Biogeosciences

Supplement of

Climatic traits on daily clearness and cloudiness indices

Estefanía Muñoz and Andrés Ochoa

Correspondence to: Estefanía Muñoz (emunozh@unal.edu.co)

List of Figures

Figure S1. Time series, annual cycle, and autocorrelation function of PAR (a–c), c (d–f), and k (g–i) at AT-Neu. Solid black and green lines in panels (a) and (b) indicate PAR_0 (no atmosphere), and PAR_{cda} (clean and dry atmosphere), respectively. Thin lines in (a), points in (b) and the ACF in (c) show PAR_{obs}. Dotted lines in the right panel indicates the 95% level of confidence.

Figure S2. Time series, annual cycle, and autocorrelation function of PAR (a–c), c (d–f), and k (g–i) at BE-Lon. Solid black and green lines in panels (a) and (b) indicate PAR_0 (no atmosphere), and PAR_{cda} (clean and dry atmosphere), respectively. Thin lines in (a), points in (b) and the ACF in (c) show PAR_{obs}. Dotted lines in the right panel indicates the 95% level of confidence.

Figure S3. Time series, annual cycle, and autocorrelation function of PAR (a–c), c (d–f), and k (g–i) at BE-Vie. Solid black and green lines in panels (a) and (b) indicate PAR_0 (no atmosphere), and PAR_{cda} (clean and dry atmosphere), respectively. Thin lines in (a), points in (b) and the ACF in (c) show PAR_{obs}. Dotted lines in the right panel indicates the 95% level of confidence.

Figure S4. Time series, annual cycle, and autocorrelation function of PAR (a–c), c (d–f), and k (g–i) at BR-Sa3. Solid black and green lines in panels (a) and (b) indicate PAR_0 (no atmosphere), and PAR_{cda} (clean and dry atmosphere), respectively. Thin lines in (a), points in (b) and the ACF in (c) show PAR_{obs}. Dotted lines in the right panel indicates the 95% level of confidence.

Figure S5. Time series, annual cycle, and autocorrelation function of PAR (a–c), c (d–f), and k (g–i) at CA-Oas. Solid black and green lines in panels (a) and (b) indicate PAR_0 (no atmosphere), and PAR_{cda} (clean and dry atmosphere), respectively. Thin lines in (a), points in (b) and the ACF in (c) show PAR_{obs}. Dotted lines in the right panel indicates the 95% level of confidence.
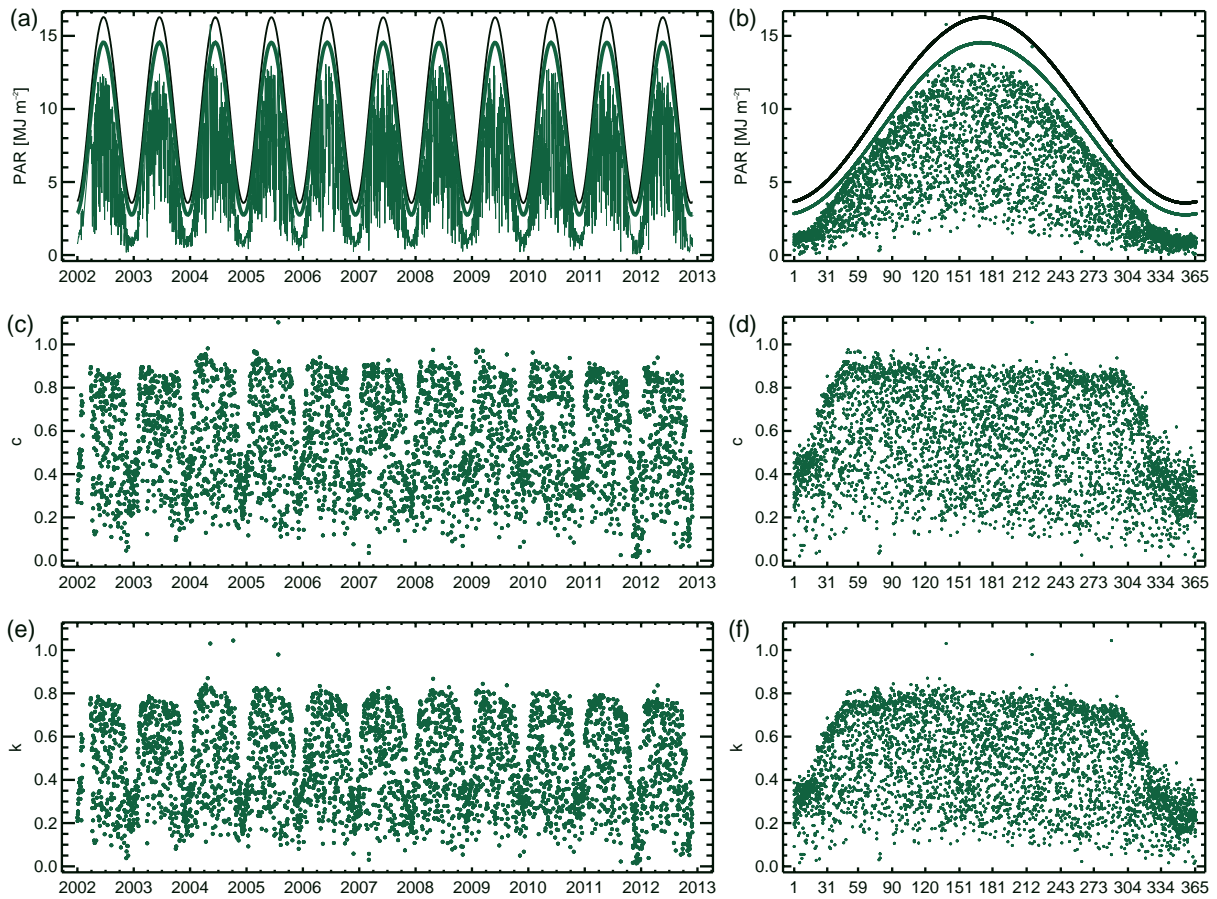
Figure S6. Time series, annual cycle, and autocorrelation function of PAR (a–c), c (d–f), and k (g–i) at CG-Tch. Solid black and green lines in panels (a) and (b) indicate PAR_0 (no atmosphere), and PAR_{cda} (clean and dry atmosphere), respectively. Thin lines in (a), points in (b) and the ACF in (c) show PAR_{obs}. Dotted lines in the right panel indicates the 95% level of confidence.
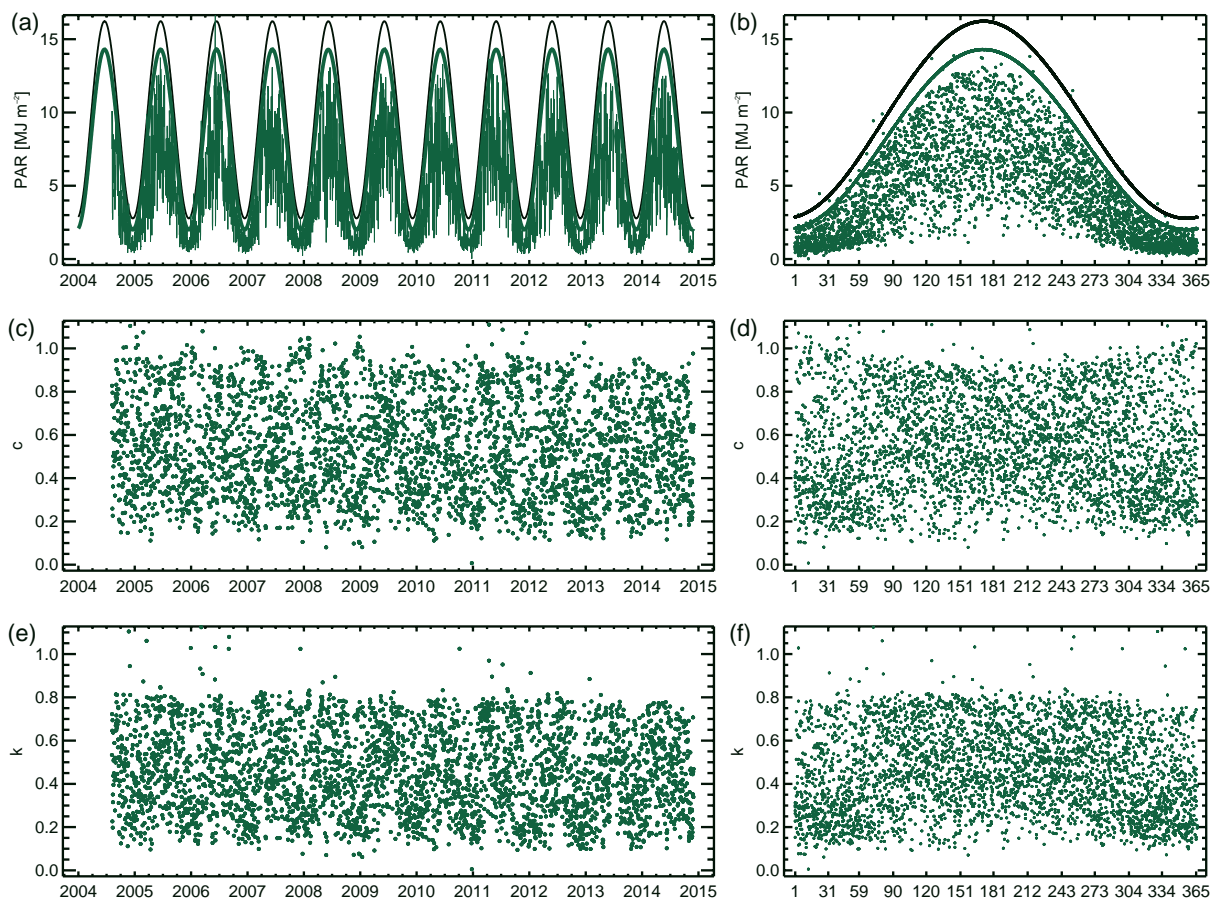
Figure S7. Time series, annual cycle, and autocorrelation function of PAR (a–c), c (d–f), and k (g–i) at CH-Oe1. Solid black and green lines in panels (a) and (b) indicate PAR_0 (no atmosphere), and PAR_{cda} (clean and dry atmosphere), respectively. Thin lines in (a), points in (b) and the ACF in (c) show PAR_{obs}. Dotted lines in the right panel indicates the 95% level of confidence.
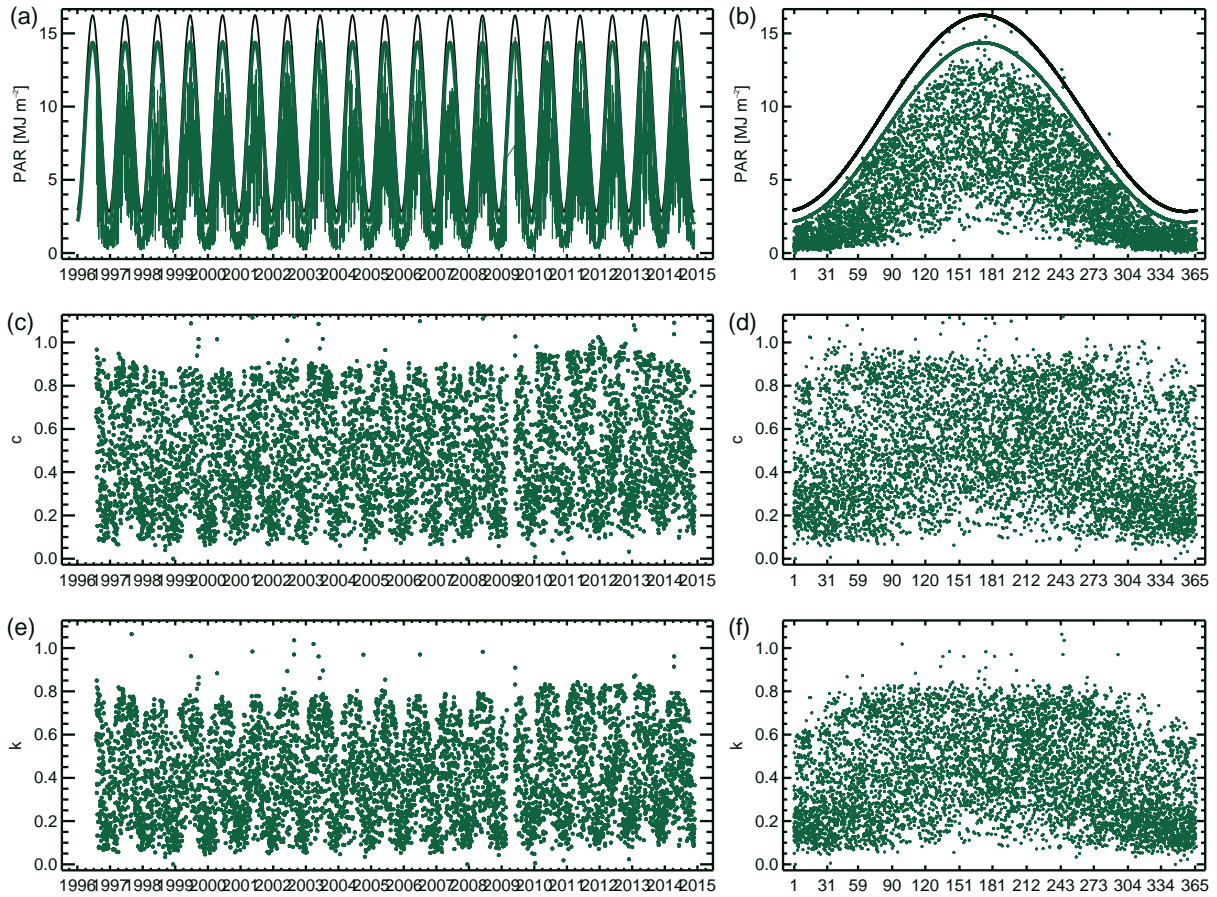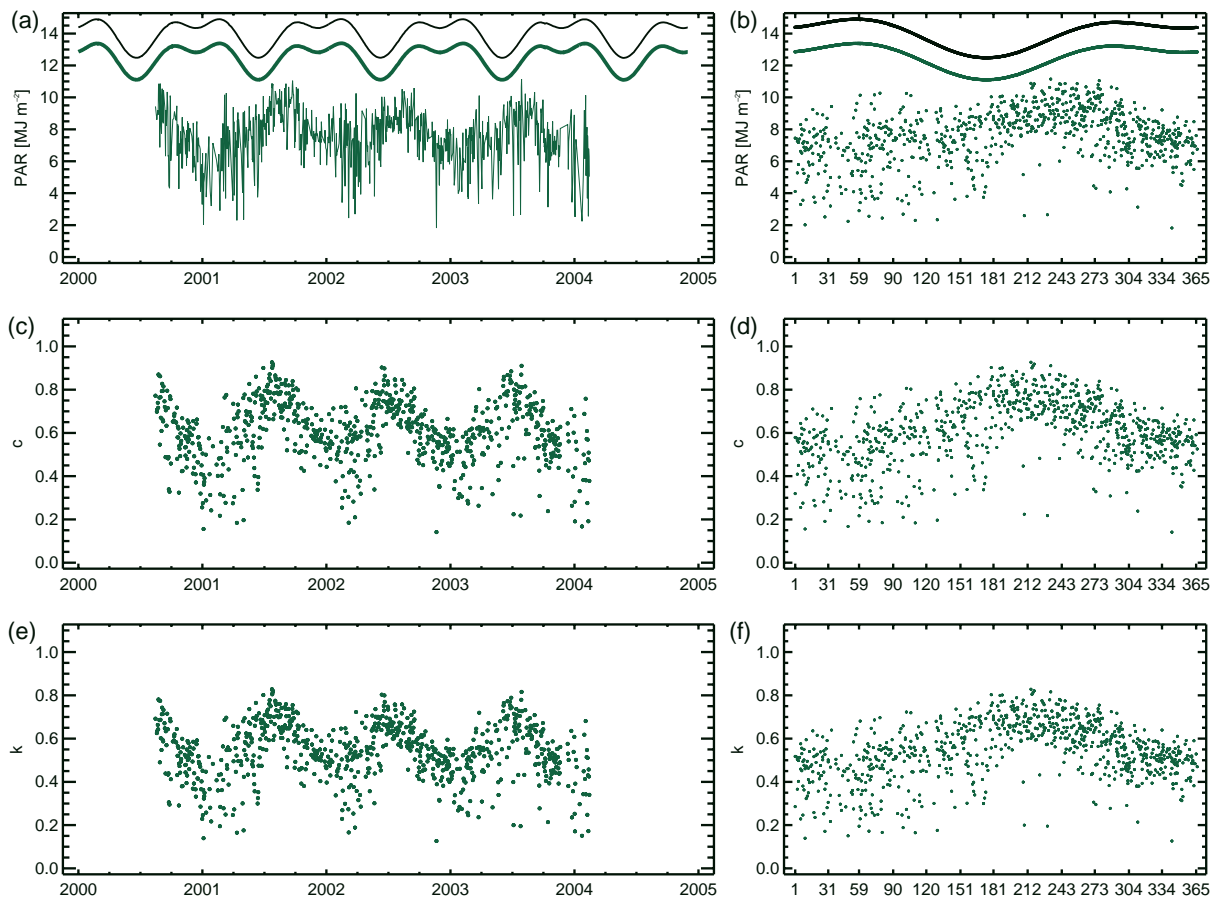
Figure S8. Time series, annual cycle, and autocorrelation function of PAR (a–c), c (d–f), and k (g–i) at CH-Oe2. Solid black and green lines in panels (a) and (b) indicate PAR_0 (no atmosphere), and PAR_{cda} (clean and dry atmosphere), respectively. Thin lines in (a), points in (b) and the ACF in (c) show PAR_{obs}. Dotted lines in the right panel indicates the 95% level of confidence.
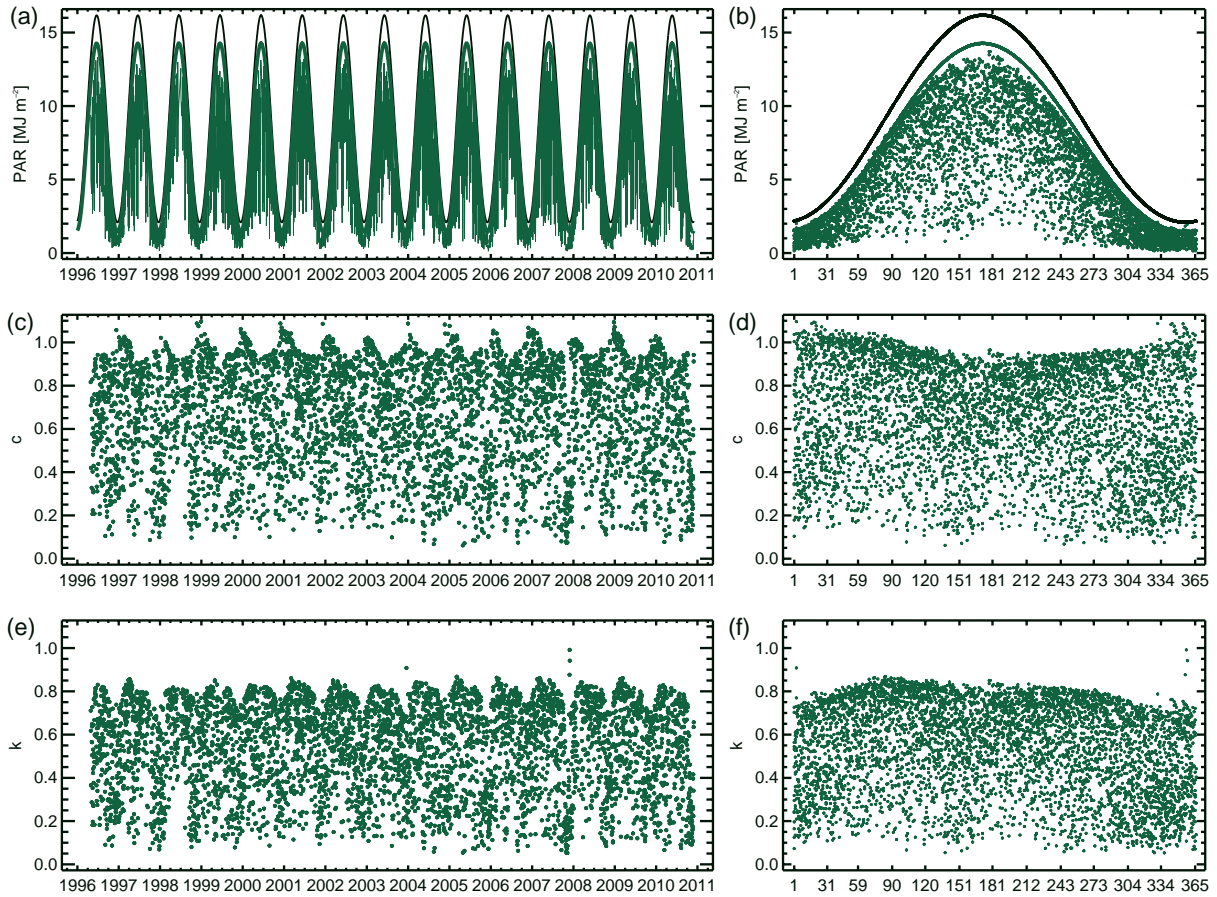
Figure S9. Time series, annual cycle, and autocorrelation function of PAR (a–c), c (d–f), and k (g–i) at DE-Geb. Solid black and green lines in panels (a) and (b) indicate PAR_0 (no atmosphere), and PAR_{cda} (clean and dry atmosphere), respectively. Thin lines in (a), points in (b) and the ACF in (c) show PAR_{obs}. Dotted lines in the right panel indicates the 95% level of confidence.
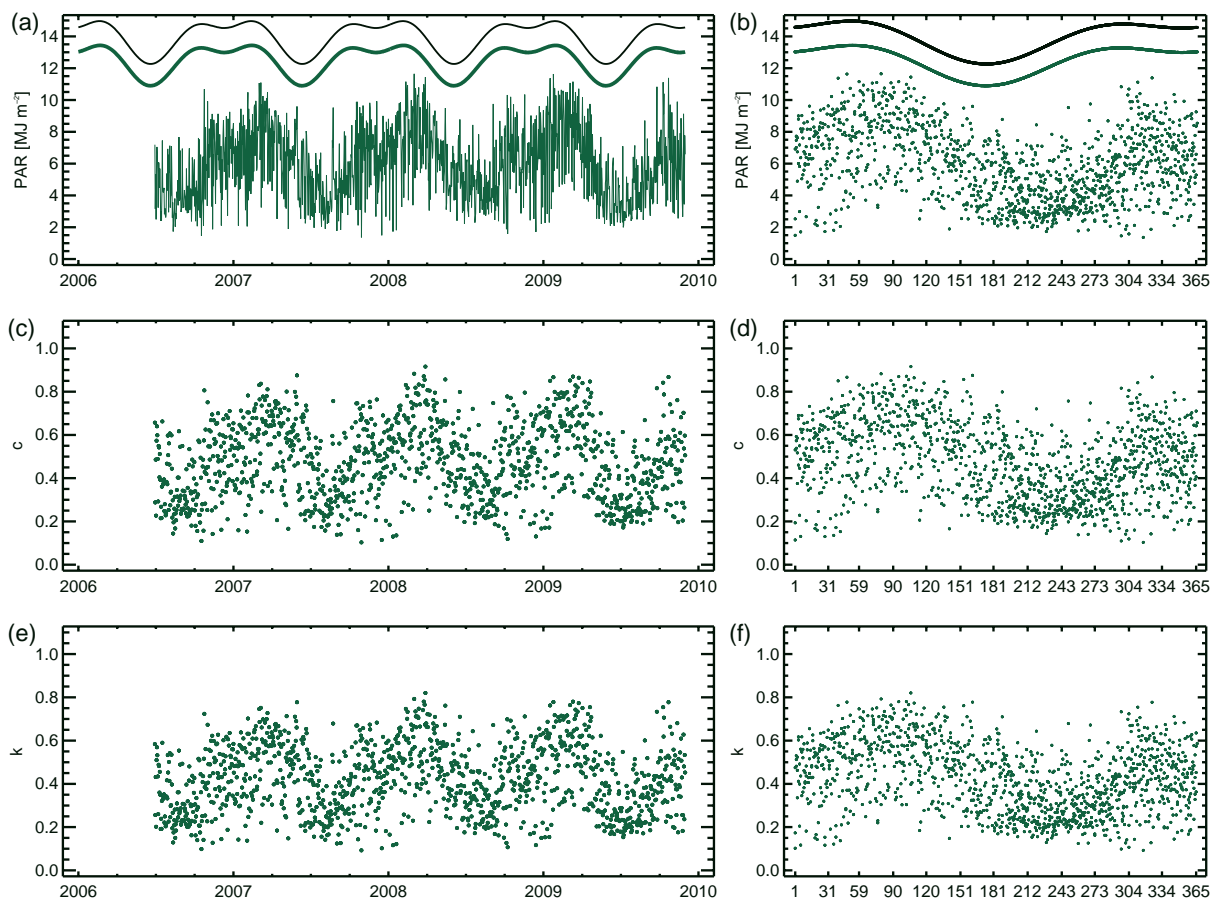
Figure S10. Time series, annual cycle, and autocorrelation function of PAR (a–c), c (d–f), and k (g–i) at DE-Gri. Solid black and green lines in panels (a) and (b) indicate PAR_0 (no atmosphere), and PAR_{cda} (clean and dry atmosphere), respectively. Thin lines in (a), points in (b) and the ACF in (c) show PAR_{obs}. Dotted lines in the right panel indicates the 95% level of confidence.
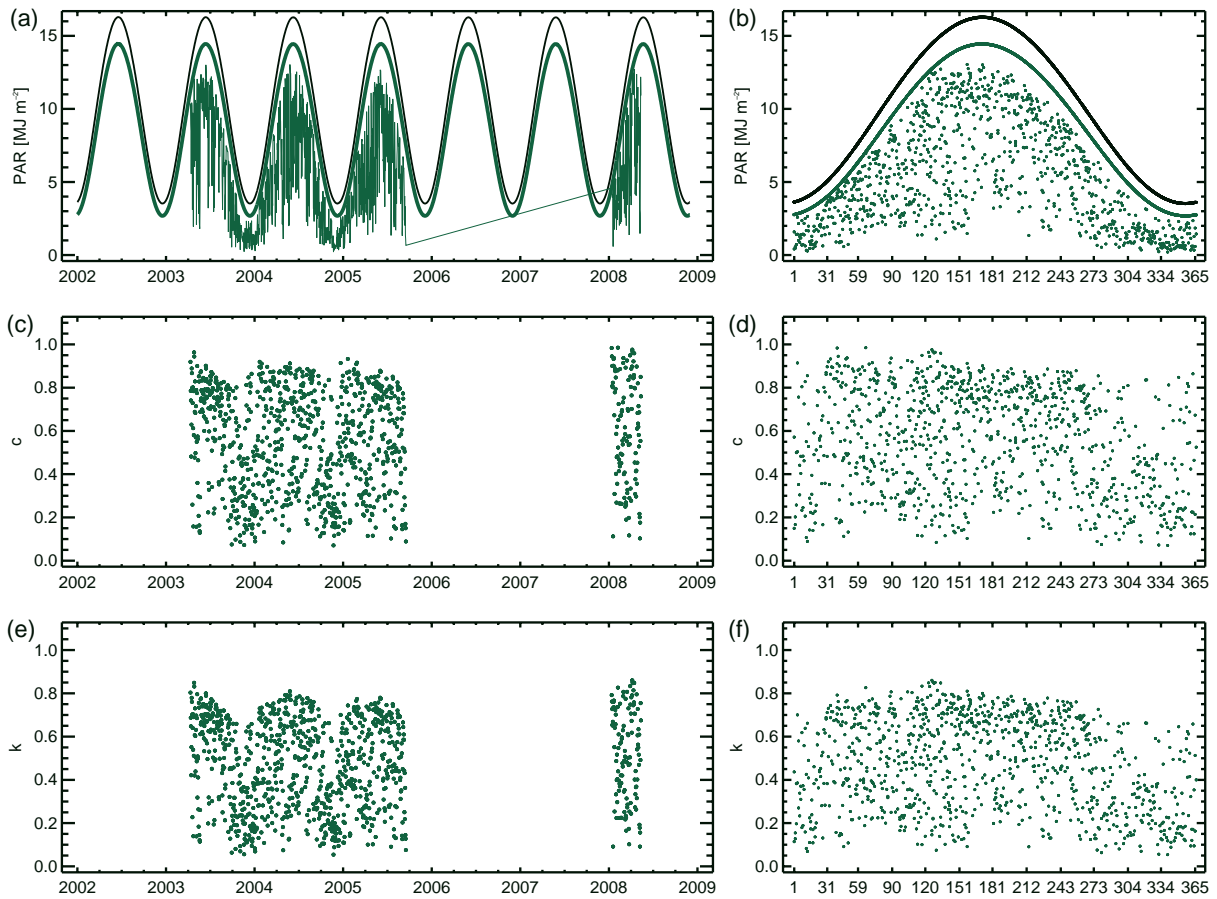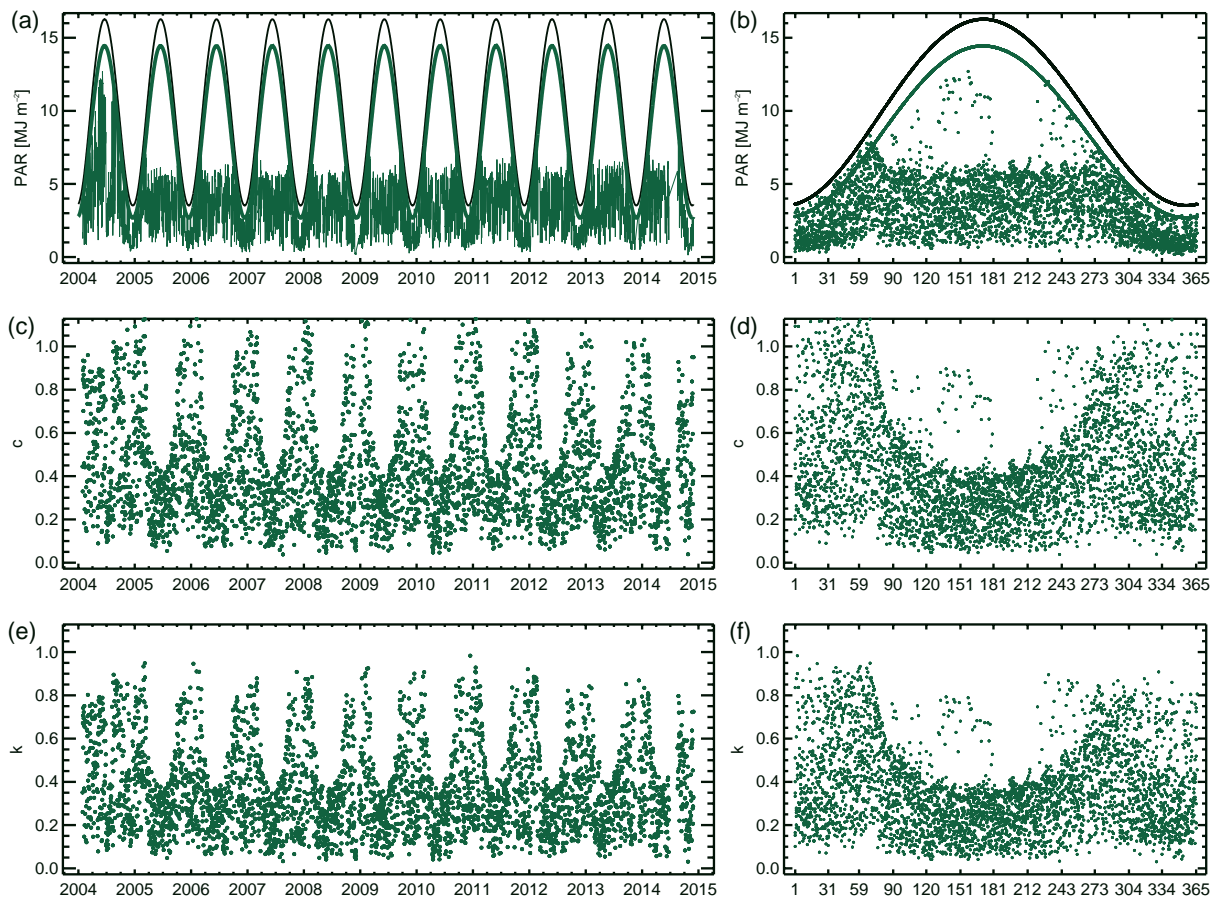
Figure S11. Time series, annual cycle, and autocorrelation function of PAR (a–c), c (d–f), and k (g–i) at DE-Hai. Solid black and green lines in panels (a) and (b) indicate PAR_0 (no atmosphere), and PAR_{cda} (clean and dry atmosphere), respectively. Thin lines in (a), points in (b) and the ACF in (c) show PAR_{obs}. Dotted lines in the right panel indicates the 95% level of confidence.
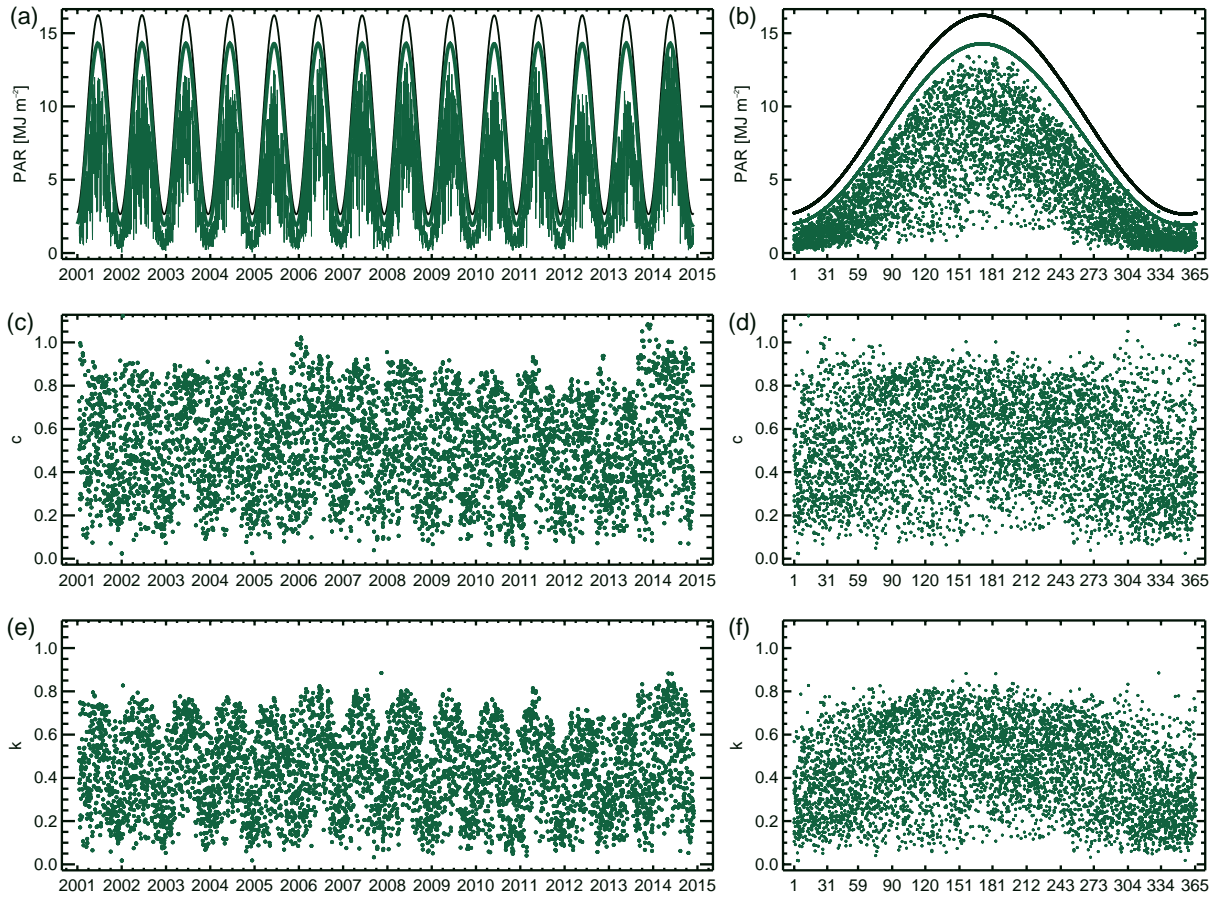
Figure S12. Time series, annual cycle, and autocorrelation function of PAR (a–c), c (d–f), and k (g–i) at DE-Obe. Solid black and green lines in panels (a) and (b) indicate PAR_0 (no atmosphere), and PAR_{cda} (clean and dry atmosphere), respectively. Thin lines in (a), points in (b) and the ACF in (c) show PAR_{obs}. Dotted lines in the right panel indicates the 95% level of confidence.
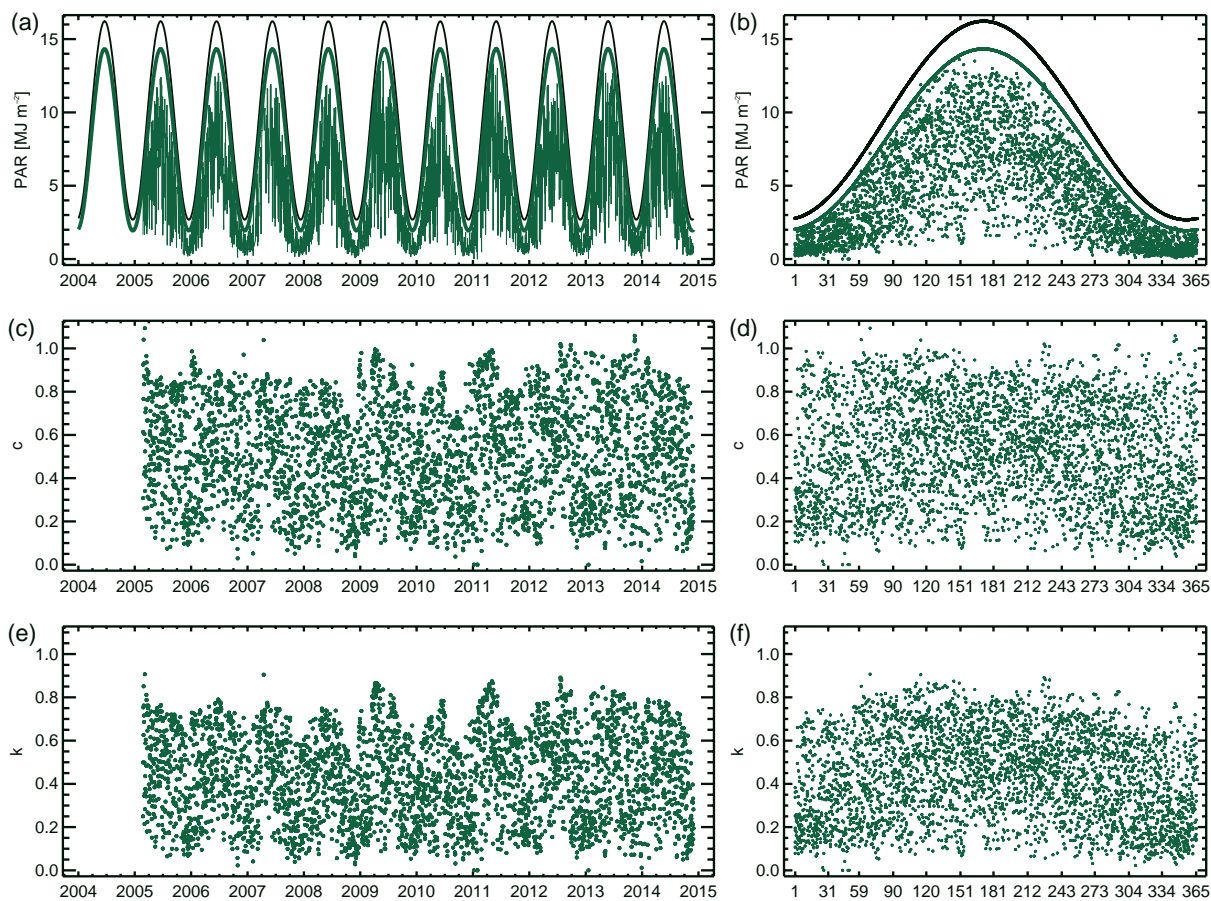
Figure S13. Time series, annual cycle, and autocorrelation function of PAR (a–c), c (d–f), and k (g–i) at DE-Tha. Solid black and green lines in panels (a) and (b) indicate PAR_0 (no atmosphere), and PAR_{cda} (clean and dry atmosphere), respectively. Thin lines in (a), points in (b) and the ACF in (c) show PAR_{obs}. Dotted lines in the right panel indicates the 95% level of confidence.
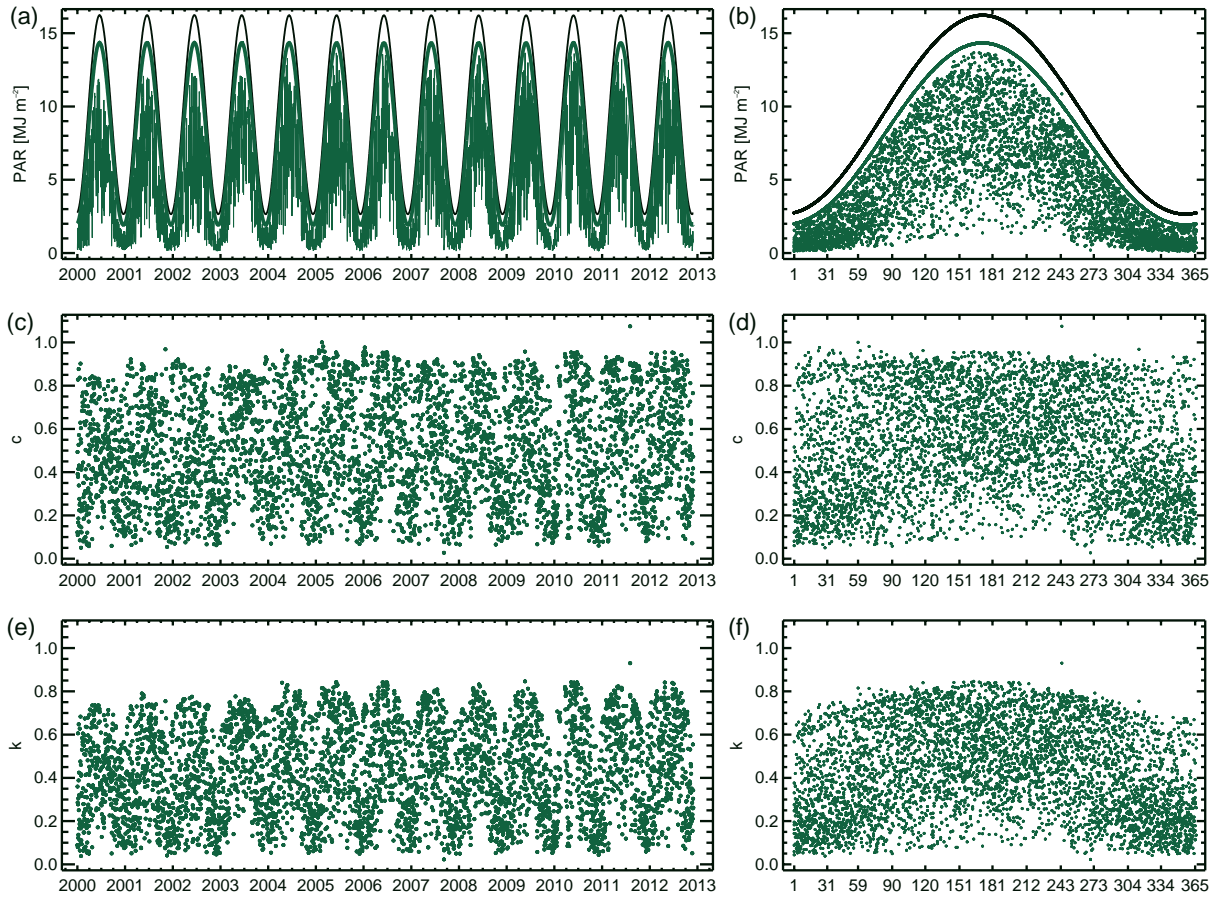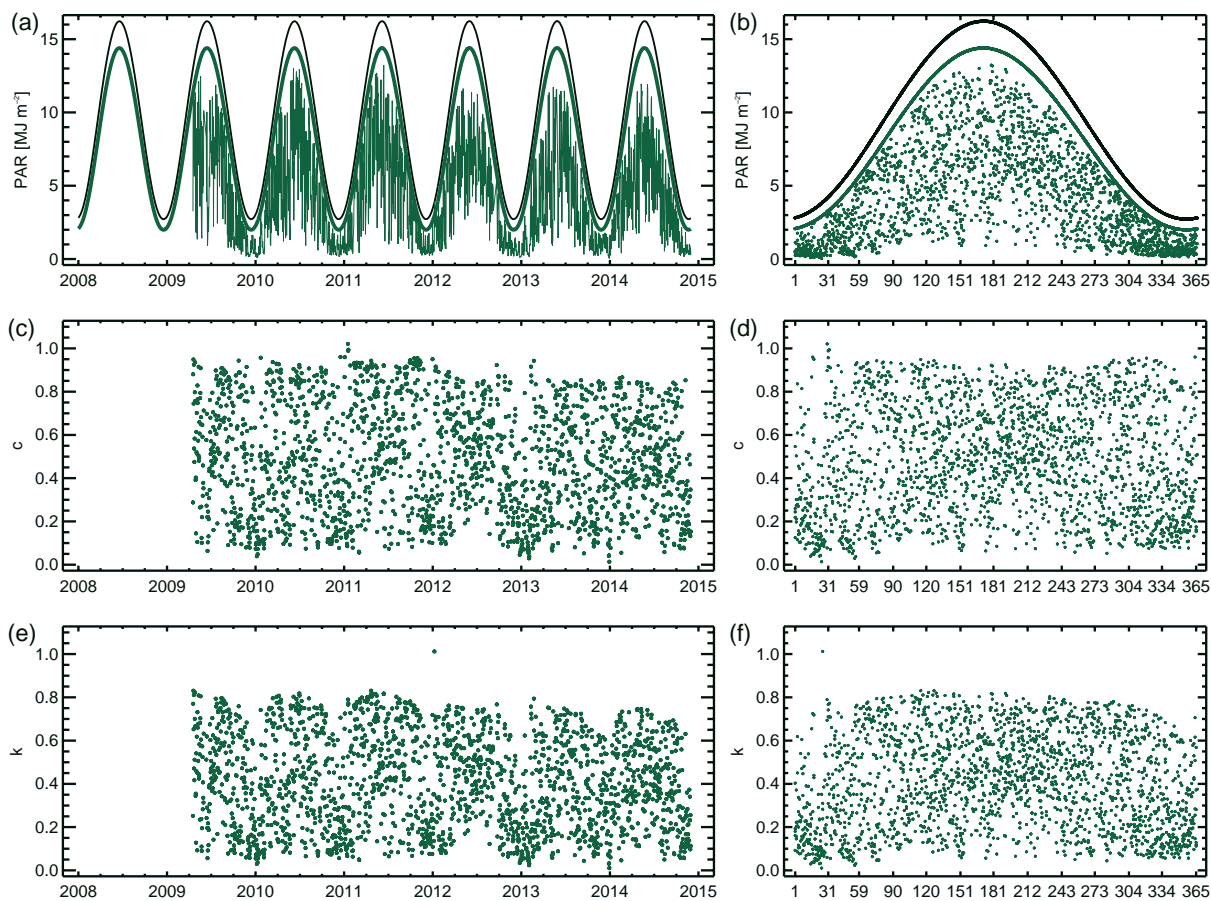
Figure S14. Time series, annual cycle, and autocorrelation function of PAR (a–c), c (d–f), and k (g–i) at GF-Guy. Solid black and green lines in panels (a) and (b) indicate PAR_0 (no atmosphere), and PAR_{cda} (clean and dry atmosphere), respectively. Thin lines in (a), points in (b) and the ACF in (c) show PAR_{obs}. Dotted lines in the right panel indicates the 95% level of confidence.
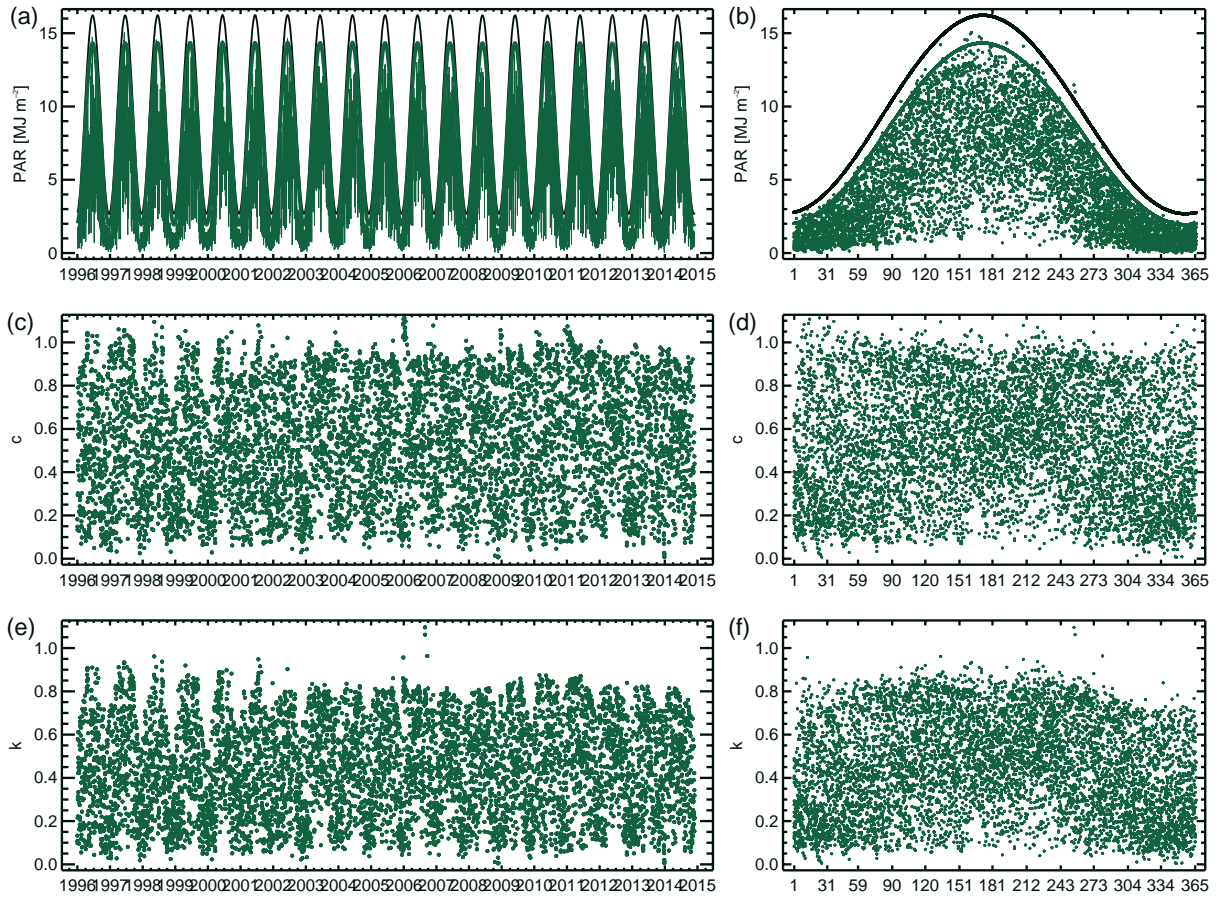
Figure S15. Time series, annual cycle, and autocorrelation function of PAR (a–c), c (d–f), and k (g–i) at GH-Ank. Solid black and green lines in panels (a) and (b) indicate PAR_0 (no atmosphere), and PAR_{cda} (clean and dry atmosphere), respectively. Thin lines in (a), points in (b) and the ACF in (c) show PAR_{obs}. Dotted lines in the right panel indicates the 95% level of confidence.
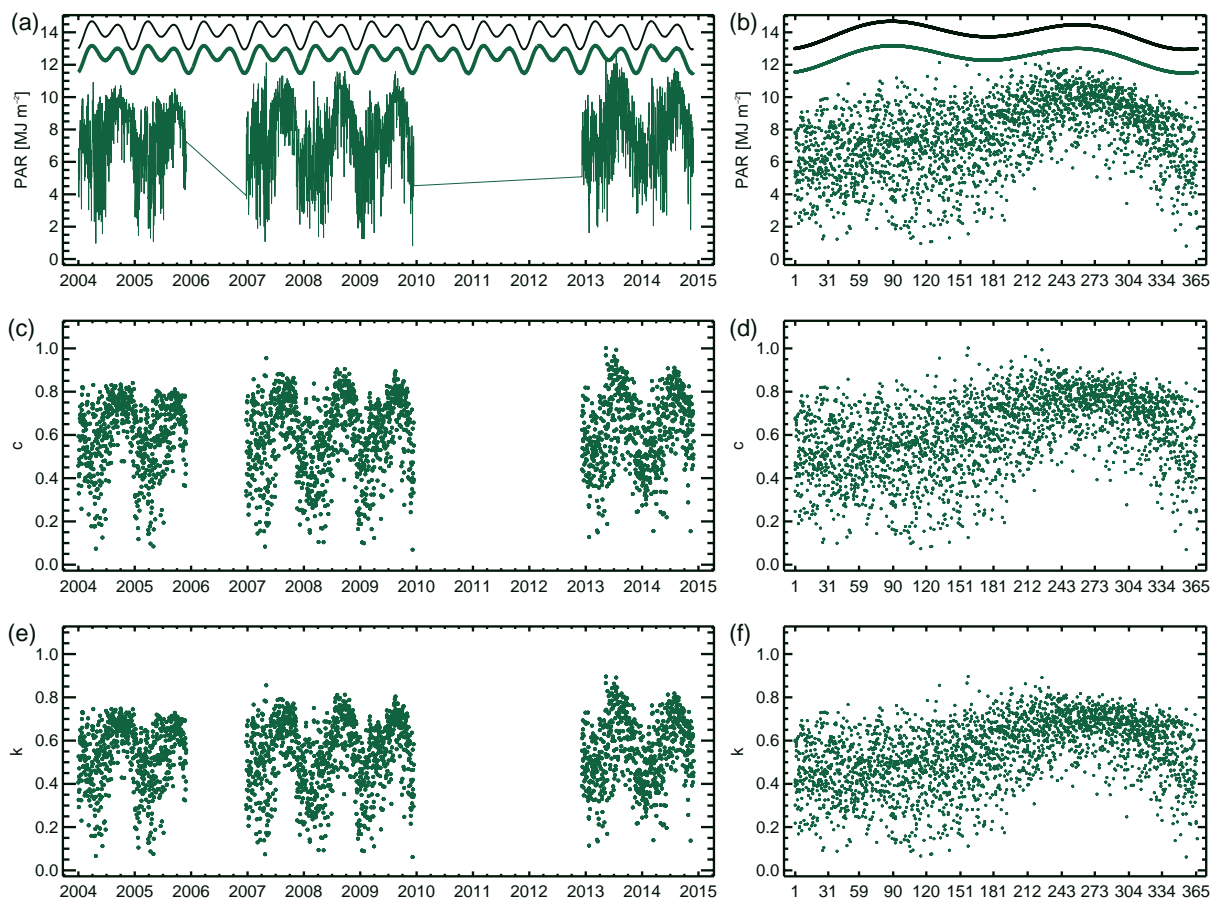
Figure S16. Time series, annual cycle, and autocorrelation function of PAR (a–c), c (d–f), and k (g–i) at IT-Lav. Solid black and green lines in panels (a) and (b) indicate PAR_0 (no atmosphere), and PAR_{cda} (clean and dry atmosphere), respectively. Thin lines in (a), points in (b) and the ACF in (c) show PAR_{obs}. Dotted lines in the right panel indicates the 95% level of confidence.
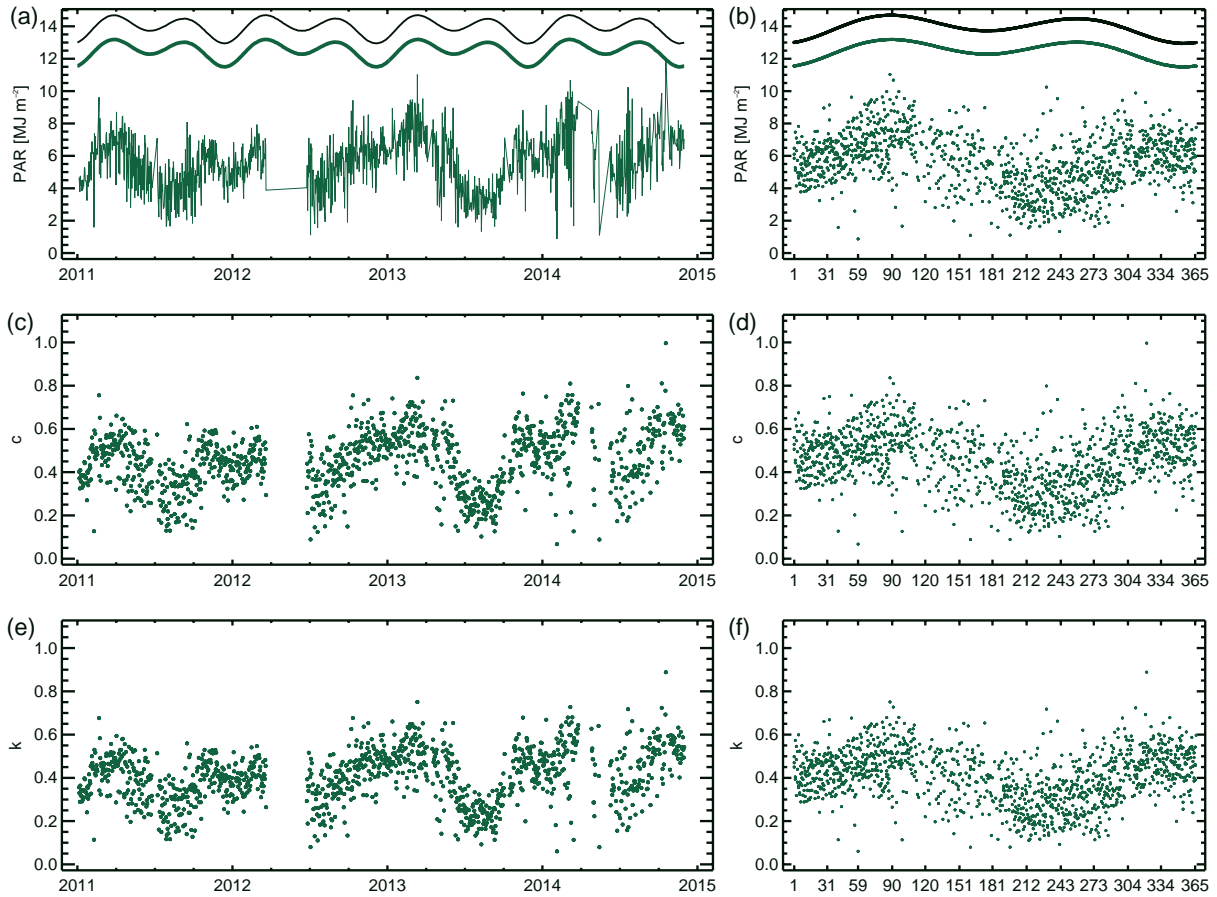
Figure S17. Time series, annual cycle, and autocorrelation function of PAR (a–c), c (d–f), and k (g–i) at IT-MBo. Solid black and green lines in panels (a) and (b) indicate PAR_0 (no atmosphere), and PAR_{cda} (clean and dry atmosphere), respectively. Thin lines in (a), points in (b) and the ACF in (c) show PAR_{obs}. Dotted lines in the right panel indicates the 95% level of confidence..
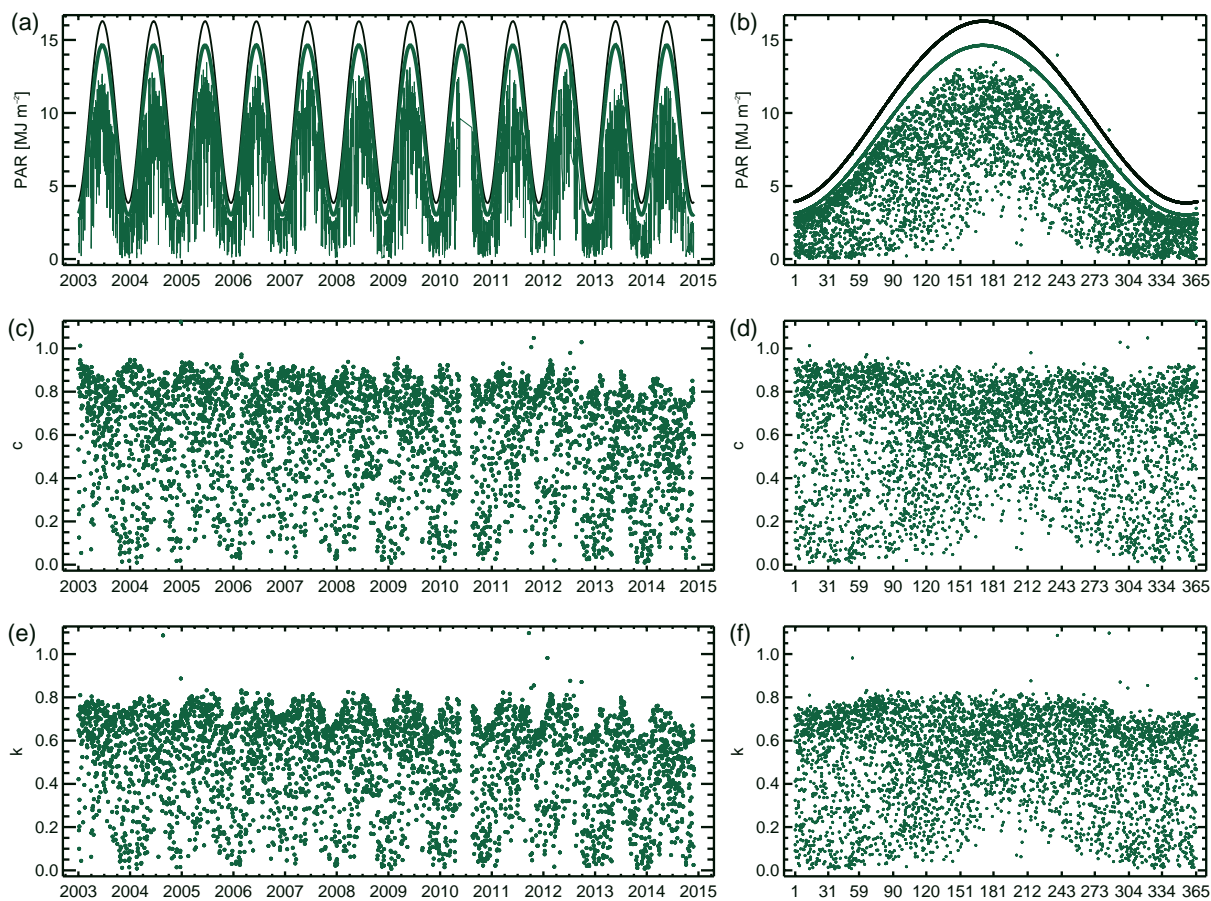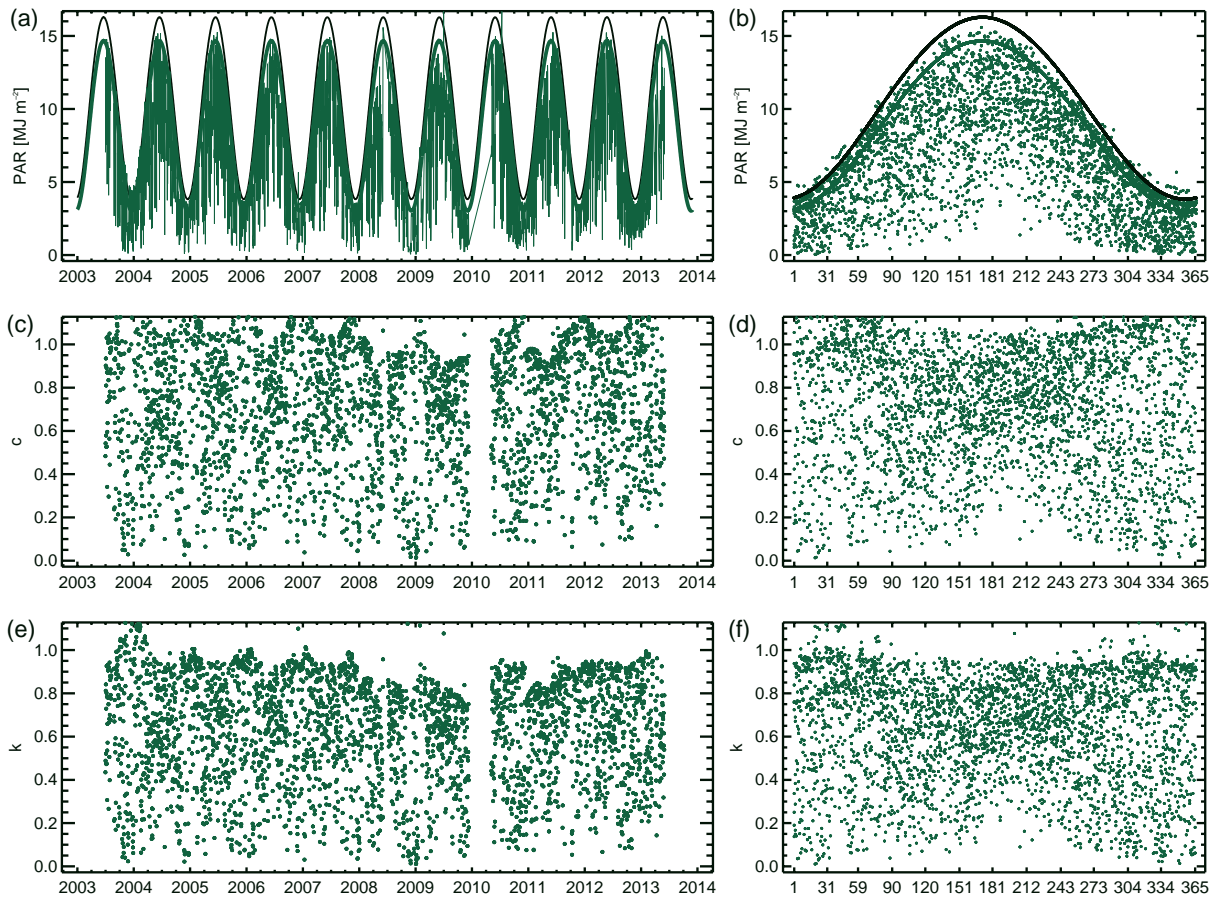
Figure S18. Time series, annual cycle, and autocorrelation function of PAR (a–c), c (d–f), and k (g–i) at IT-SRo. Solid black and green lines in panels (a) and (b) indicate PAR_0 (no atmosphere), and PAR_{cda} (clean and dry atmosphere), respectively. Thin lines in (a), points in (b) and the ACF in (c) show PAR_{obs}. Dotted lines in the right panel indicates the 95% level of confidence.
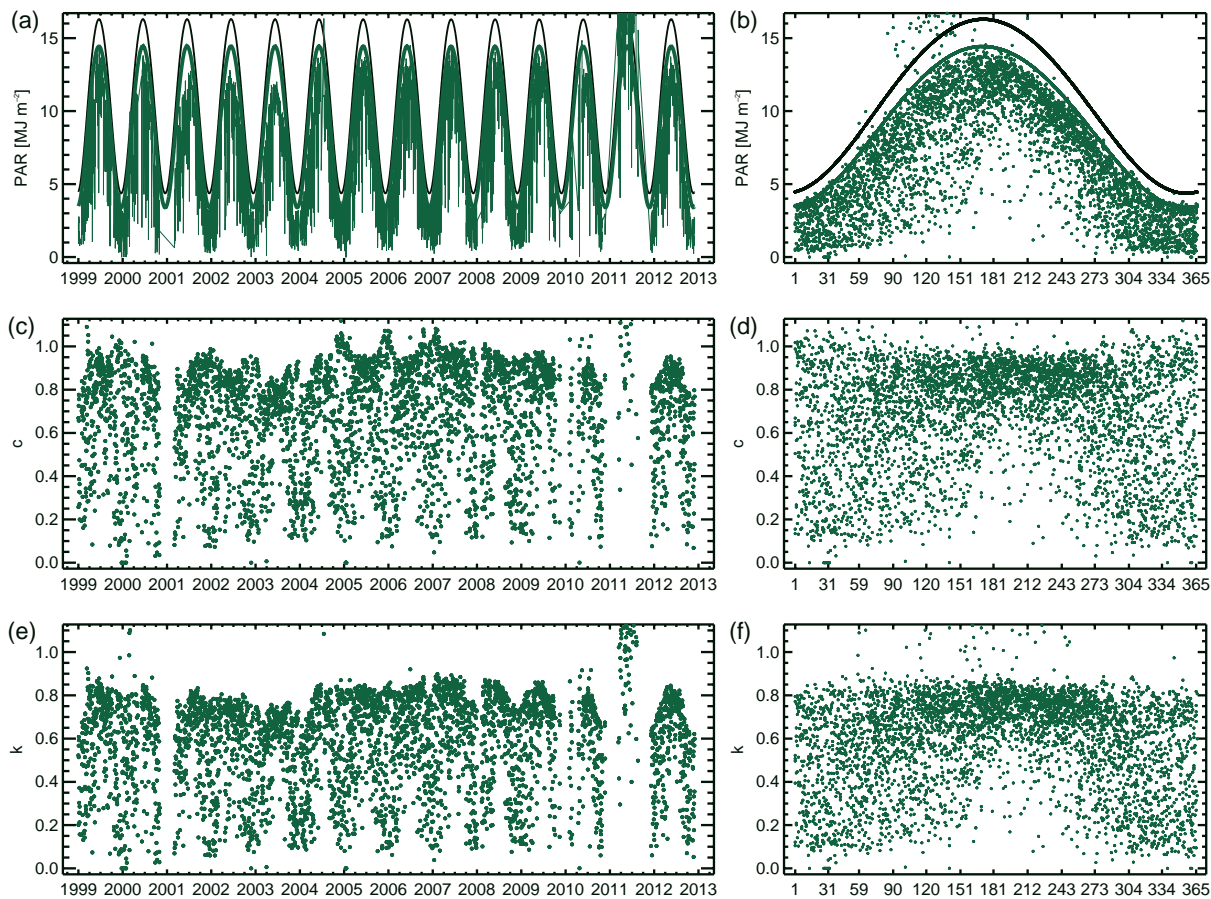
Figure S19. Time series, annual cycle, and autocorrelation function of PAR (a–c), c (d–f), and k (g–i) at MY-PSO. Solid black and green lines in panels (a) and (b) indicate PAR_0 (no atmosphere), and PAR_{cda} (clean and dry atmosphere), respectively. Thin lines in (a), points in (b) and the ACF in (c) show PAR_{obs}. Dotted lines in the right panel indicates the 95% level of confidence.
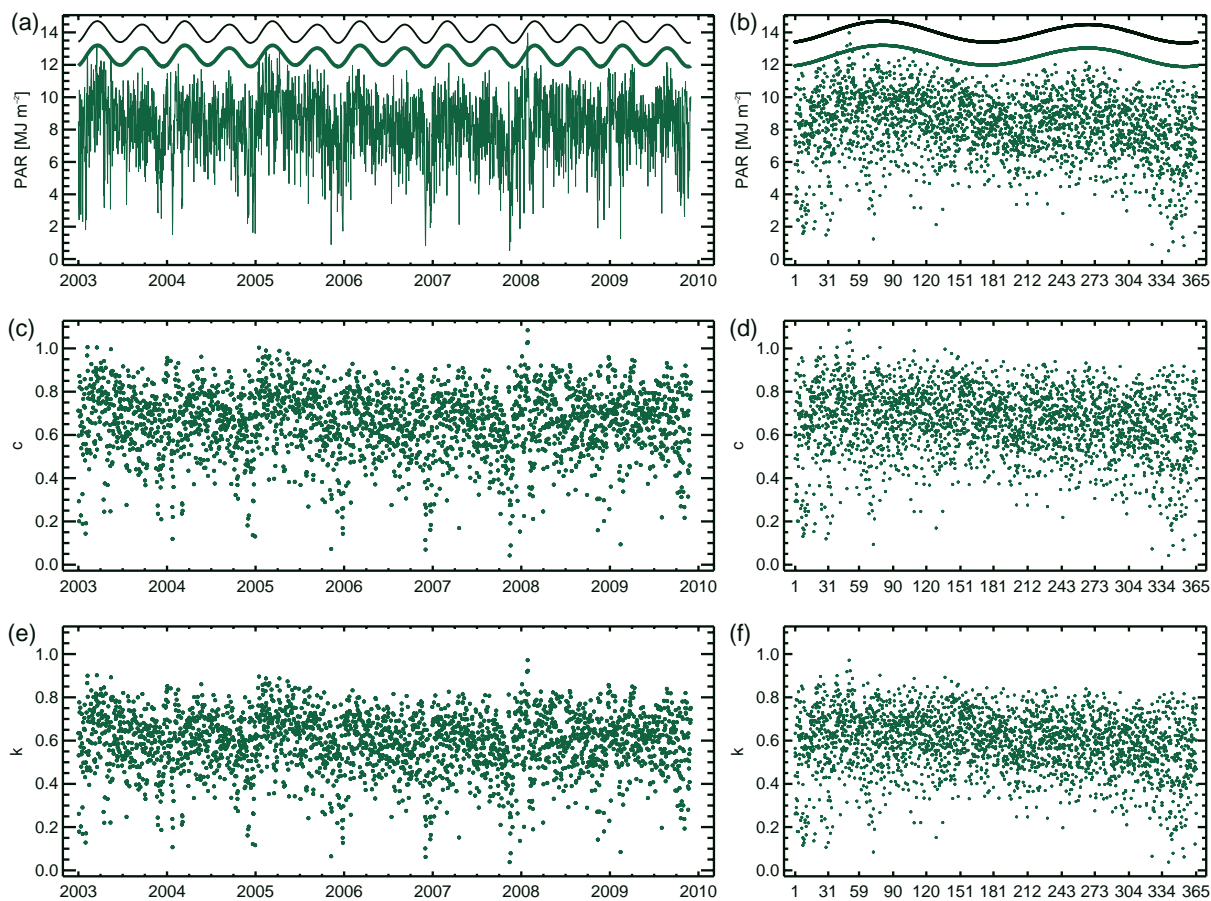
Figure S20. Time series, annual cycle, and autocorrelation function of PAR (a–c), c (d–f), and k (g–i) at PA-SPs. Solid black and green lines in panels (a) and (b) indicate PAR_0 (no atmosphere), and PAR_{cda} (clean and dry atmosphere), respectively. Thin lines in (a), points in (b) and the ACF in (c) show PAR_{obs}. Dotted lines in the right panel indicates the 95% level of confidence.
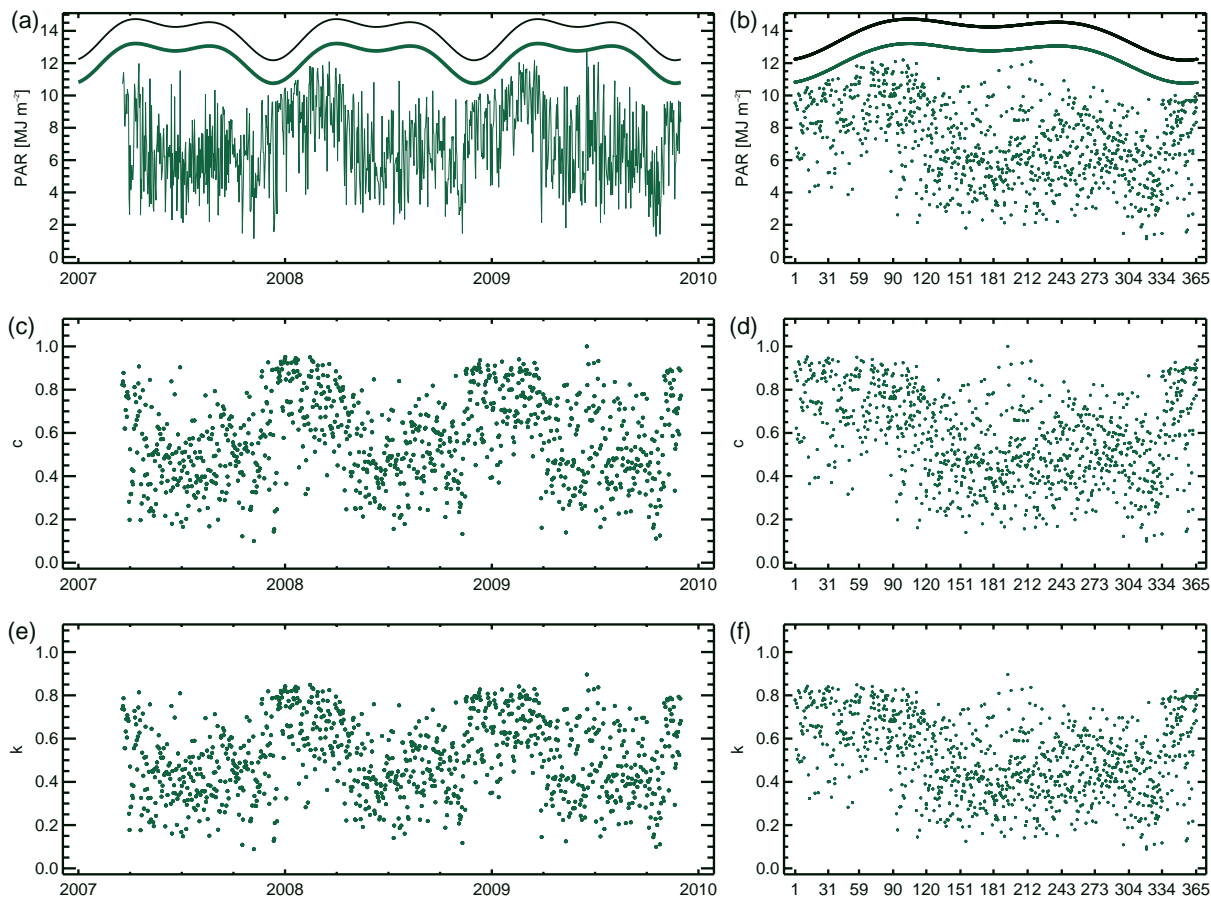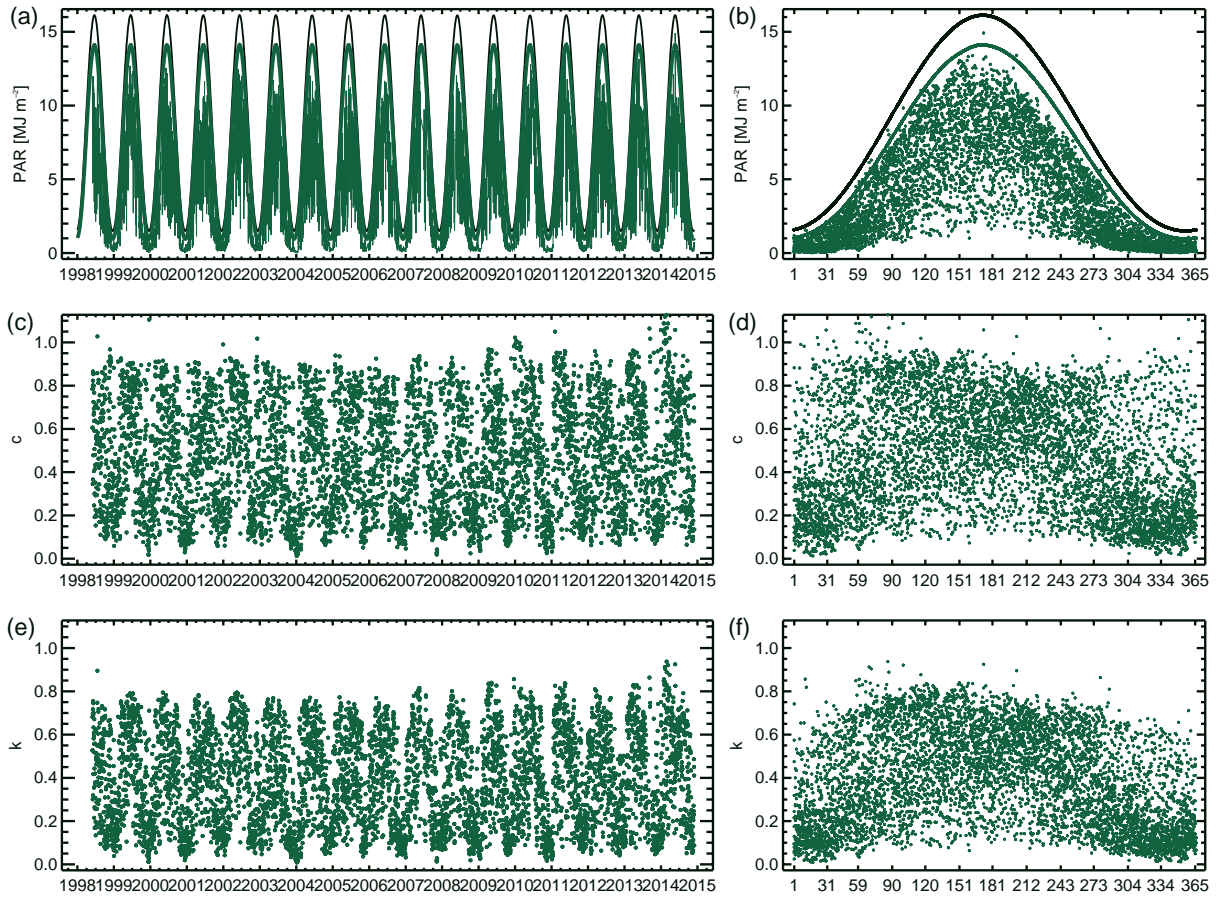
Figure S21. Time series, annual cycle, and autocorrelation function of PAR (a–c), c (d–f), and k (g–i) at RU-Fyo. Solid black and green lines in panels (a) and (b) indicate PAR_0 (no atmosphere), and PAR_{cda} (clean and dry atmosphere), respectively. Thin lines in (a), points in (b) and the ACF in (c) show PAR_{obs}. Dotted lines in the right panel indicates the 95% level of confidence.
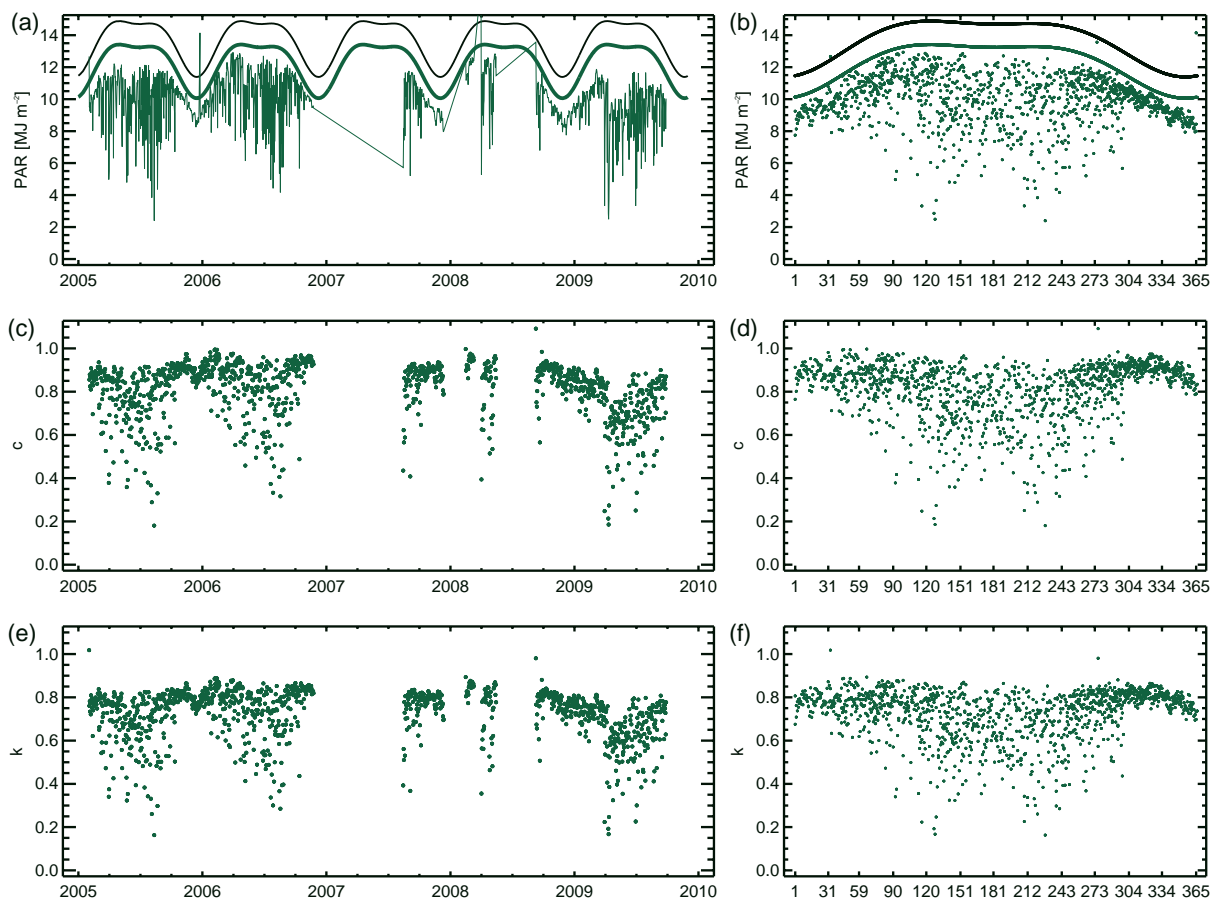
Figure S22. Time series, annual cycle, and autocorrelation function of PAR (a–c), c (d–f), and k (g–i) at SD-Dem. Solid black and green lines in panels (a) and (b) indicate PAR_0 (no atmosphere), and PAR_{cda} (clean and dry atmosphere), respectively. Thin lines in (a), points in (b) and the ACF in (c) show PAR_{obs}. Dotted lines in the right panel indicates the 95% level of confidence.
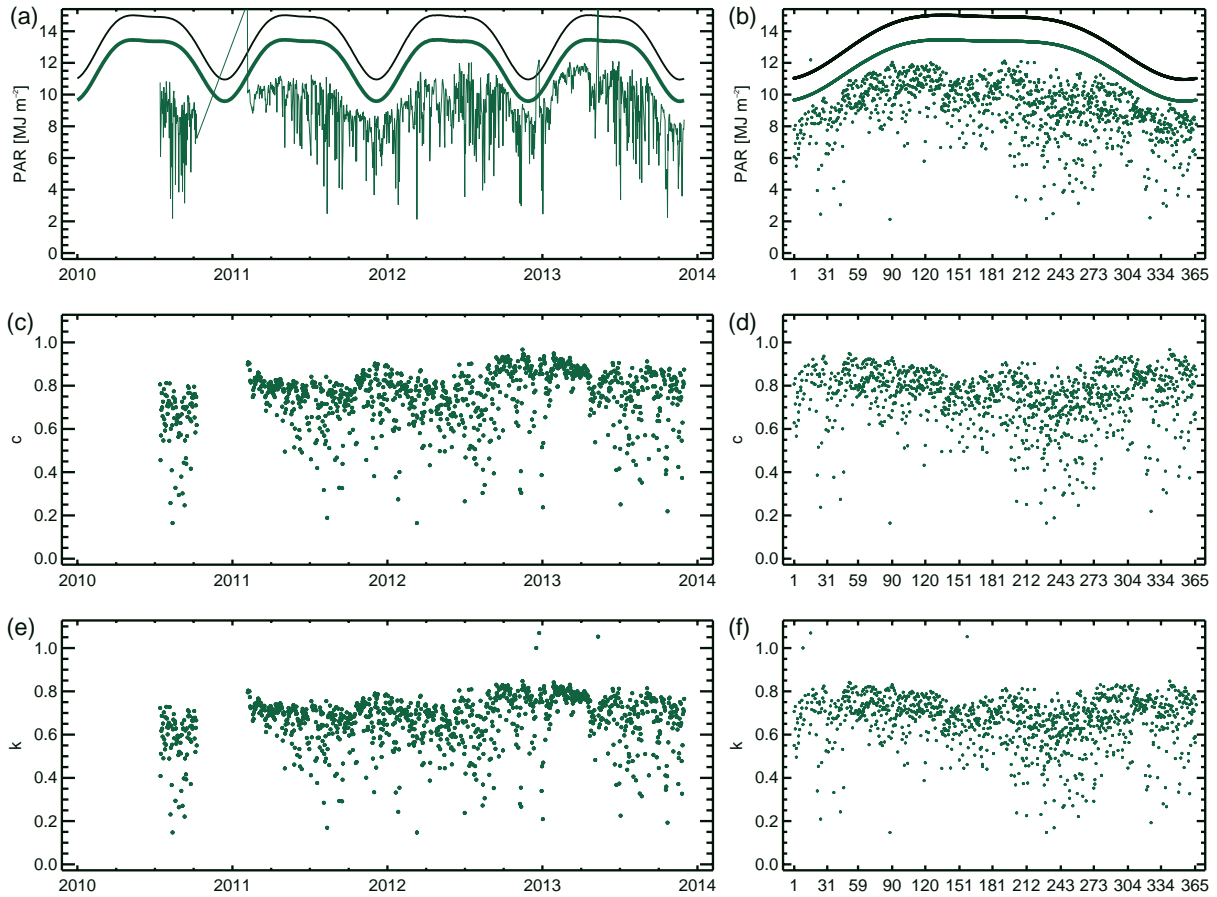
Figure S23. Time series, annual cycle, and autocorrelation function of PAR (a–c), c (d–f), and k (g–i) at SN-Dhr. Solid black and green lines in panels (a) and (b) indicate PAR_0 (no atmosphere), and PAR_{cda} (clean and dry atmosphere), respectively. Thin lines in (a), points in (b) and the ACF in (c) show PAR_{obs}. Dotted lines in the right panel indicates the 95% level of confidence.
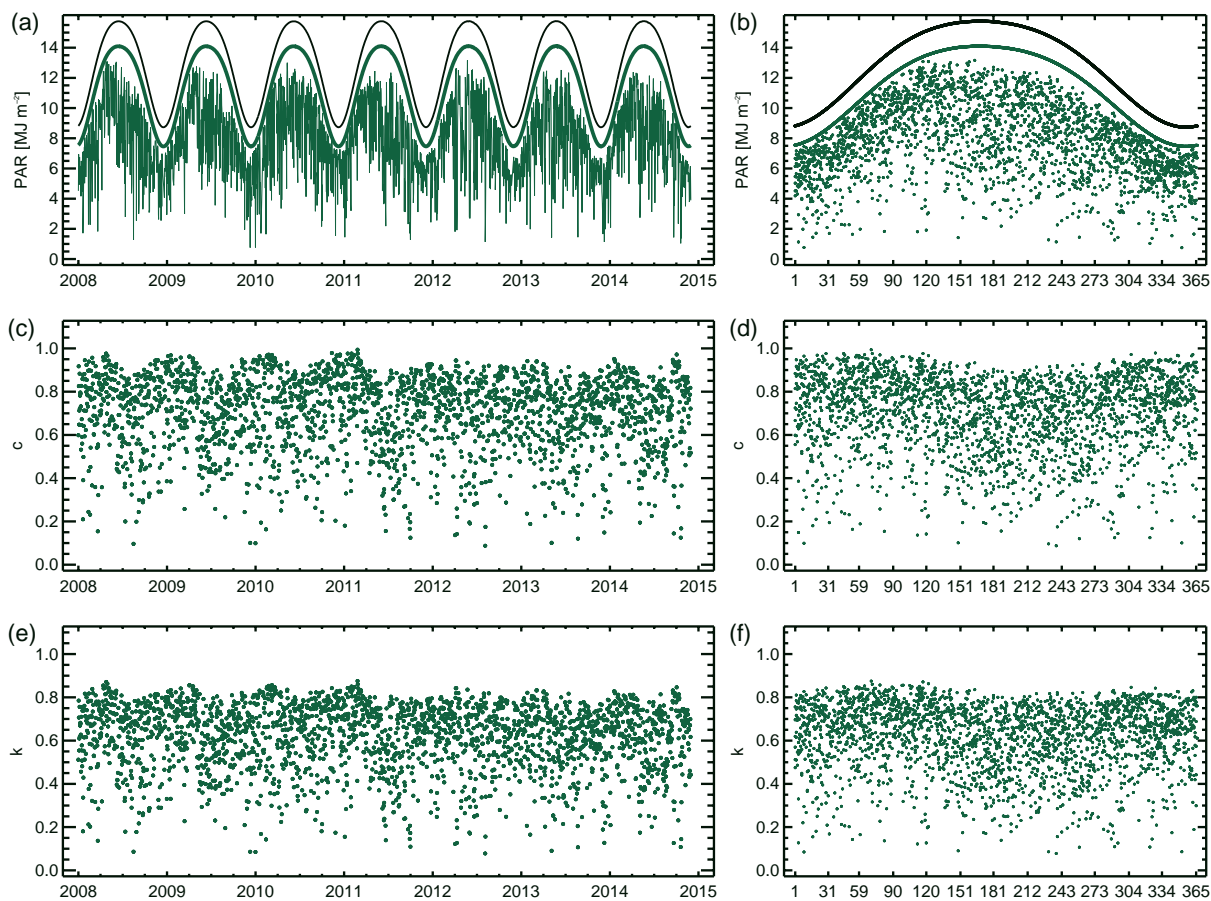
Figure S24. Time series, annual cycle, and autocorrelation function of PAR (a–c), c (d–f), and k (g–i) at US-Esm. Solid black and green lines in panels (a) and (b) indicate PAR_0 (no atmosphere), and PAR_{cda} (clean and dry atmosphere), respectively. Thin lines in (a), points in (b) and the ACF in (c) show PAR_{obs}. Dotted lines in the right panel indicates the 95% level of confidence.
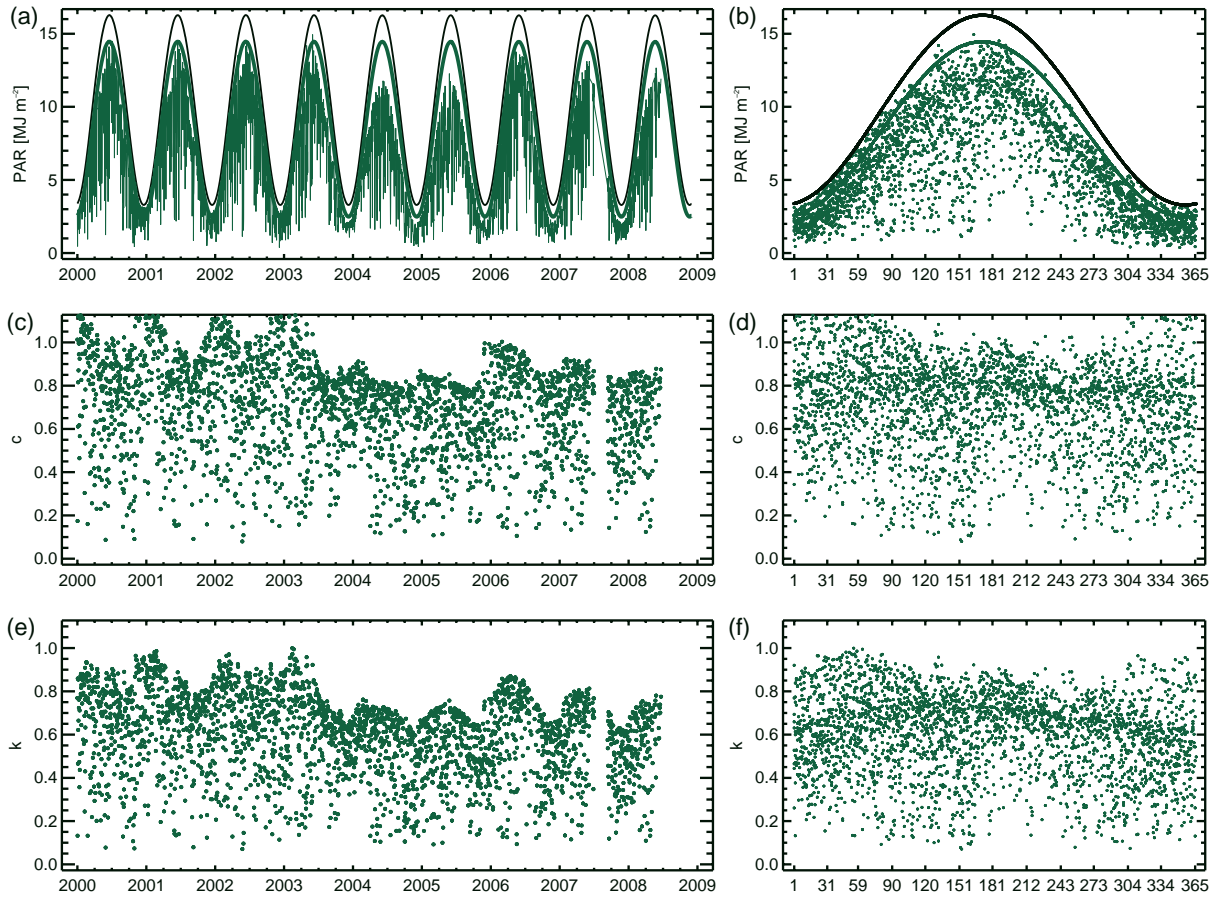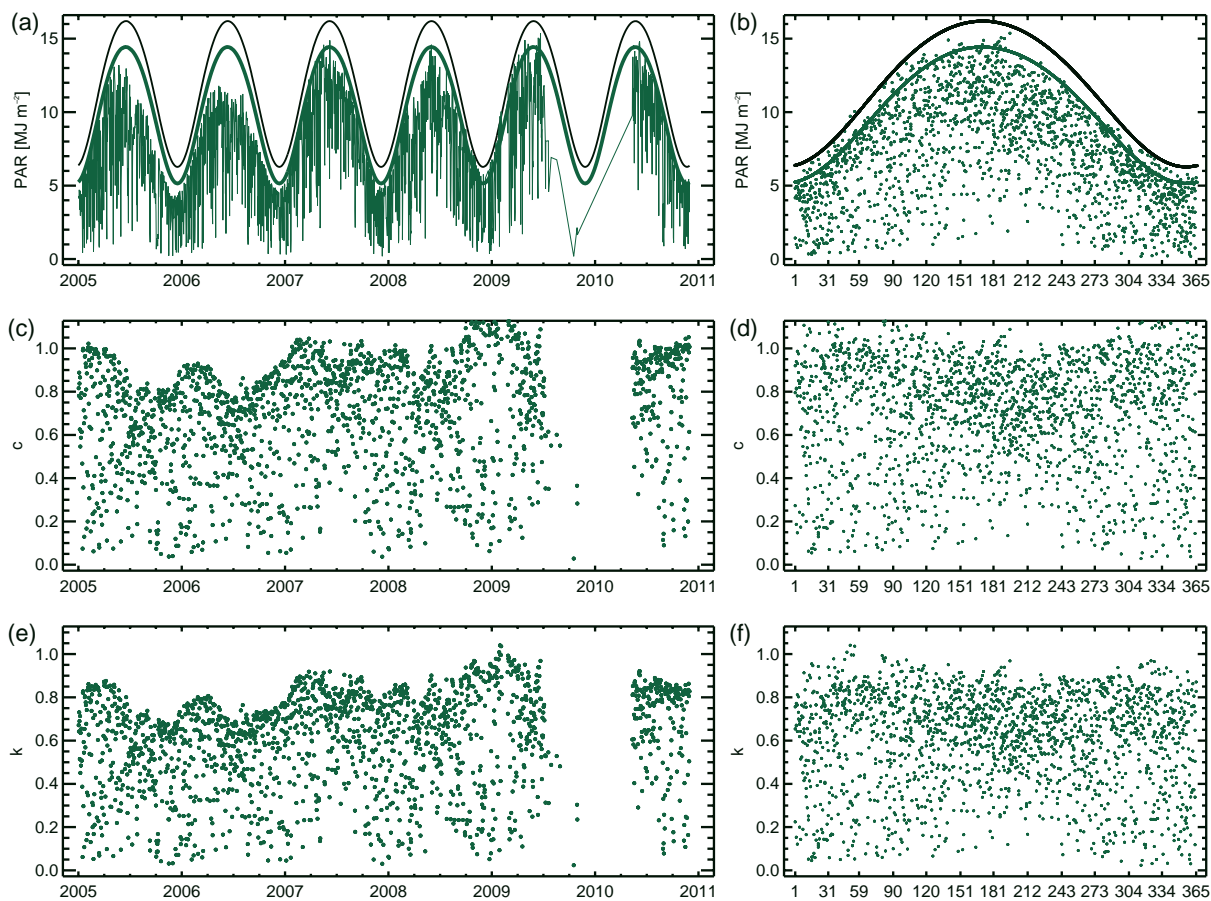
Figure S25. Time series, annual cycle, and autocorrelation function of PAR (a–c), c (d–f), and k (g–i) at US-FPe. Solid black and green lines in panels (a) and (b) indicate PAR_0 (no atmosphere), and PAR_{cda} (clean and dry atmosphere), respectively. Thin lines in (a), points in (b) and the ACF in (c) show PAR_{obs}. Dotted lines in the right panel indicates the 95% level of confidence.
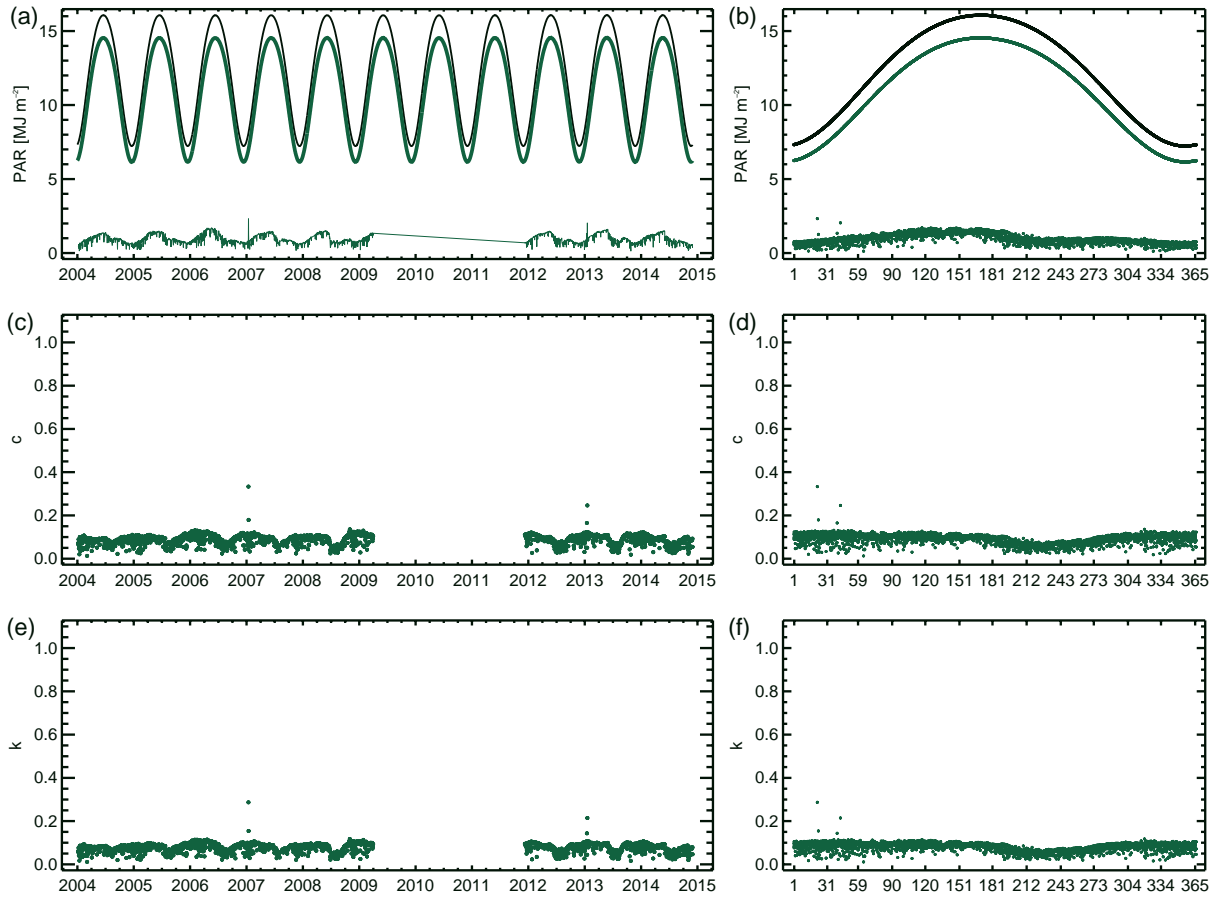
Figure S26. Time series, annual cycle, and autocorrelation function of PAR (a–c), c (d–f), and k (g–i) at US-NC2. Solid black and green lines in panels (a) and (b) indicate PAR_0 (no atmosphere), and PAR_{cda} (clean and dry atmosphere), respectively. Thin lines in (a), points in (b) and the ACF in (c) show PAR_{obs}. Dotted lines in the right panel indicates the 95% level of confidence.
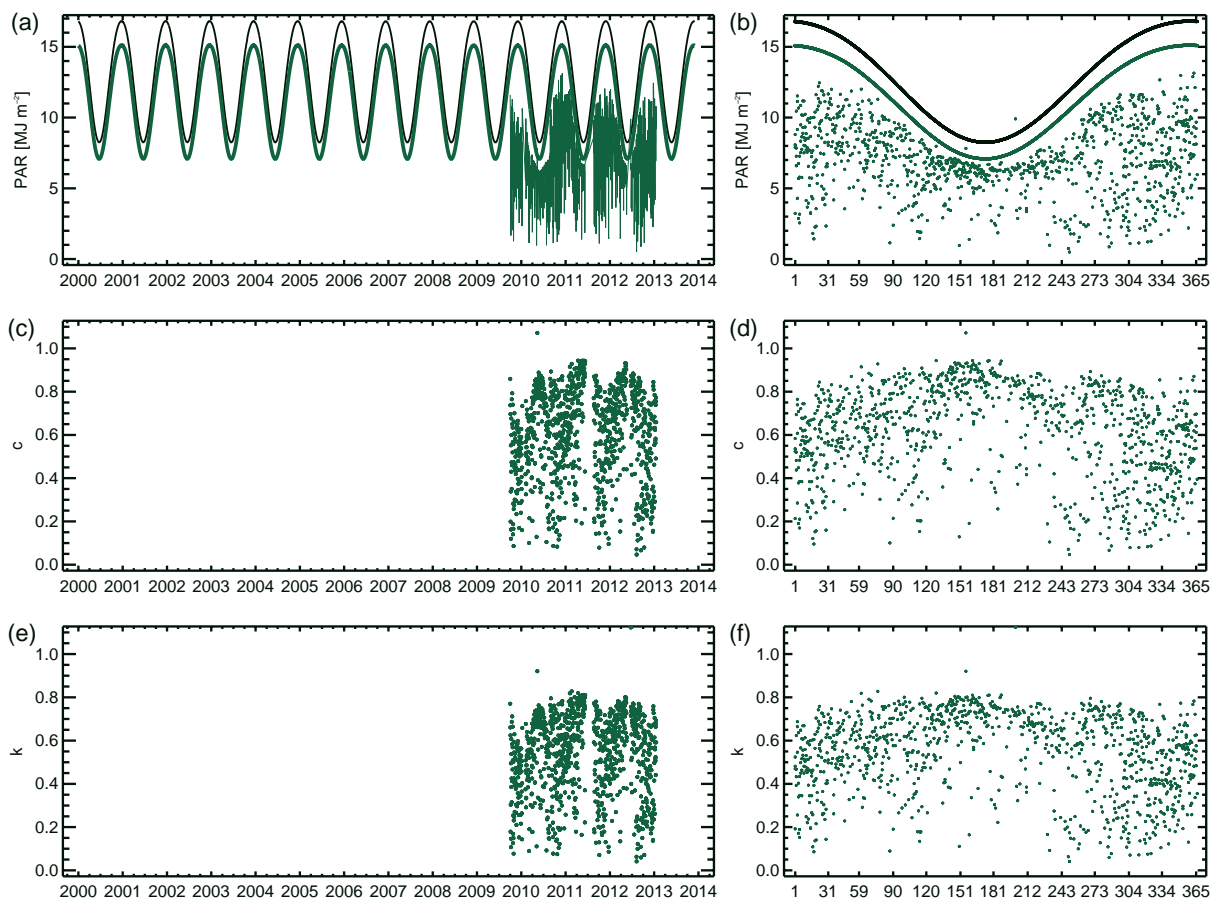
Figure S27. Time series, annual cycle, and autocorrelation function of PAR (a–c), c (d–f), and k (g–i) at US-SRM. Solid black and green lines in panels (a) and (b) indicate PAR_0 (no atmosphere), and PAR_{cda} (clean and dry atmosphere), respectively. Thin lines in (a), points in (b) and the ACF in (c) show PAR_{obs}. Dotted lines in the right panel indicates the 95% level of confidence.
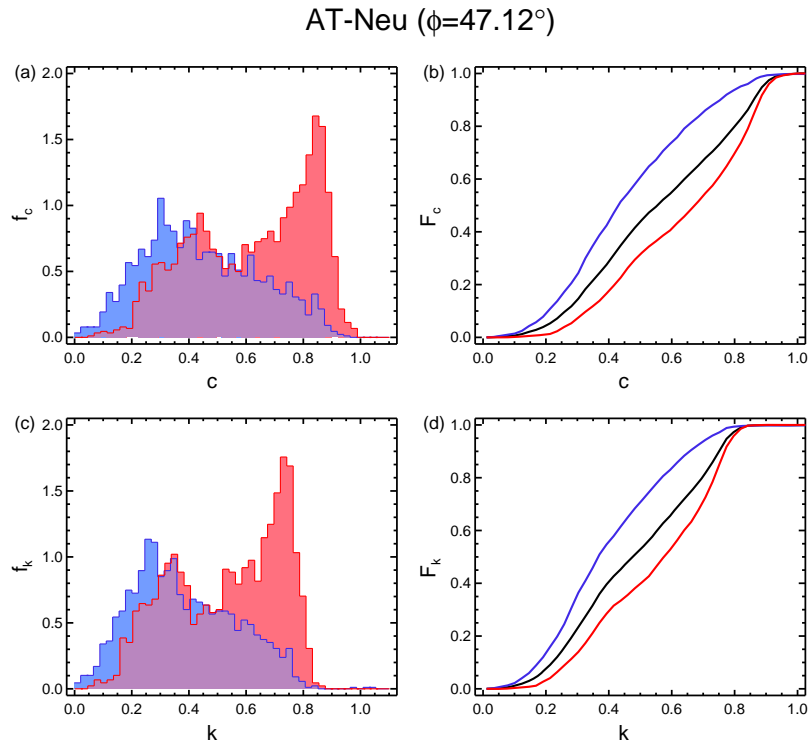
Figure S28. Time series, annual cycle, and autocorrelation function of PAR (a–c), c (d–f), and k (g–i) at ZA-Kru. Solid black and green lines in panels (a) and (b) indicate PAR_0 (no atmosphere), and PAR_{cda} (clean and dry atmosphere), respectively. Thin lines in (a), points in (b) and the ACF in (c) show PAR_{obs}. Dotted lines in the right panel indicates the 95% level of confidence.

AT-Neu (ϕ=47.12°)

Figure S29. PDFs and CDFs during wet days (blue) and dry (red) of (a-b) c and (c-d) k at AT-Neu.

BE-Lon (ϕ=50.55°)
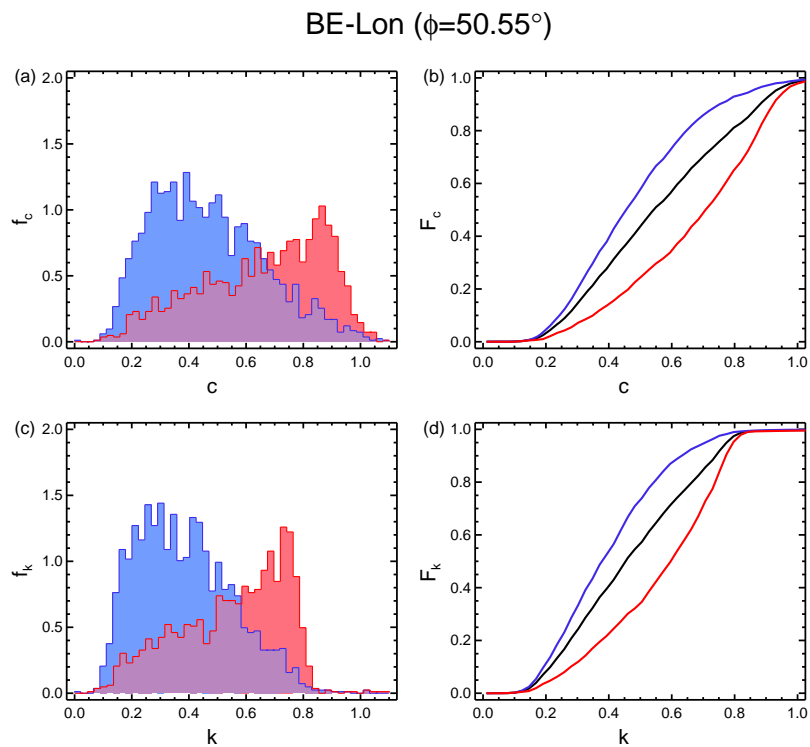
Figure S30. PDFs and CDFs during wet days (blue) and dry (red) of (a-b) c and (c-d) k at BE-Lon.

BE-Vie (φ=50.31°)
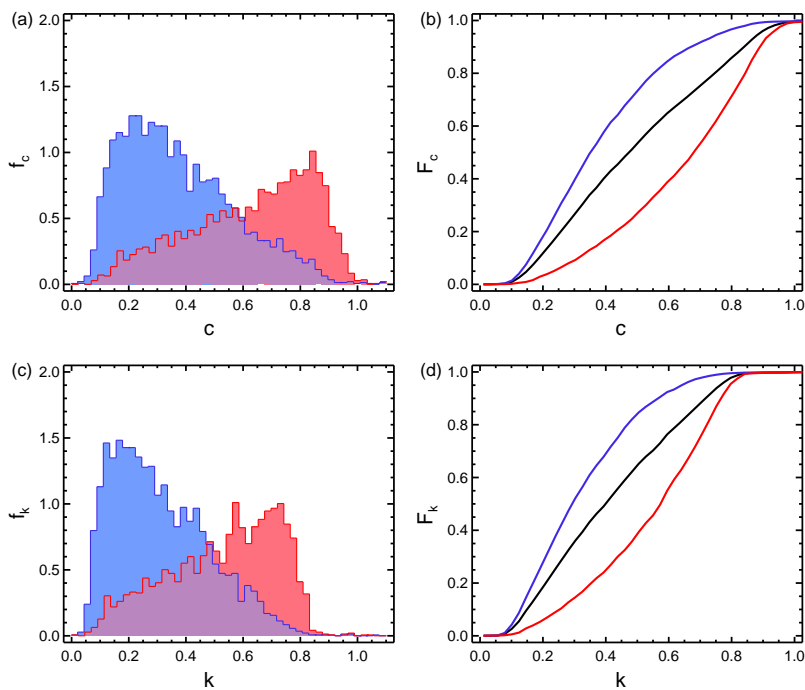
Figure S31. PDFs and CDF during wet days (blue) and dry (red) of (a-b) c and (c-d) k at BE-Vie.
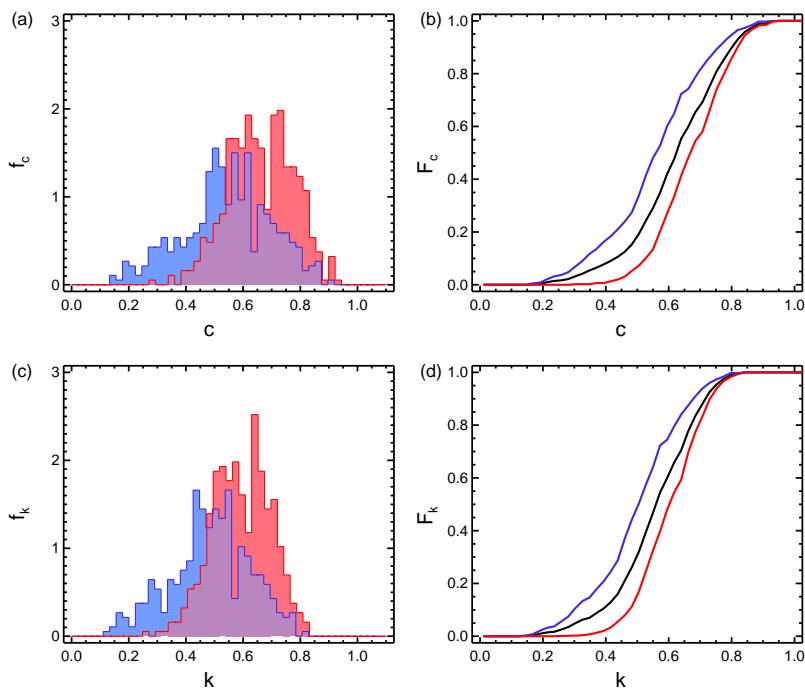
BR-Sa3 (φ= -3.02°)

Figure S32. PDFs and CDFs during wet days (blue) and dry (red) of (a-b) c and (c-d) k at BR-Sa3.

CA-Oas (φ=53.63°)
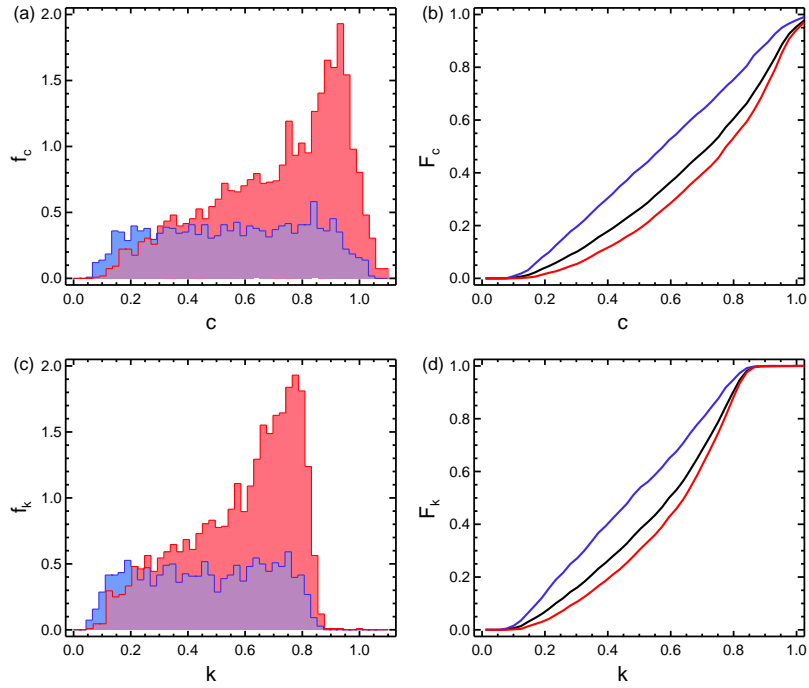
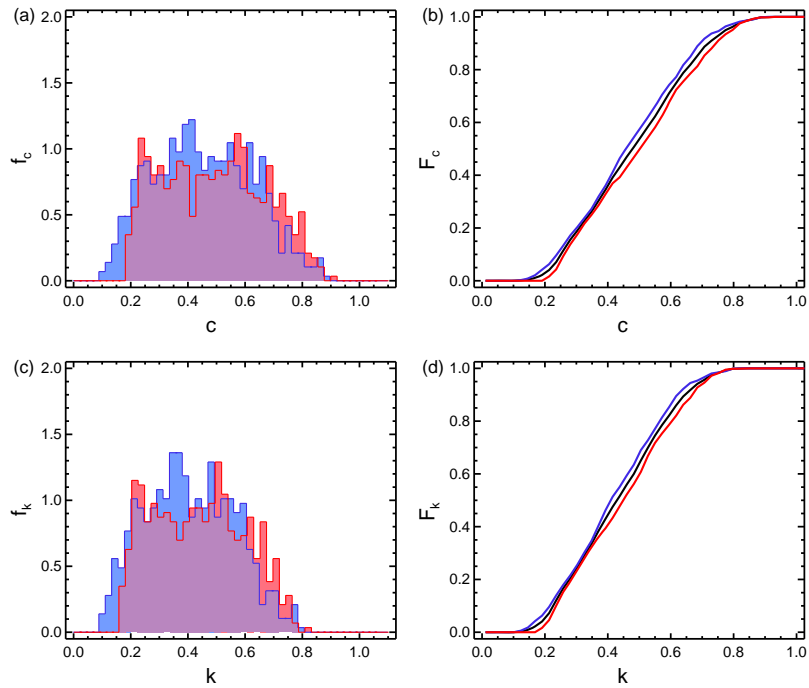**Figure S33.** PDFs and CDFs during wet days (blue) and dry (red) of (a-b) c and (c-d) k at CA-Oas.

CG-Tch (φ= -4.29°)

Figure S34. PDFs and CDFs during wet days (blue) and dry (red) of (a-b) c and (c-d) k at CG-Tch.

CH-Oe1 (φ=47.29°)
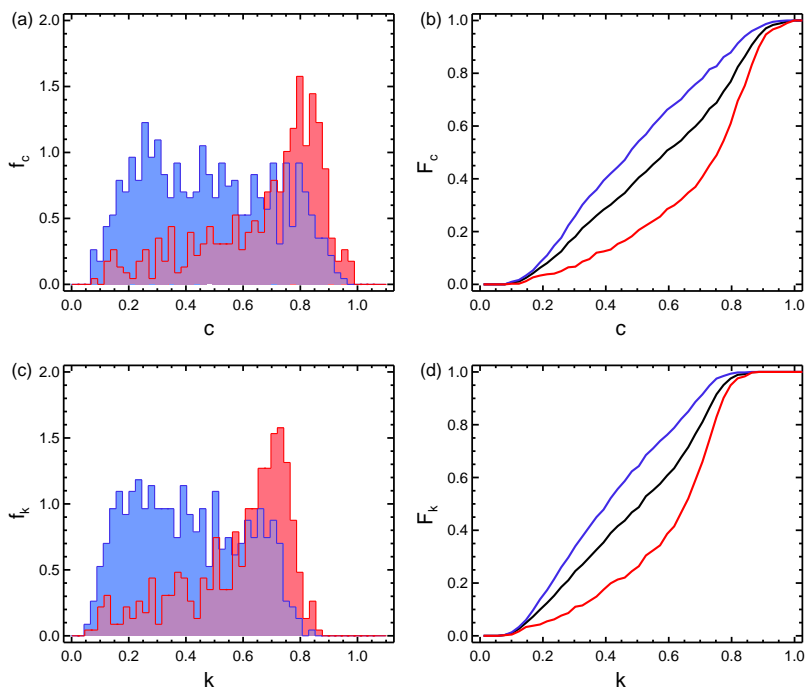
Figure S35. PDFs and CDFs during wet days (blue) and dry (red) of (a-b) c and (c-d) k at CH-Oe1.
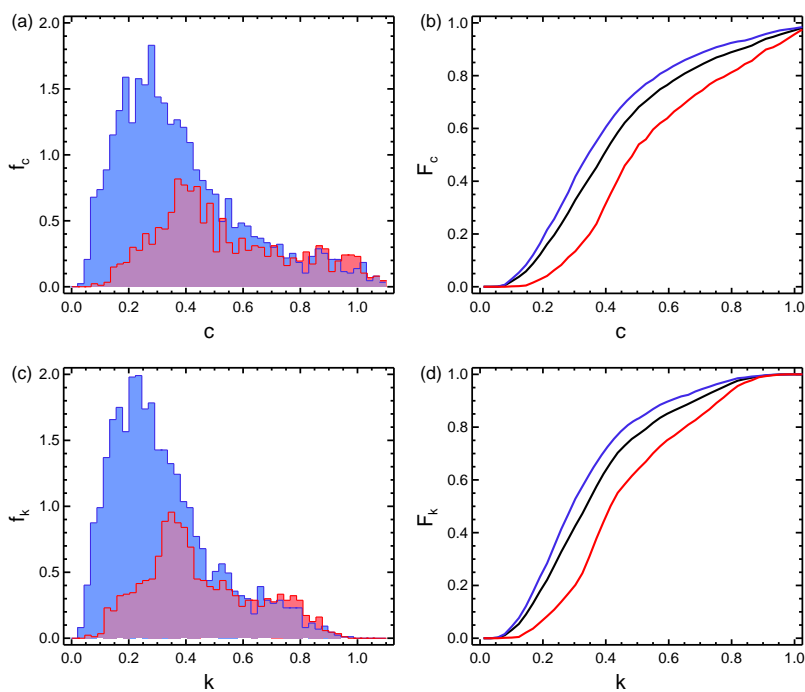
CH-Oe2 (φ=47.29°)

Figure S36. PDFs and CDFs during wet days (blue) and dry (red) of (a-b) c and (c-d) k at CH-Oe2.
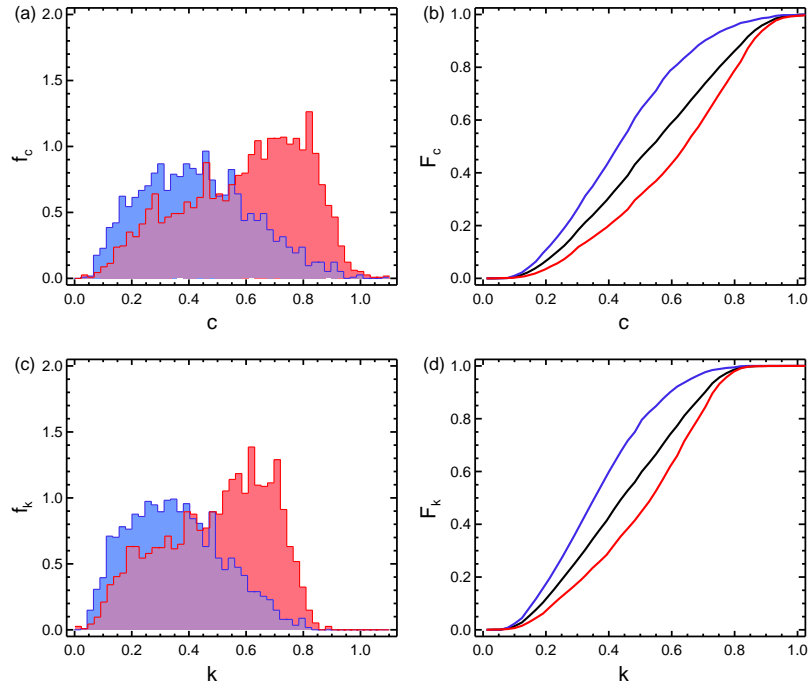
DE-Geb (ϕ=51.10°)

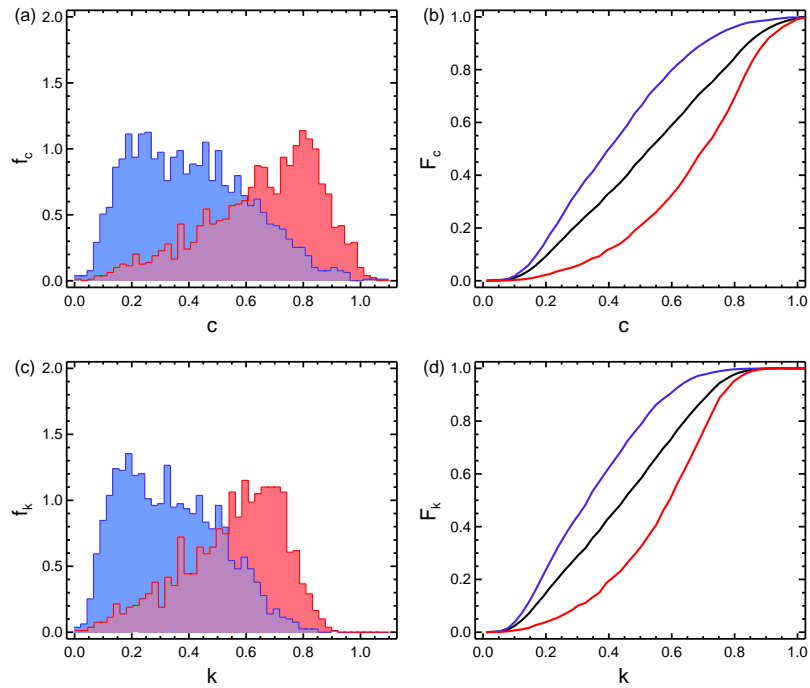**Figure S37.** PDFs and CDFs during wet days (blue) and dry (red) of (a-b) c and (c-d) k at DE-Geb.

DE-Gri (ϕ=50.95°)

Figure S38. PDFs and CDFs during wet days (blue) and dry (red) of (a-b) c and (c-d) k at DE-Gri.
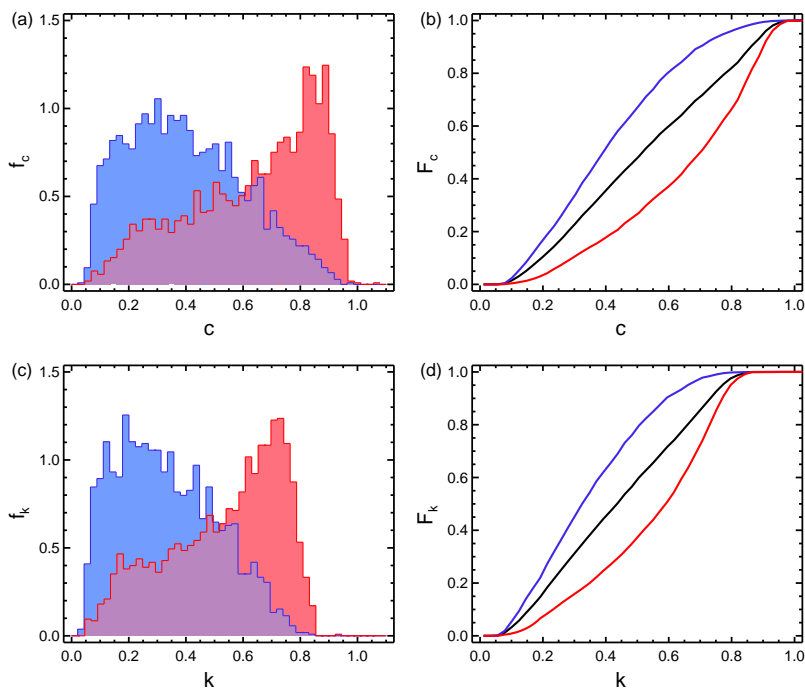
DE-Hai (φ=51.08°)

Figure S39. PDFs and CDFs during wet days (blue) and dry (red) of (a-b) c and (c-d) k at DE-Hai.

DE-Obe (φ=50.79°)
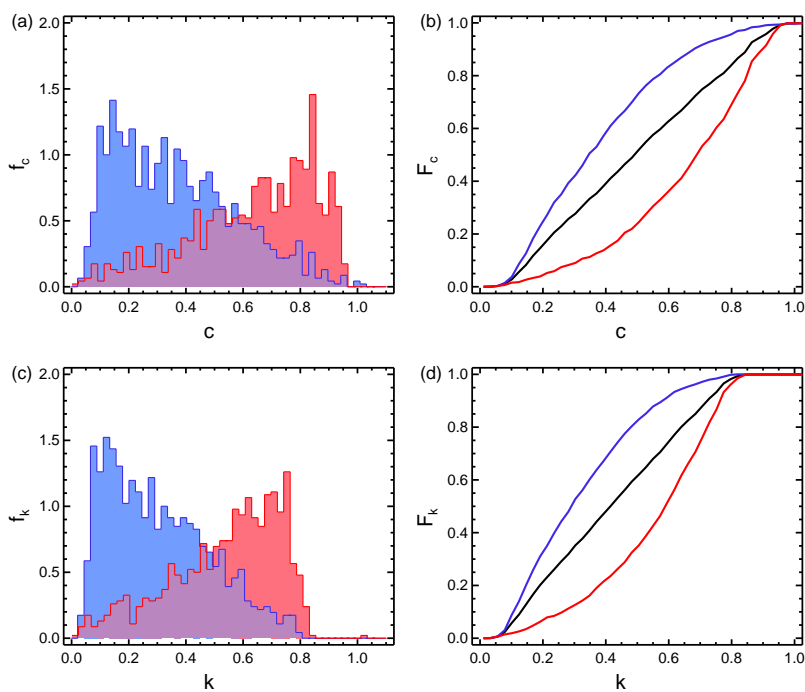
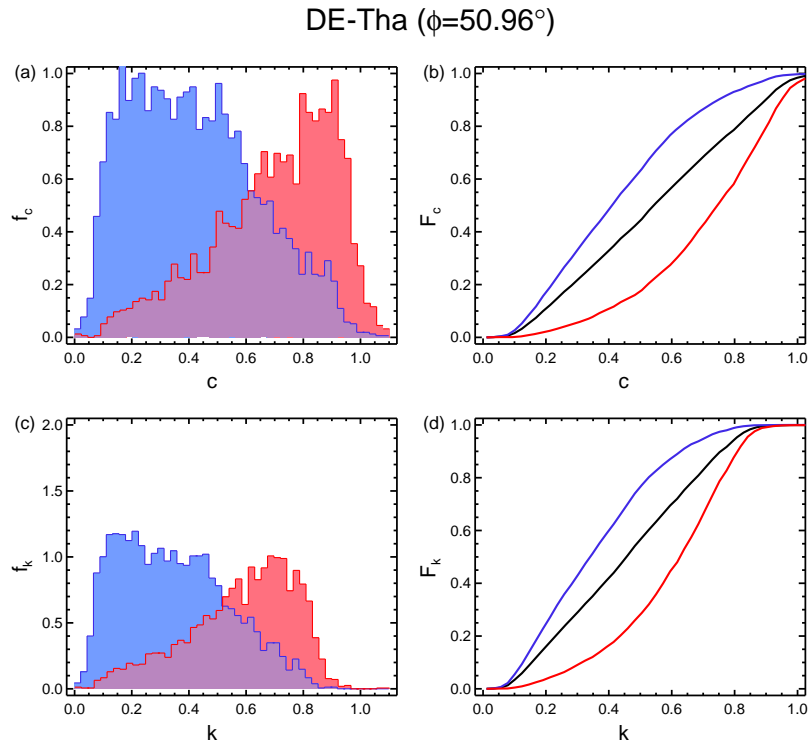**Figure S40.** PDFs and CDFs during wet days (blue) and dry (red) of (a-b) c and (c-d) k at DE-Obe.

DE-Tha (ϕ=50.96°)

Figure S41. PDFs and CDFs during wet days (blue) and dry (red) of (a-b) c and (c-d) k at DE-Tha.

GF-Guy (ϕ= 5.28°)

Figure S42. PDFs and CDFs during wet days (blue) and dry (red) of (a-b) c and (c-d) k at GF-Guy.

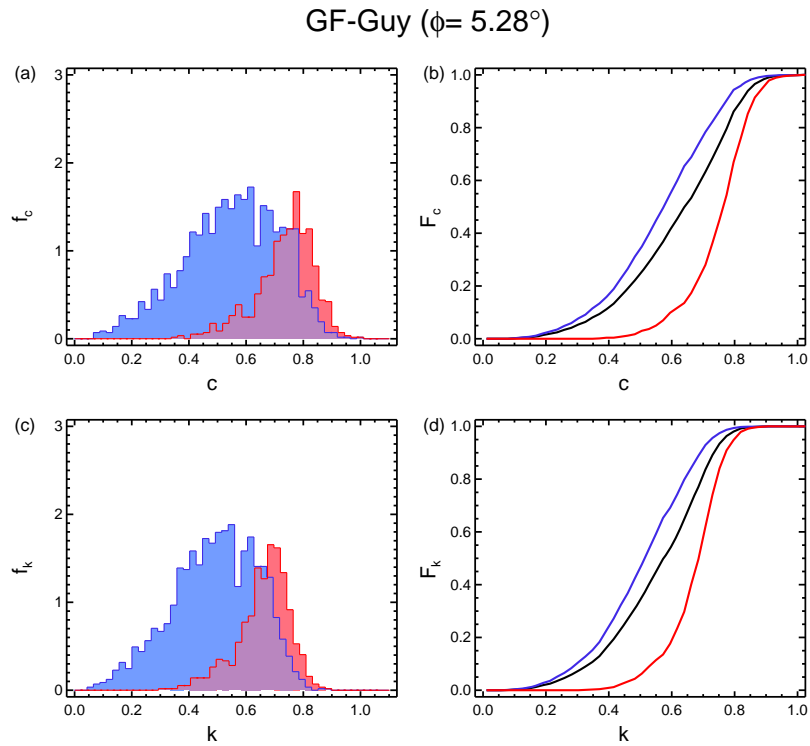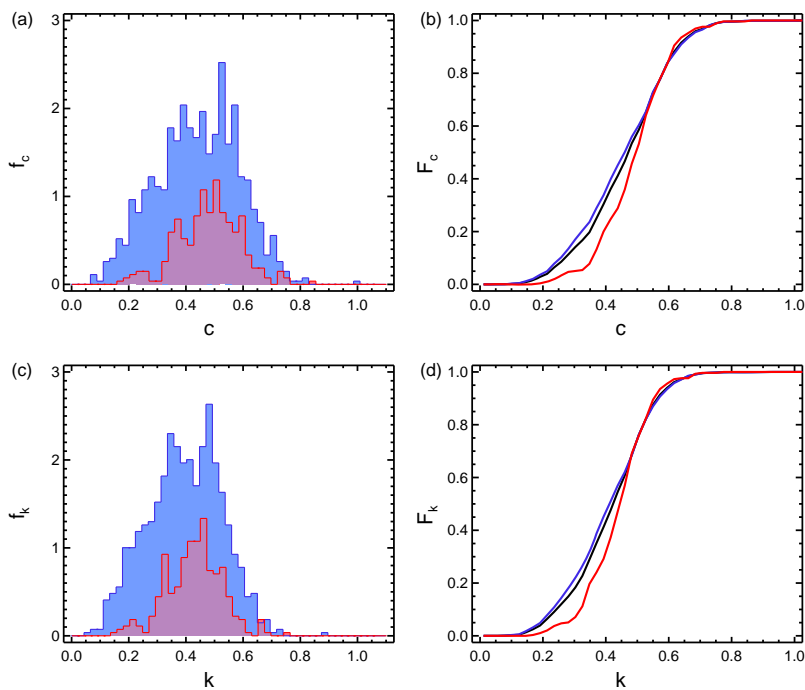**Figure S43.** PDFs and CDFs during wet days (blue) and dry (red) of (a-b) c and (c-d) k at GH-Ank.
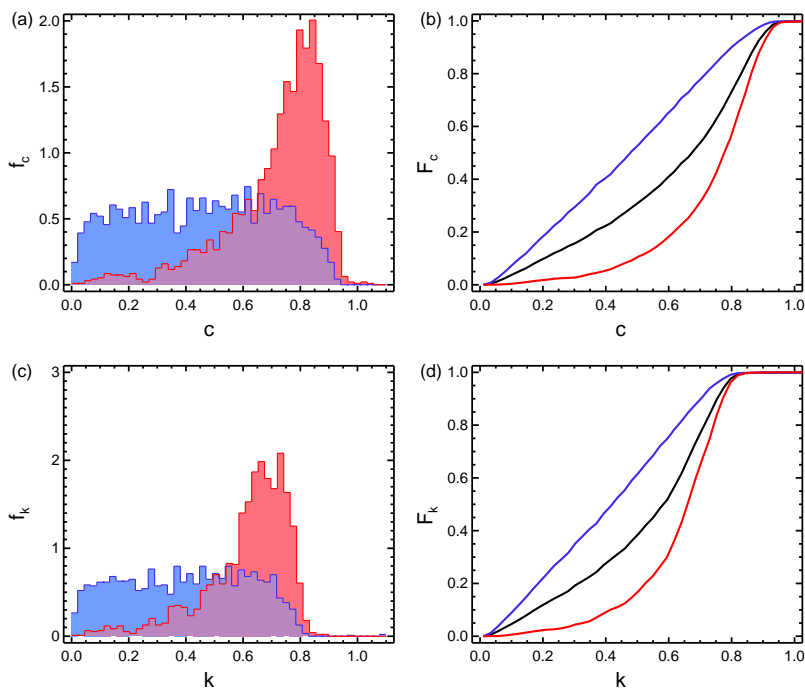

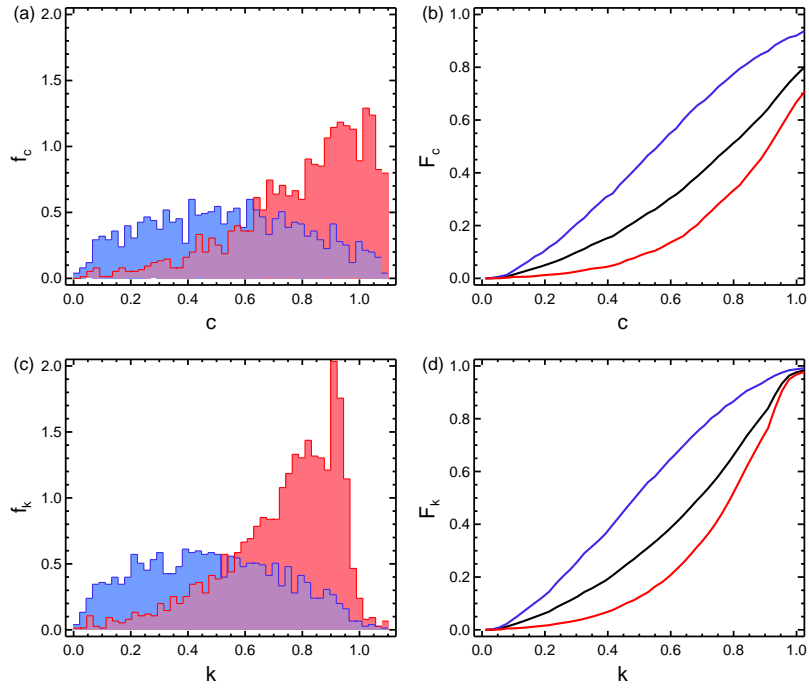**Figure S44.** PDFs and CDFs during wet days (blue) and dry (red) of (a-b) c and (c-d) k at IT-Lav.

IT-MBo (φ=46.01°)

Figure S45. PDFs and CDFs during wet days (blue) and dry (red) of (a-b) c and (c-d) k at IT-MBo.
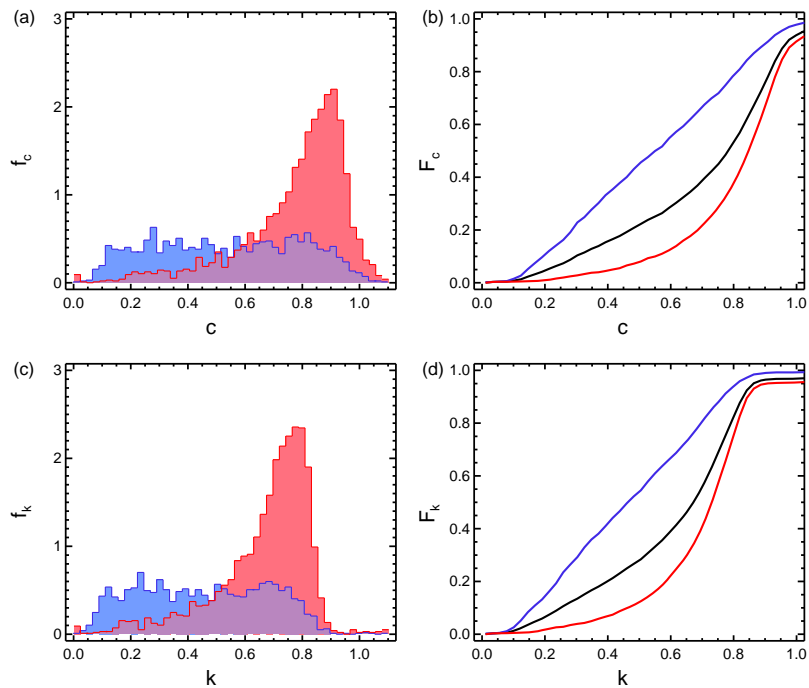
IT-SRo (φ=43.73°)

Figure S46. PDFs and CDFs during wet days (blue) and dry (red) of (a-b) c and (c-d) k at IT-SRo.

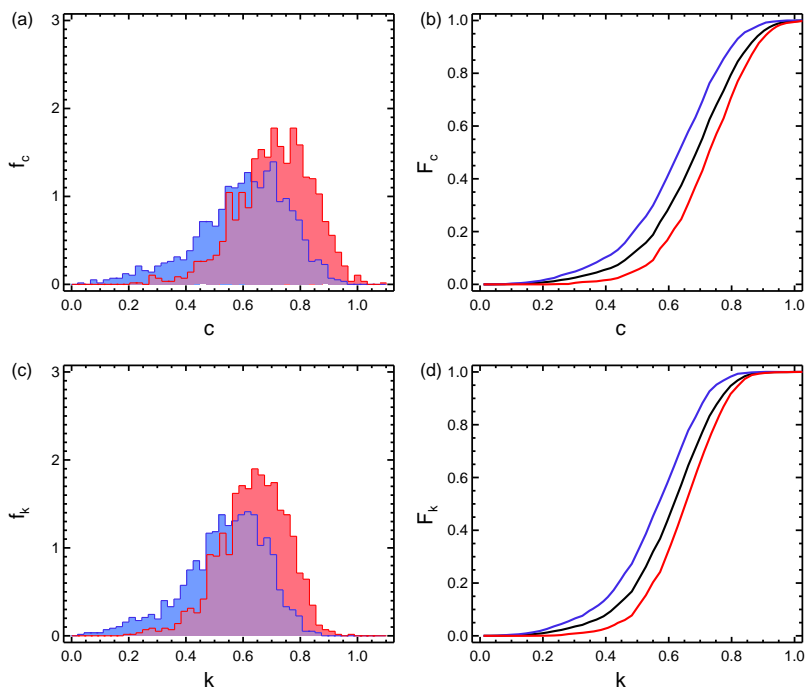## MY-PSO (ϕ = 2.97°)

Figure S47. PDFs and CDFs during wet days (blue) and dry (red) of (a-b) c and (c-d) k at MY-PSO.
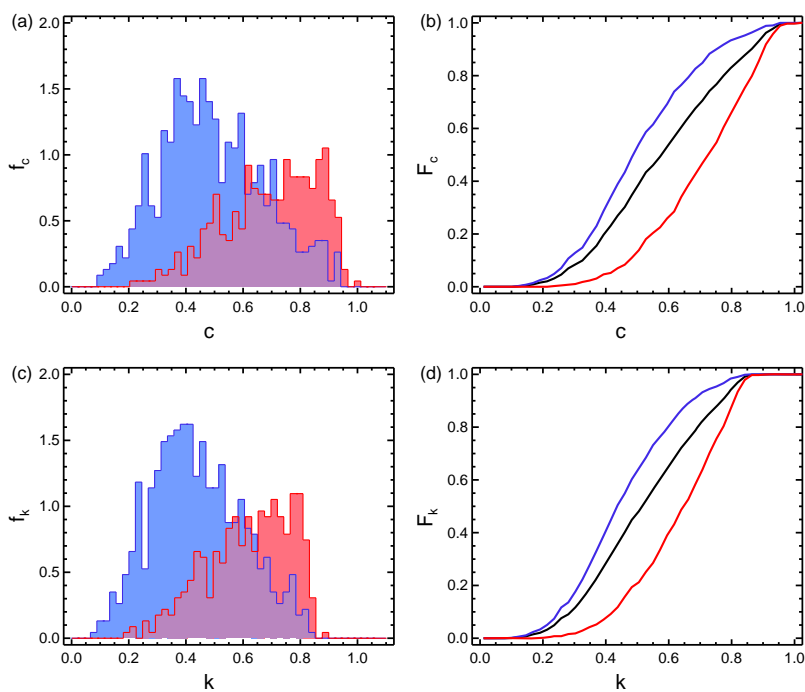
PA-SPs (ϕ = 9.31°)

Figure S48. PDFs and CDFs during wet days (blue) and dry (red) of (a-b) c and (c-d) k at PA-SPs.
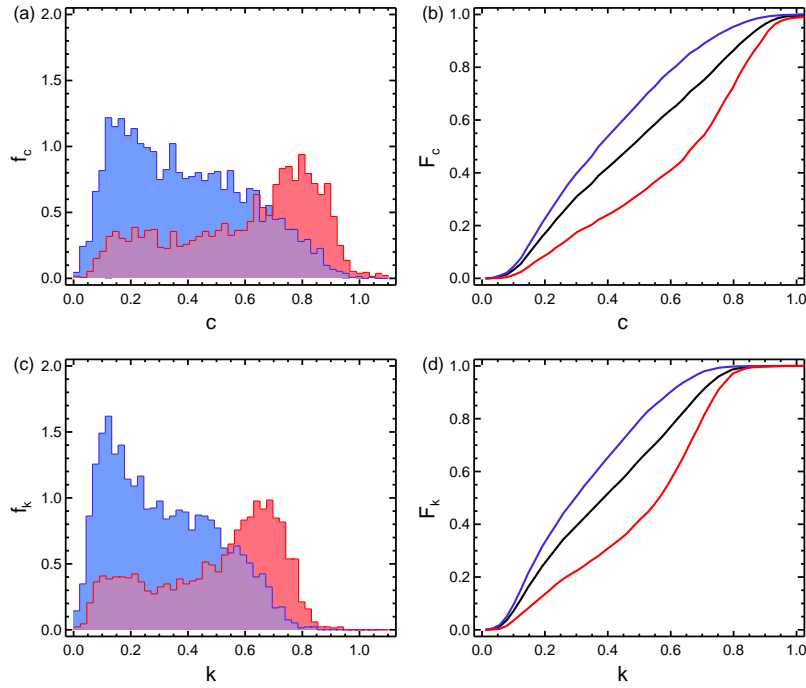
RU-Fyo (ϕ=56.46°)

Figure S49. PDFs and CDFs during wet days (blue) and dry (red) of (a-b) c and (c-d) k at RU-Fyo.
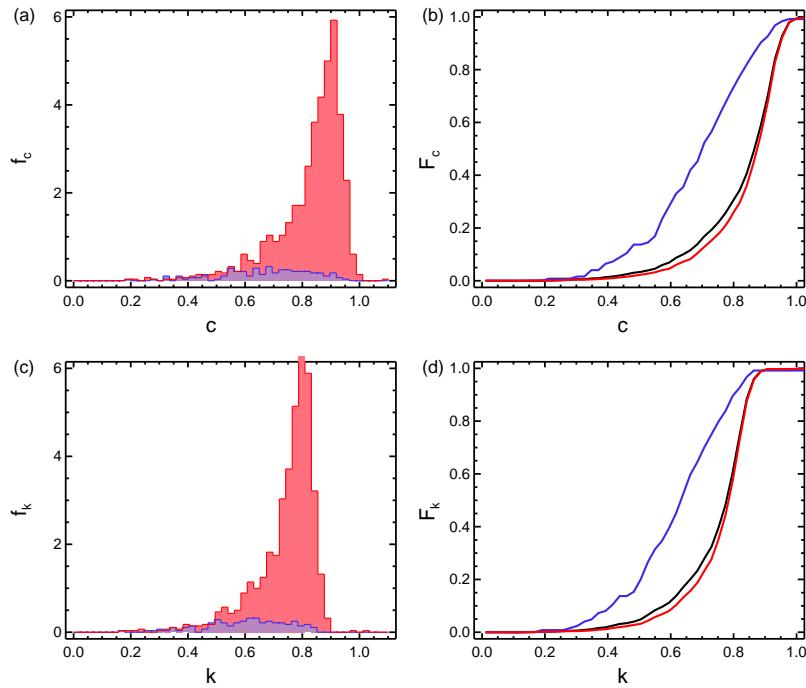
SD-Dem (ϕ=13.28°)

Figure S50. PDFs and CDFs during wet days (blue) and dry (red) of (a-b) c and (c-d) k at SD-Dem.
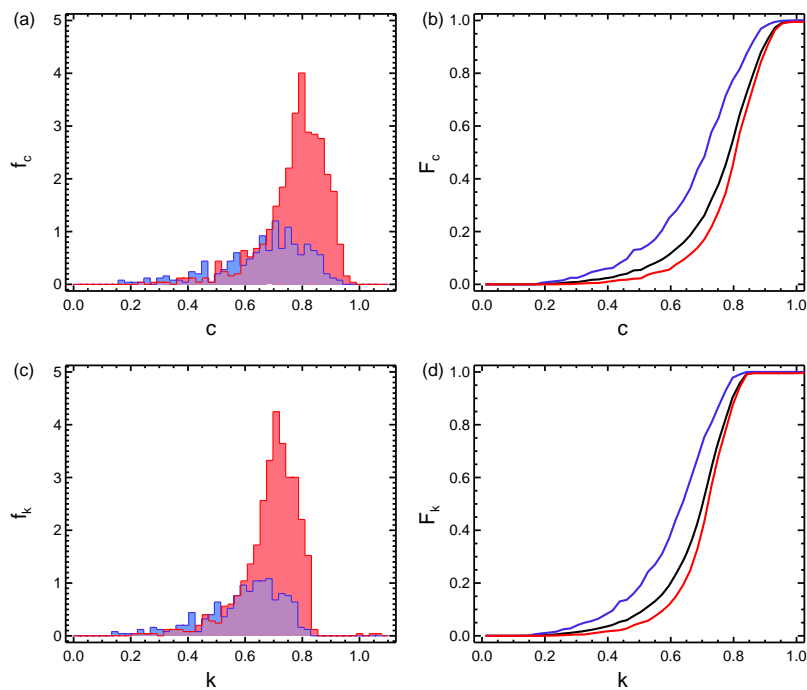
SN-Dhr (φ=15.40°)

Figure S51. PDFs and CDFs during wet days (blue) and dry (red) of (a-b) c and (c-d) k at SN-Dhr.
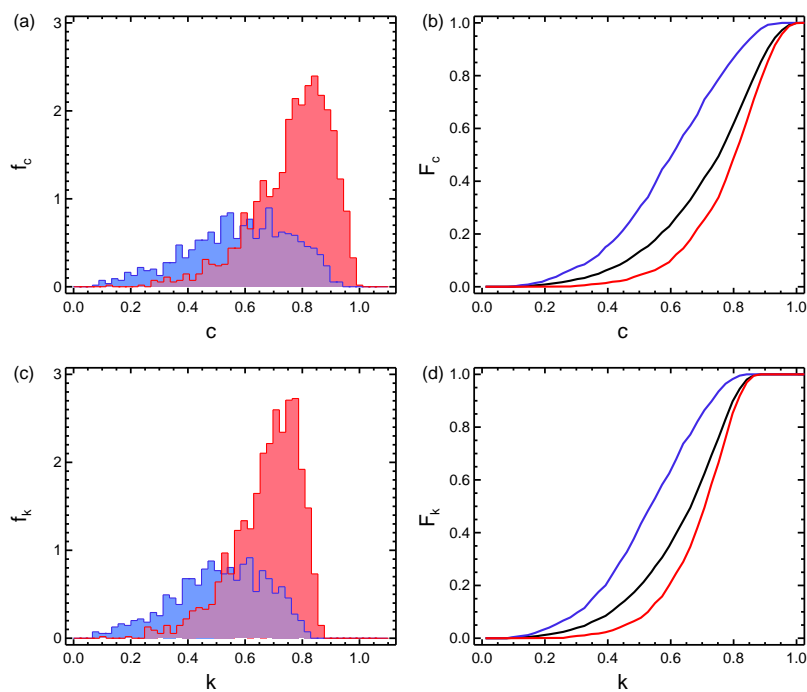
US-Esm (φ=25.44°)

Figure S52. PDFs and CDFs during wet days (blue) and dry (red) of (a-b) c and (c-d) k at US-Esm.
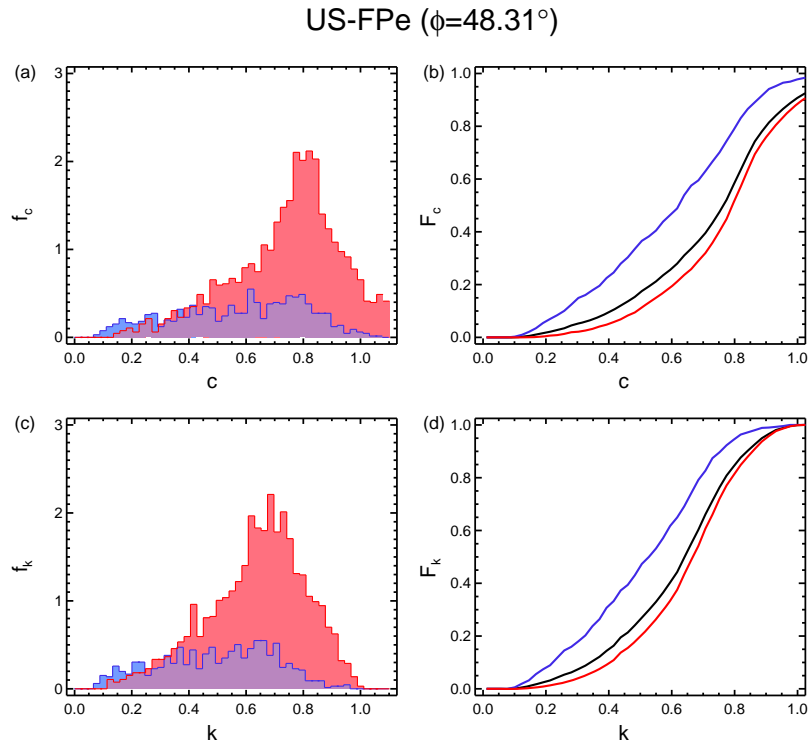
US-FPe (φ=48.31°)

Figure S53. PDFs and CDFs during wet days (blue) and dry (red) of (a-b) c and (c-d) k at US-FPe.
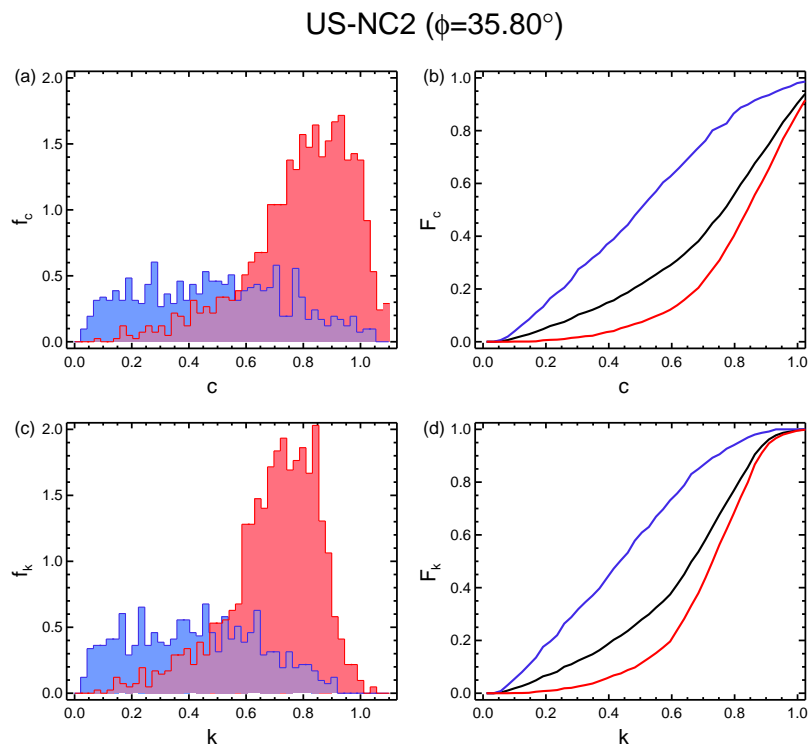
US-NC2 (φ=35.80°)

Figure S54. PDFs and CDFs during wet days (blue) and dry (red) of (a-b) c and (c-d) k at US-NC2.
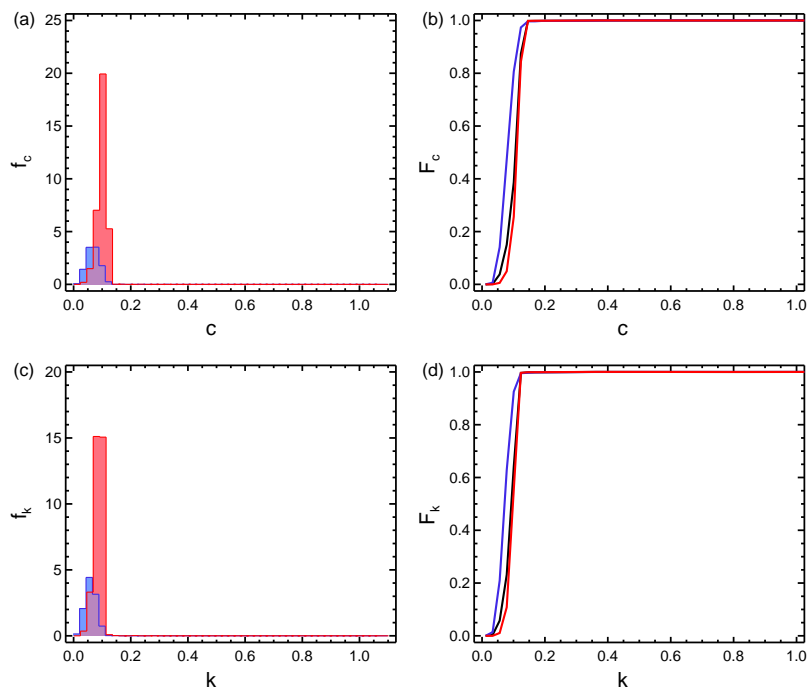
US-SRM (ϕ=31.82°)

Figure S55. PDFs and CDFs during wet days (blue) and dry (red) of (a-b) c and (c-d) k at US-SRM.
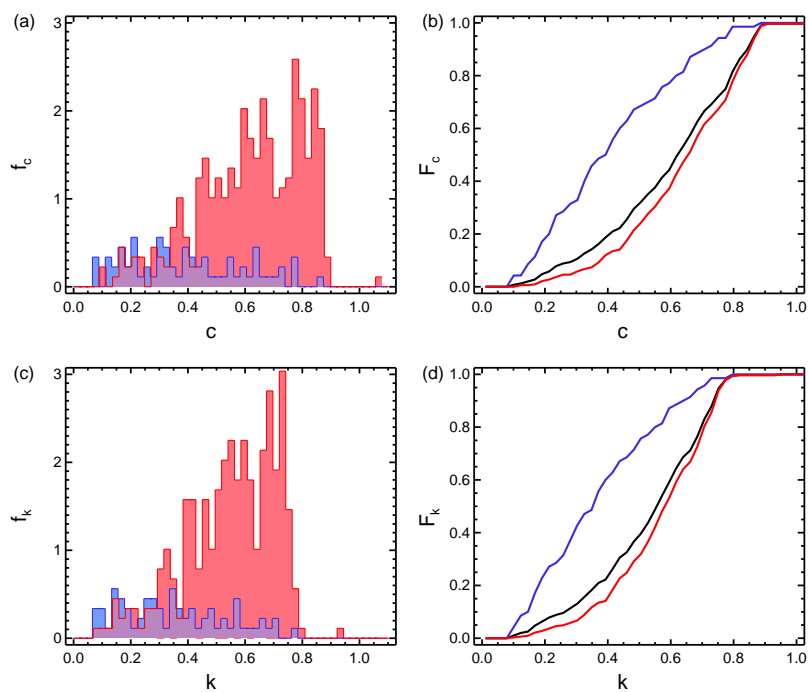
ZA-Kru (ϕ=31.82°)

Figure S56. PDFs and CDFs during wet days (blue) and dry (red) of (a-b) c and (c-d) k at ZA-Kru.

Figure S57. Monthly CDFs of (a) c, and (b) k. (c-j) p-value of the 2-sample KS and AD tests applied to all combinations of monthly CDF of c and k during wet (blue) and dry (red) days at AT-Neu.
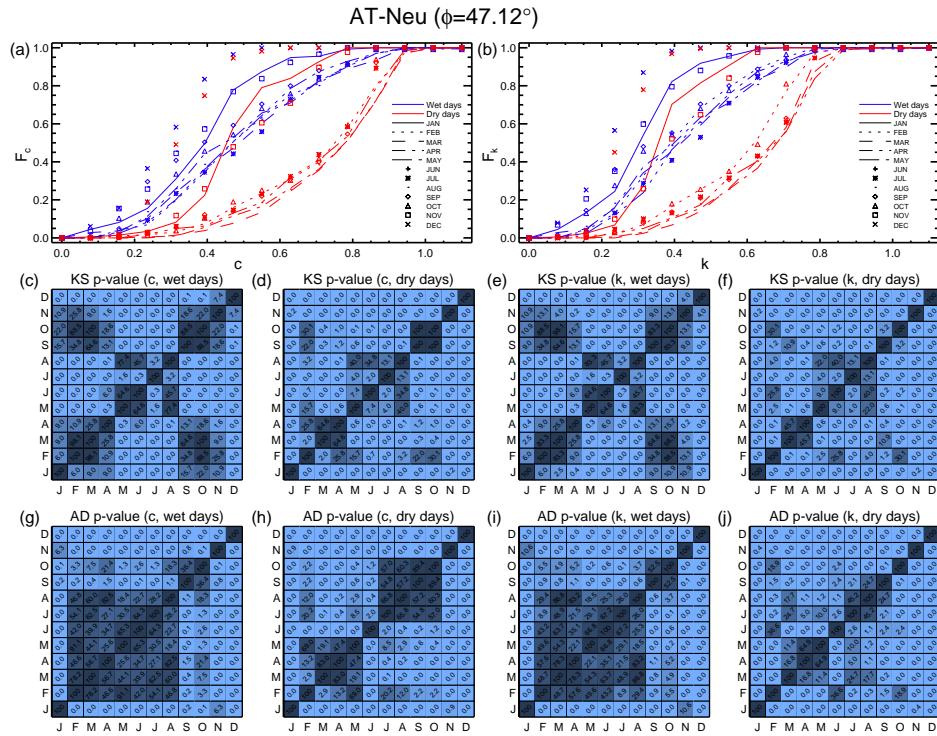

Figure S58. Monthly CDFs of (a) c, and (b) k. (c-j) p-value of the 2-sample KS and AD tests applied to all combinations of monthly CDF of c and k during wet (blue) and dry (red) days at BE-Lon.

Figure S59. Monthly CDFs of (a) c, and (b) k. (c-j) p-value of the 2-sample KS and AD tests applied to all combinations of monthly CDF of c and k during wet (blue) and dry (red) days at BE-Vie.
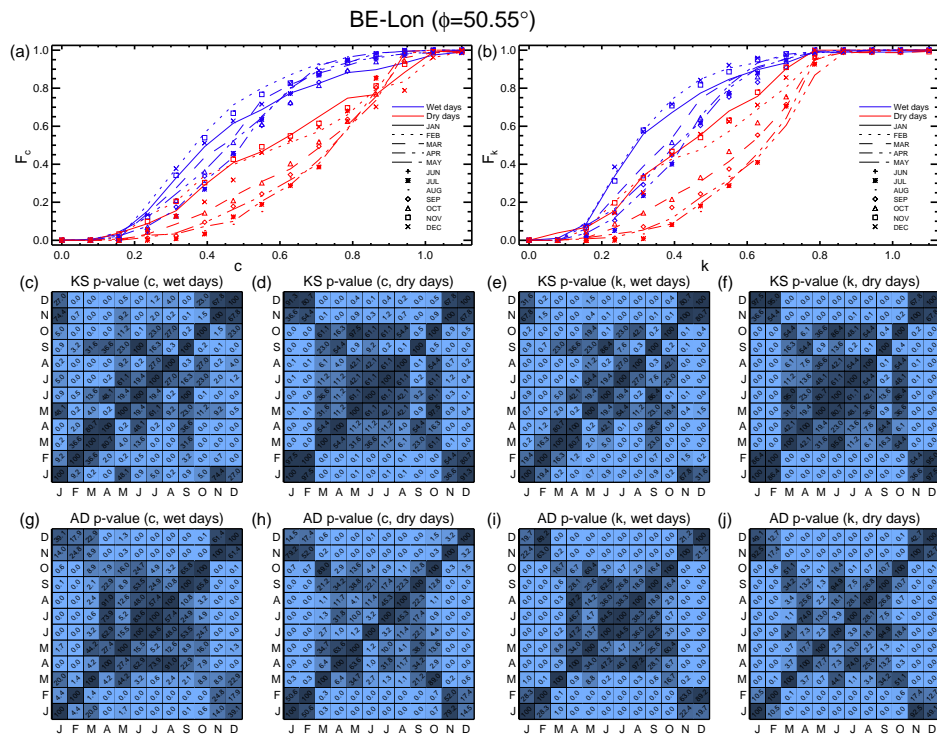

Figure S60. Monthly CDFs of (a) c, and (b) k. (c-j) p-value of the 2-sample KS and AD tests applied to all combinations of monthly CDF of c and k during wet (blue) and dry (red) days at BR-Sa3.
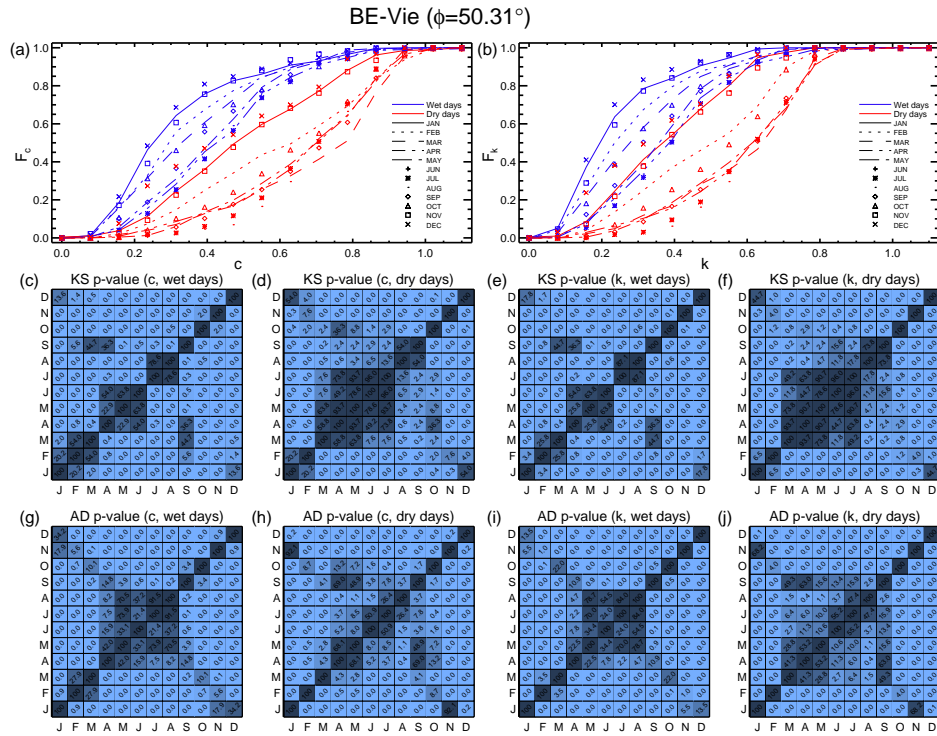
Figure S61. Monthly CDFs of (a) c, and (b) k. (c-j) p-value of the 2-sample KS and AD tests applied to all combinations of monthly CDF of c and k during wet (blue) and dry (red) days at CA-Oas.
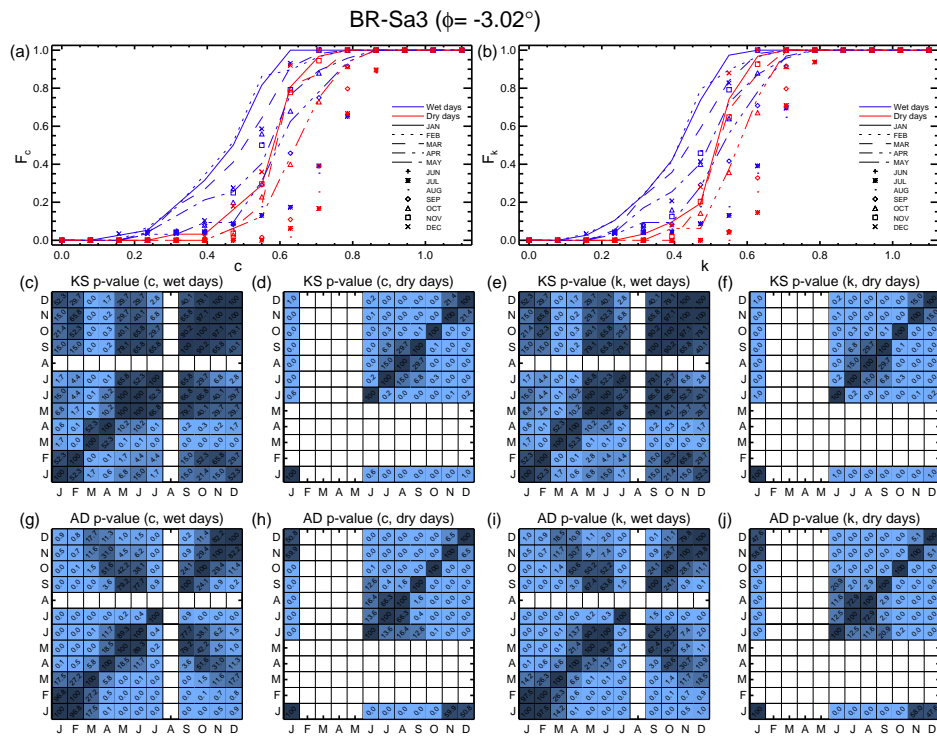

Figure S62. Monthly CDFs of (a) c, and (b) k. (c-j) p-value of the 2-sample KS and AD tests applied to all combinations of monthly CDF of c and k during wet (blue) and dry (red) days at CG-Tch.
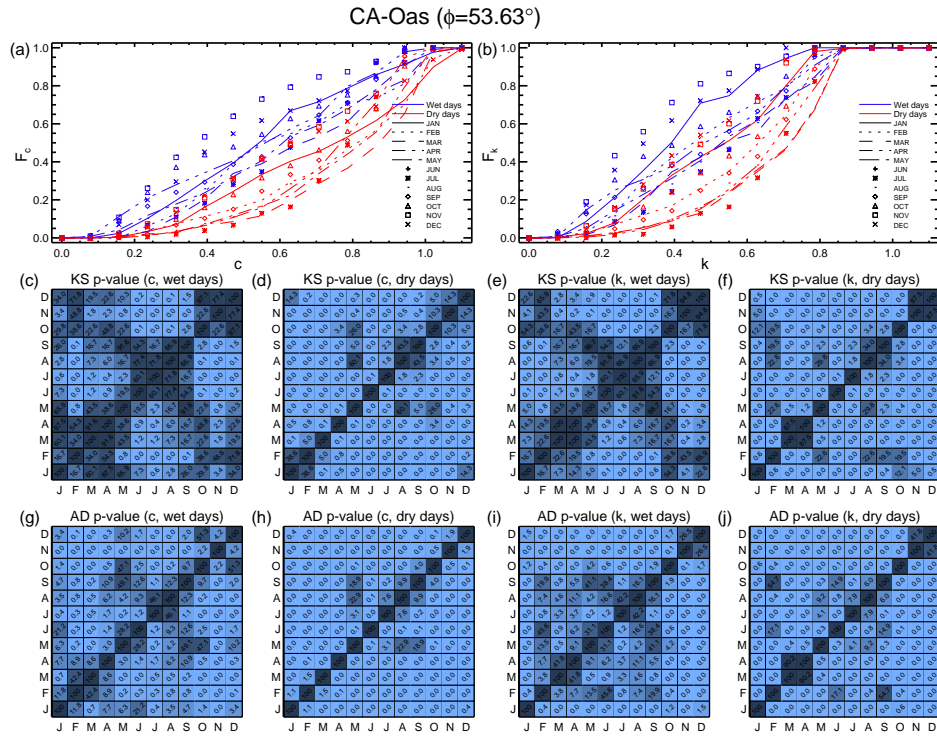
Figure S63. Monthly CDFs of (a) c, and (b) k. (c-j) p-value of the 2-sample KS and AD tests applied to all combinations of monthly CDF of c and k during wet (blue) and dry (red) days at CH-Oe1.
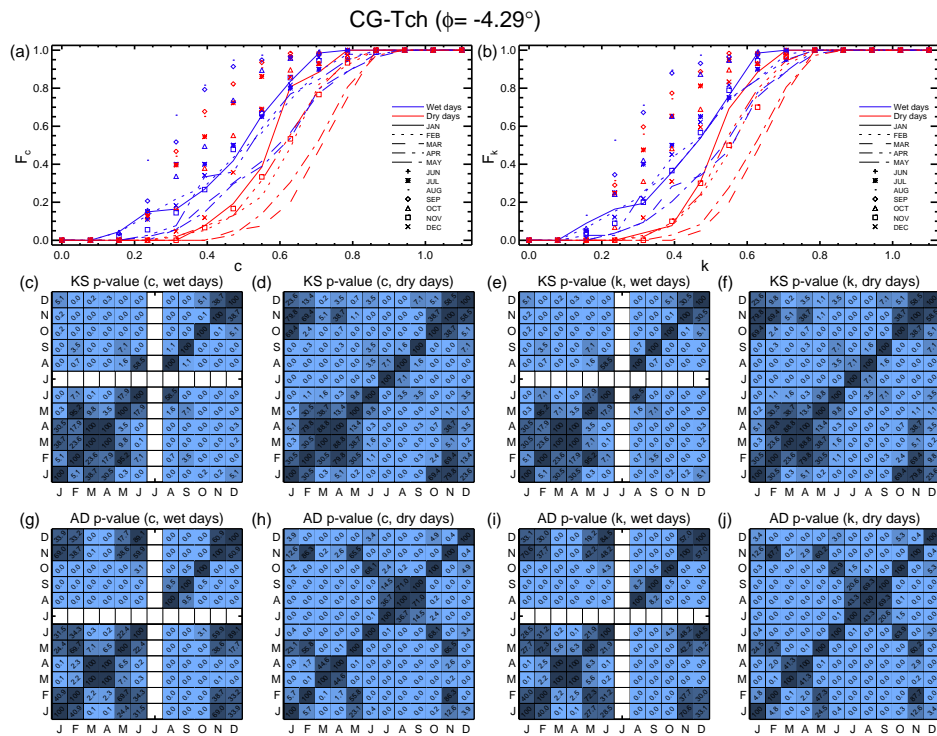

Figure S64. Monthly CDFs of (a) c, and (b) k. (c-j) p-value of the 2-sample KS and AD tests applied to all combinations of monthly CDF of c and k during wet (blue) and dry (red) days at CH-Oe2.
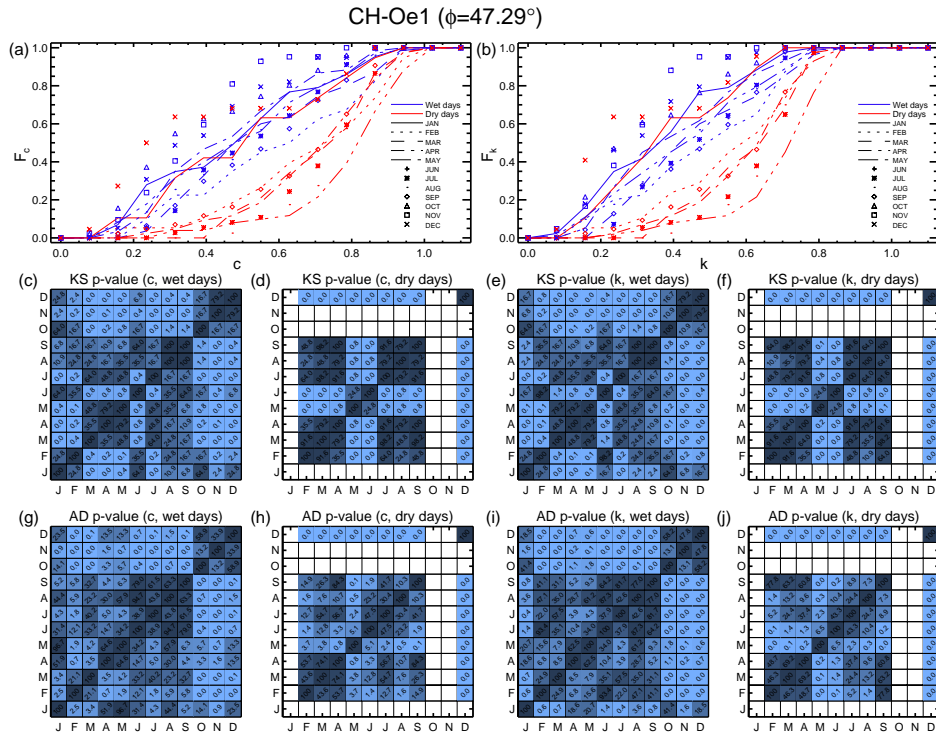
DE-Geb (ɸ=51.10°)

Figure S65. Monthly CDFs of (a) c, and (b) k. (c-j) p-value of the 2-sample KS and AD tests applied to all combinations of monthly CDF of c and k during wet (blue) and dry (red) days at DE-Geb.
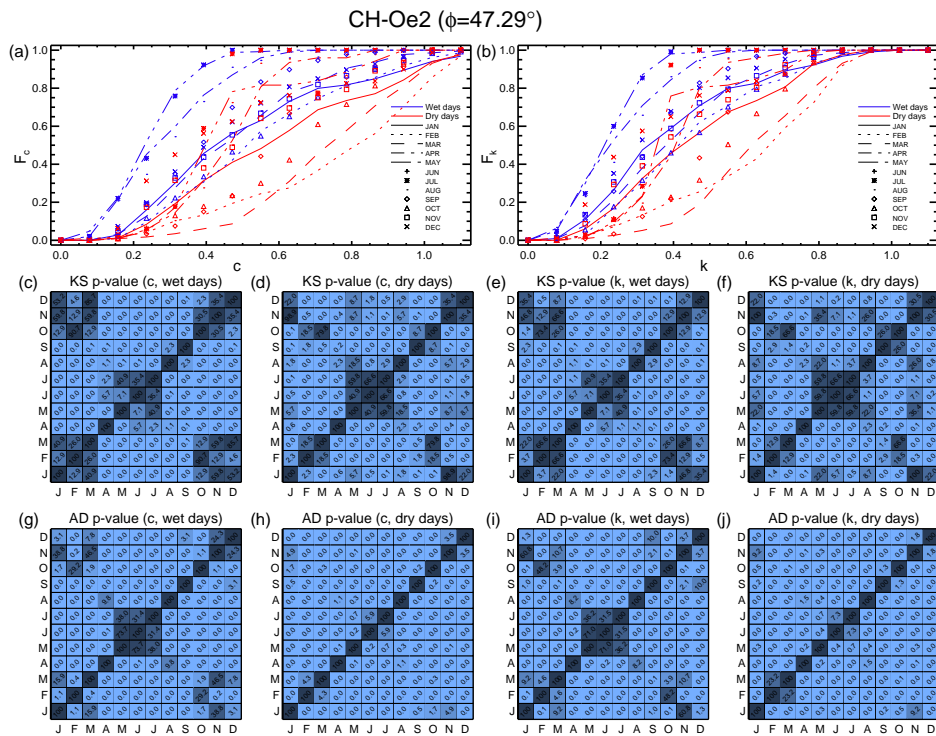
DE-Gri (ɸ=50.95°)

Figure S66. Monthly CDFs of (a) c, and (b) k. (c-j) p-value of the 2-sample KS and AD tests applied to all combinations of monthly CDF of c and k during wet (blue) and dry (red) days at DE-Gri.
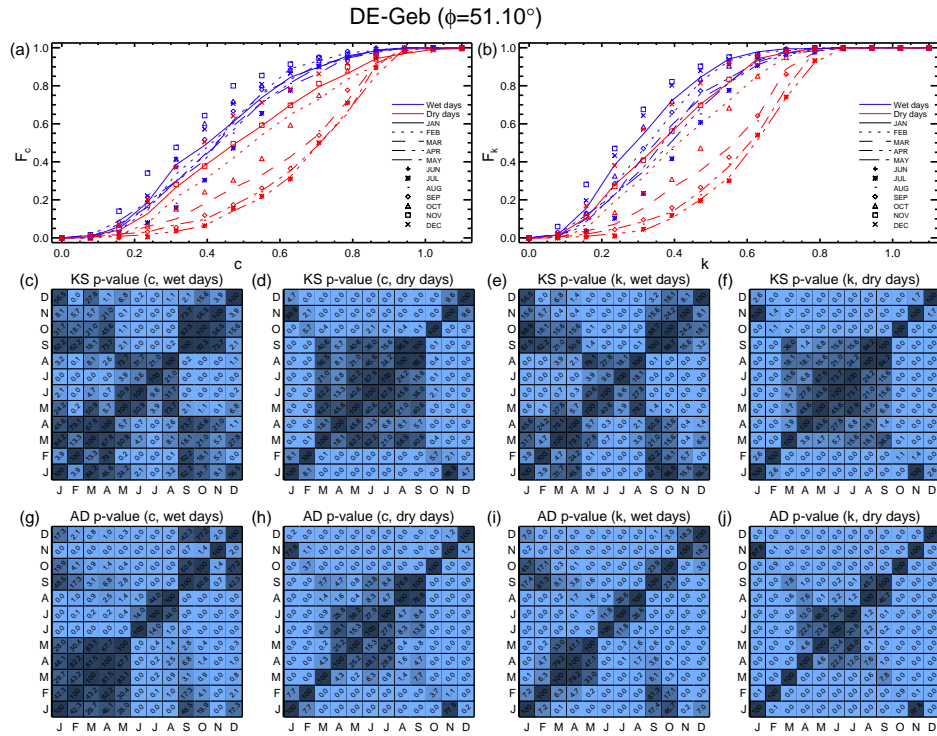
Figure S67. Monthly CDFs of (a) c, and (b) k. (c-j) p-value of the 2-sample KS and AD tests applied to all combinations of monthly CDF of c and k during wet (blue) and dry (red) days at DE-Hai.
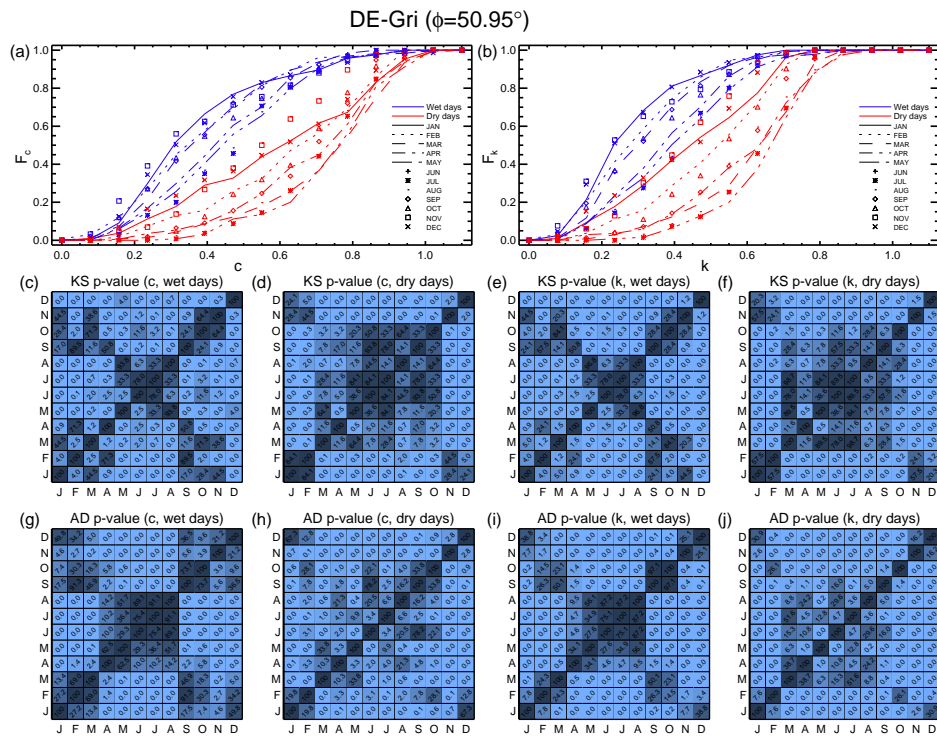

Figure S68. Monthly CDFs of (a) c, and (b) k. (c-j) p-value of the 2-sample KS and AD tests applied to all combinations of monthly CDF of c and k during wet (blue) and dry (red) days at DE-Obe.
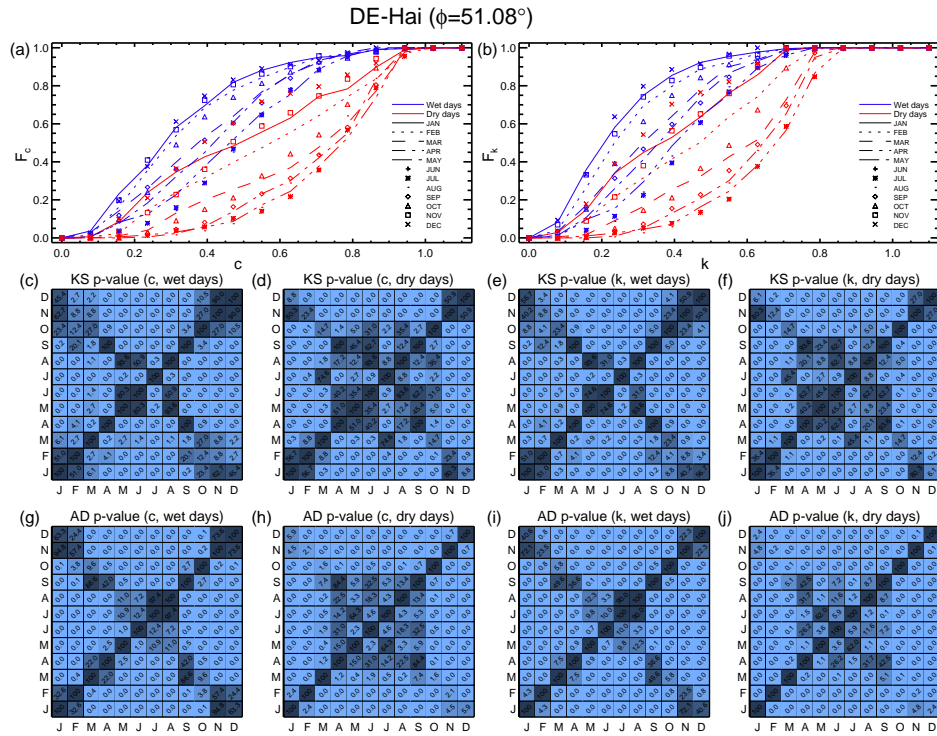
Figure S69. Monthly CDFs of (a) c, and (b) k. (c-j) p-value of the 2-sample KS and AD tests applied to all combinations of monthly CDF of c and k during wet (blue) and dry (red) days at DE-Tha.
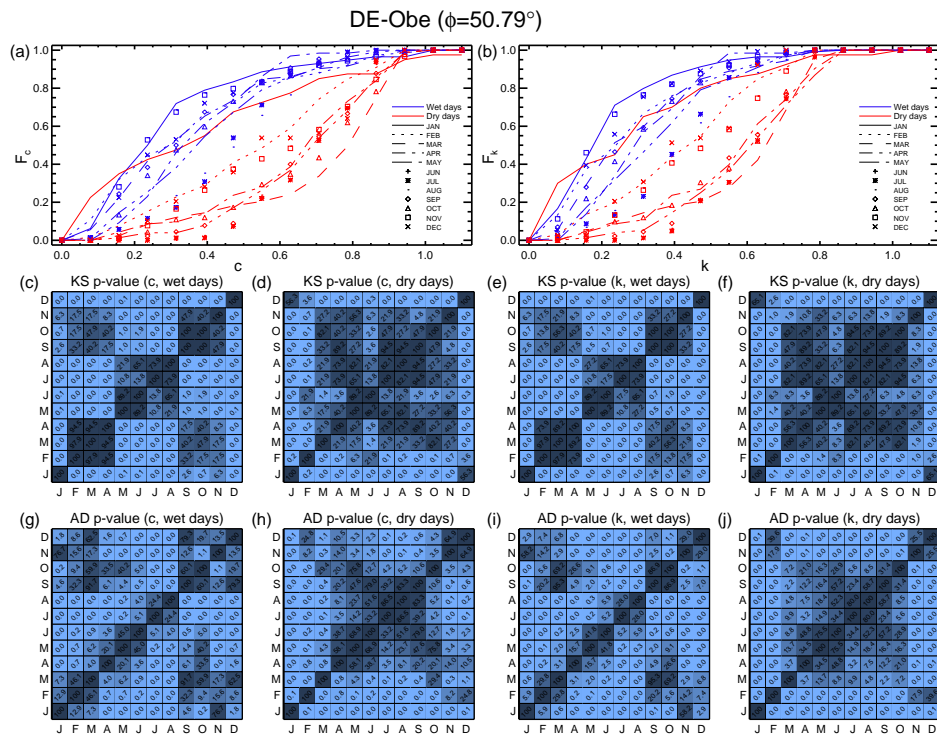

Figure S70. Monthly CDFs of (a) c, and (b) k. (c-j) p-value of the 2-sample KS and AD tests applied to all combinations of monthly CDF of c and k during wet (blue) and dry (red) days at GF-Guy.
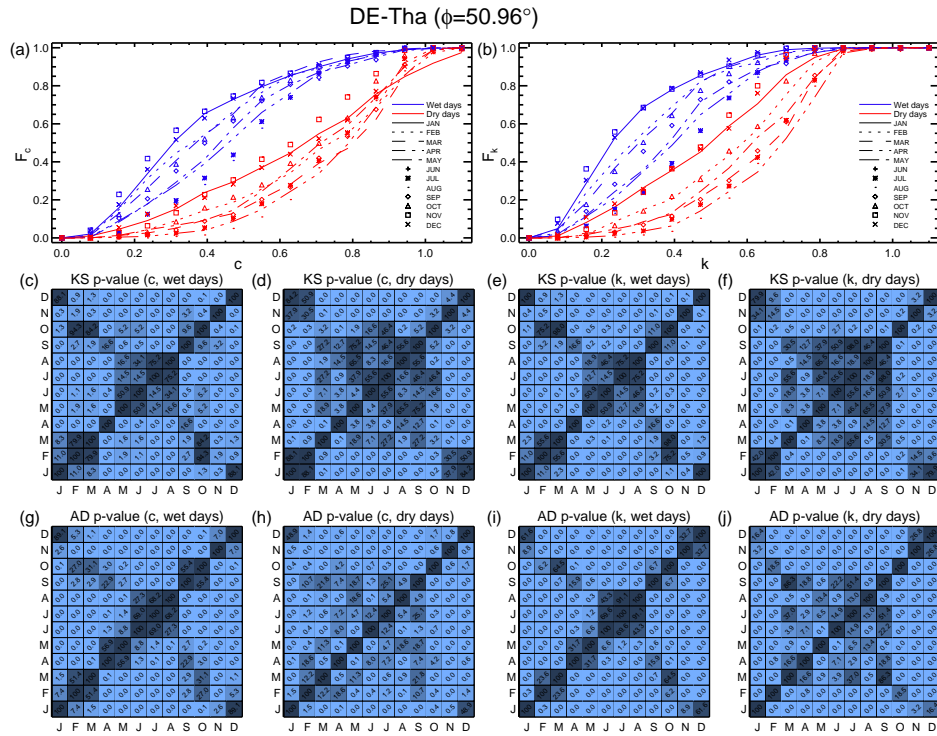
Figure S71. Monthly CDFs of (a) c, and (b) k. (c-j) p-value of the 2-sample KS and AD tests applied to all combinations of monthly CDF of c and k during wet (blue) and dry (red) days at GH-Ank.
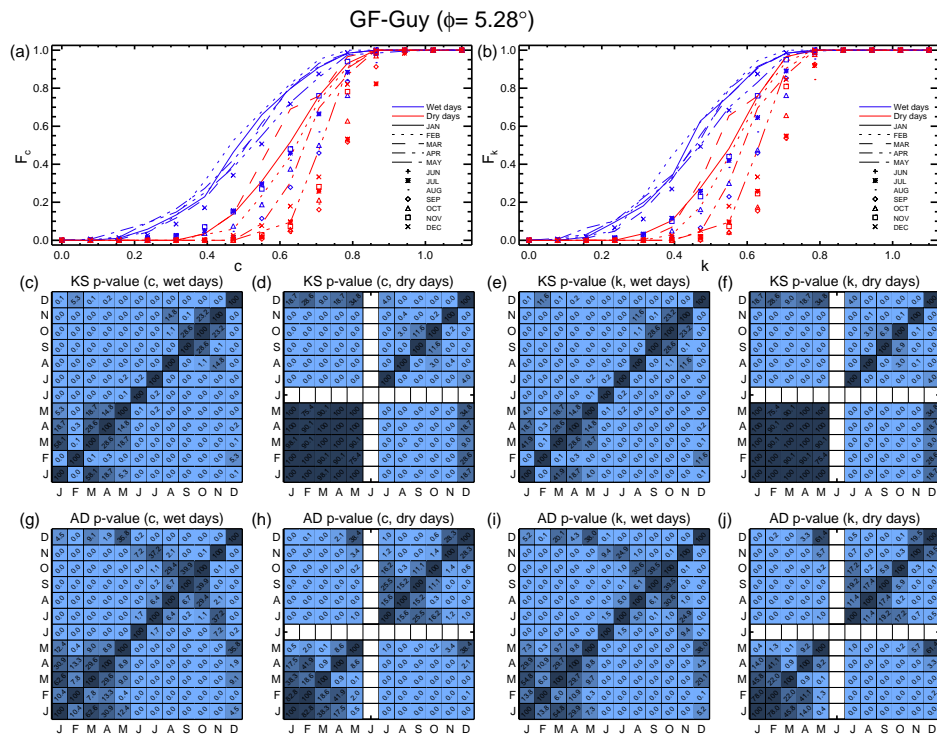

Figure S72. Monthly CDFs of (a) c, and (b) k. (c-j) p-value of the 2-sample KS and AD tests applied to all combinations of monthly CDF of c and k during wet (blue) and dry (red) days at IT-Lav.
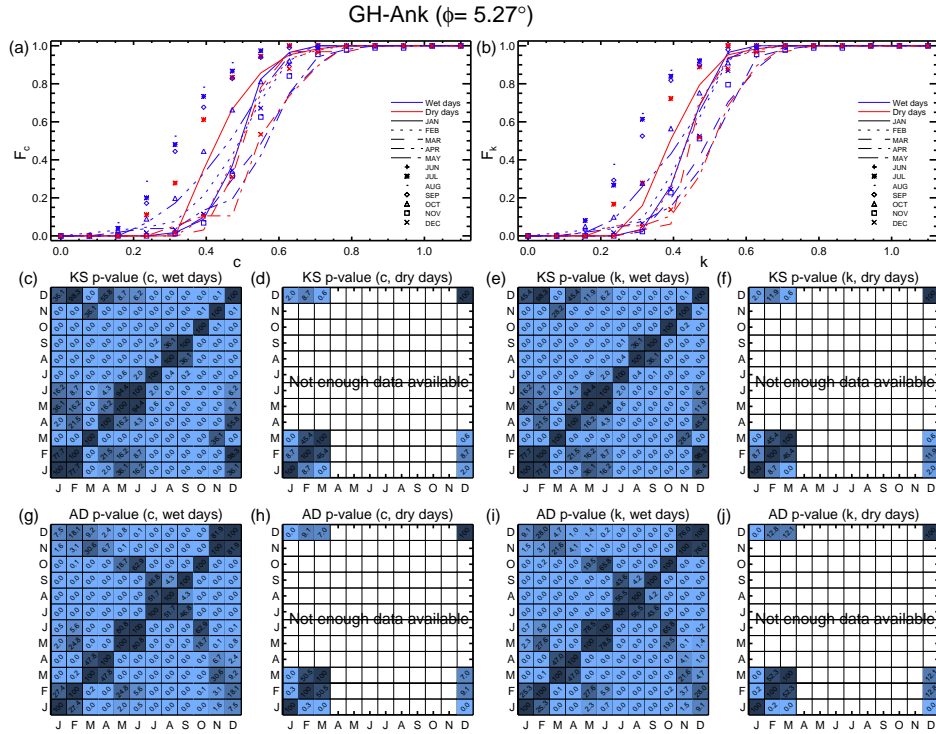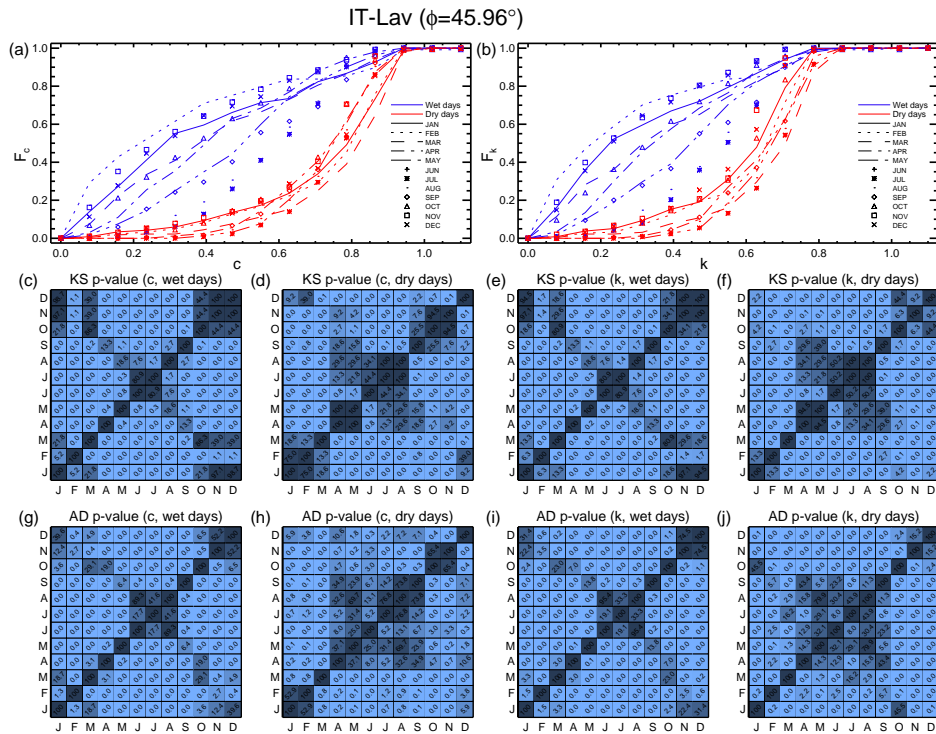
Figure S73. Monthly CDFs of (a) c, and (b) k. (c-j) p-value of the 2-sample KS and AD tests applied to all combinations of monthly CDF of c and k during wet (blue) and dry (red) days at IT-MBo.
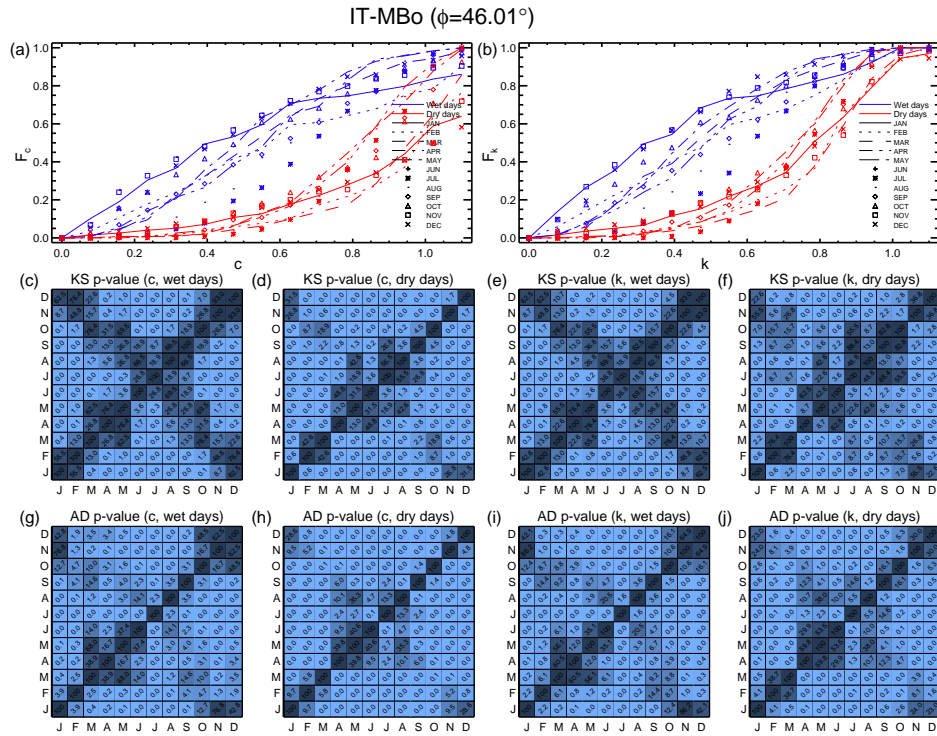

Figure S74. Monthly CDFs of (a) c, and (b) k. (c-j) p-value of the 2-sample KS and AD tests applied to all combinations of monthly CDF of c and k during wet (blue) and dry (red) days at IT-SRo.
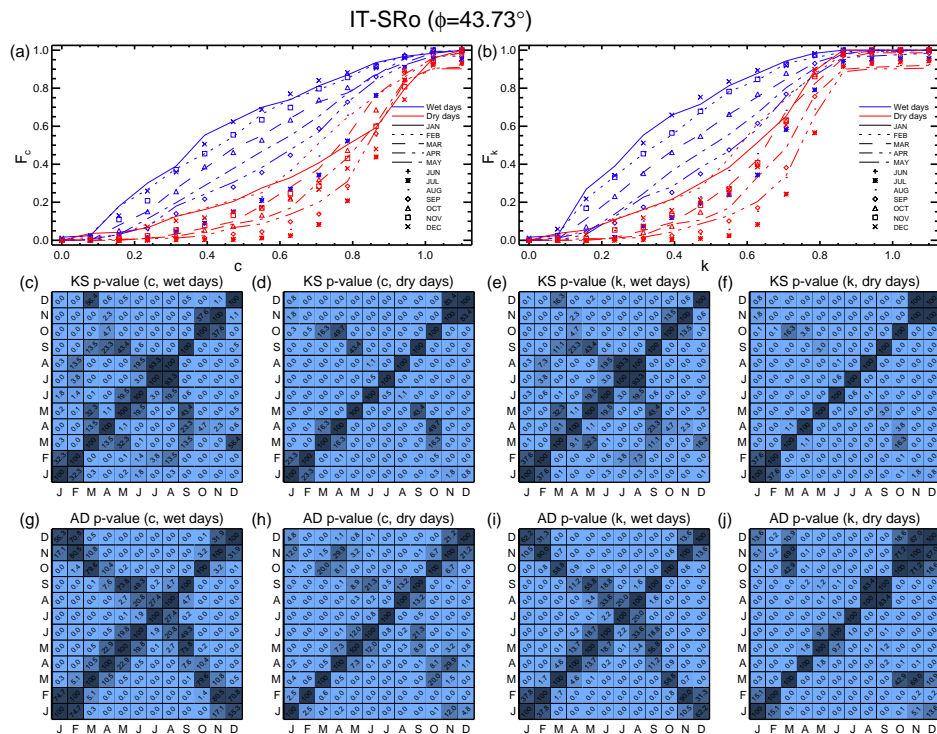
Figure S75. Monthly CDFs of (a) c, and (b) k. (c-j) p-value of the 2-sample KS and AD tests applied to all combinations of monthly CDF of c and k during wet (blue) and dry (red) days at MY-PSO.
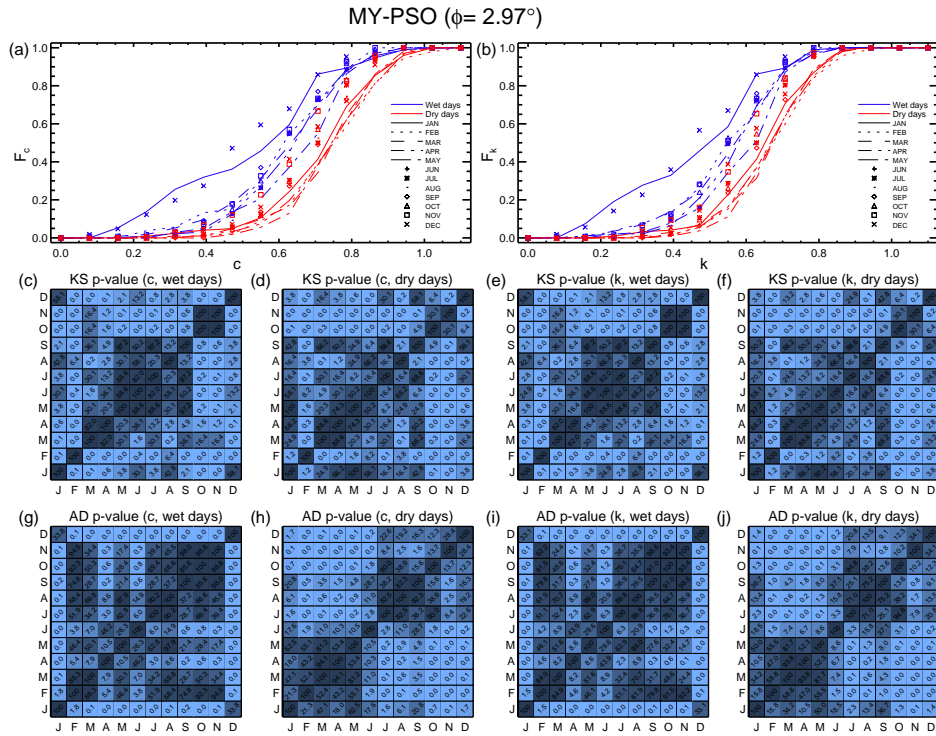

Figure S76. Monthly CDFs of (a) c, and (b) k. (c-j) p-value of the 2-sample KS and AD tests applied to all combinations of monthly CDF of c and k during wet (blue) and dry (red) days at PA-SPs.
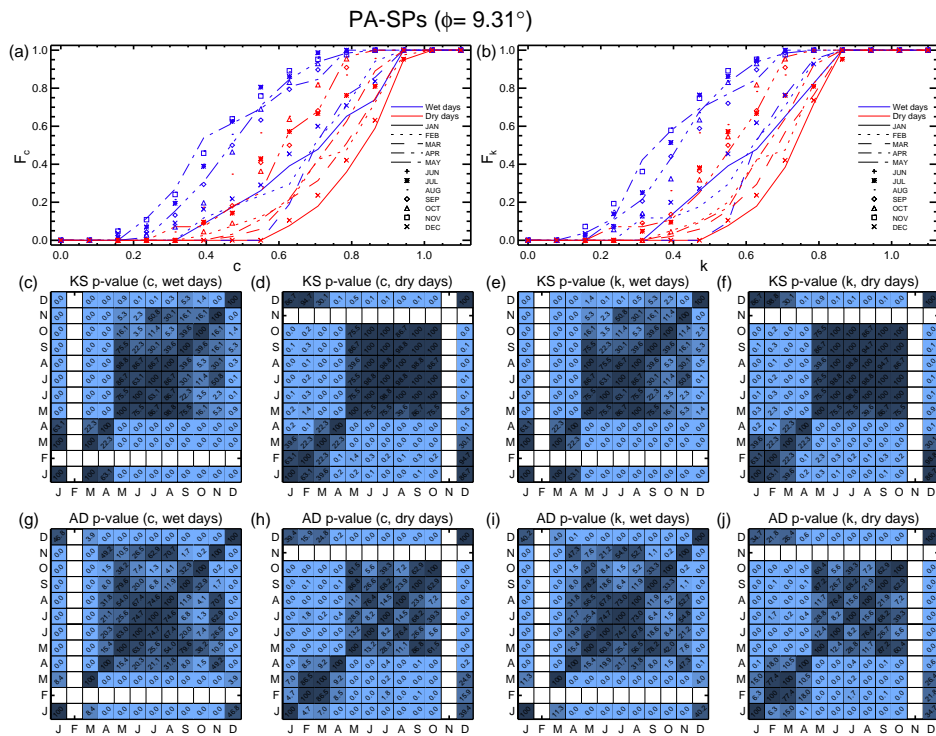
RU-Fyo (ϕ=56.46°)

Figure S77. Monthly CDFs of (a) c, and (b) k. (c-j) p-value of the 2-sample KS and AD tests applied to all combinations of monthly CDF of c and k during wet (blue) and dry (red) days at RU-Fyo.
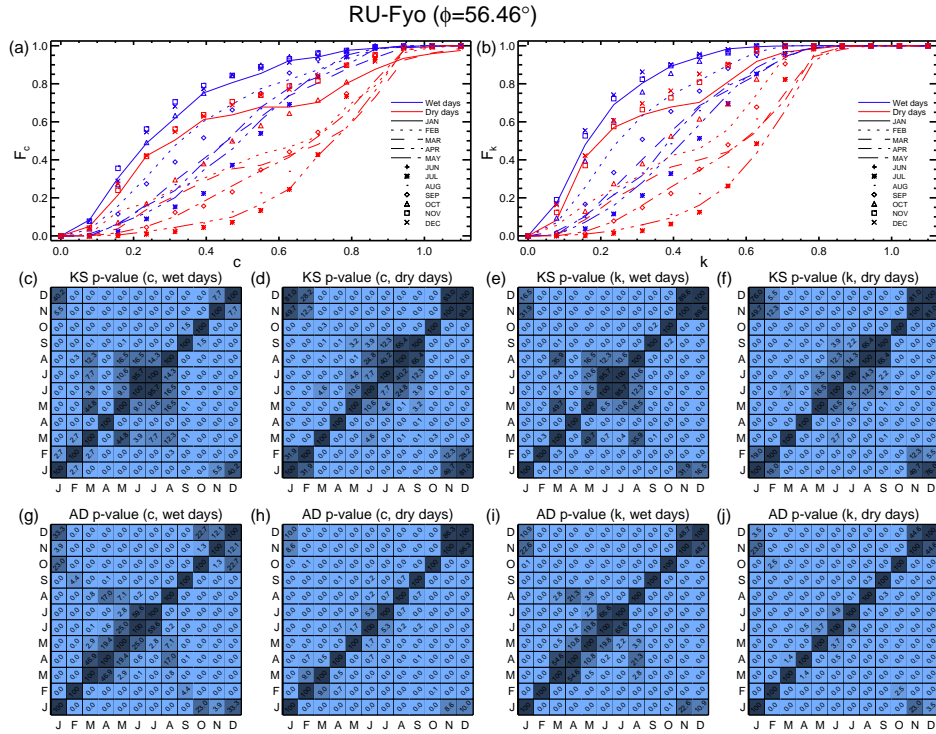
SD-Dem (ϕ=13.28°)

Figure S78. Monthly CDFs of (a) c, and (b) k. (c-j) p-value of the 2-sample KS and AD tests applied to all combinations of monthly CDF of c and k during wet (blue) and dry (red) days at SD-Dem.
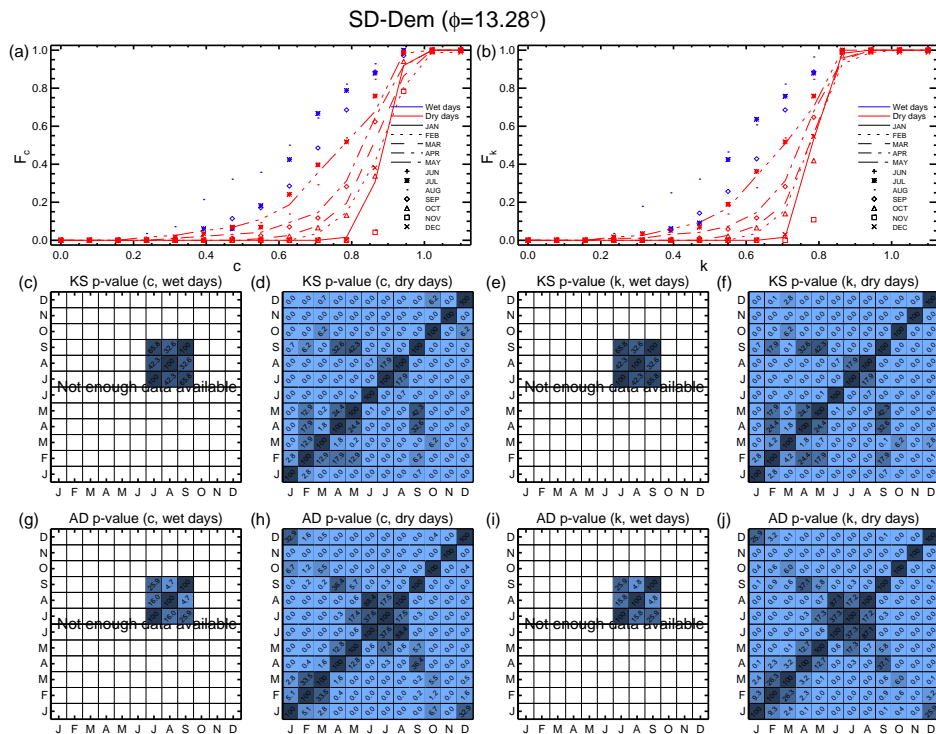
Figure S79. Monthly CDFs of (a) c, and (b) k. (c-j) p-value of the 2-sample KS and AD tests applied to all combinations of monthly CDF of c and k during wet (blue) and dry (red) days at SN-Dhr.
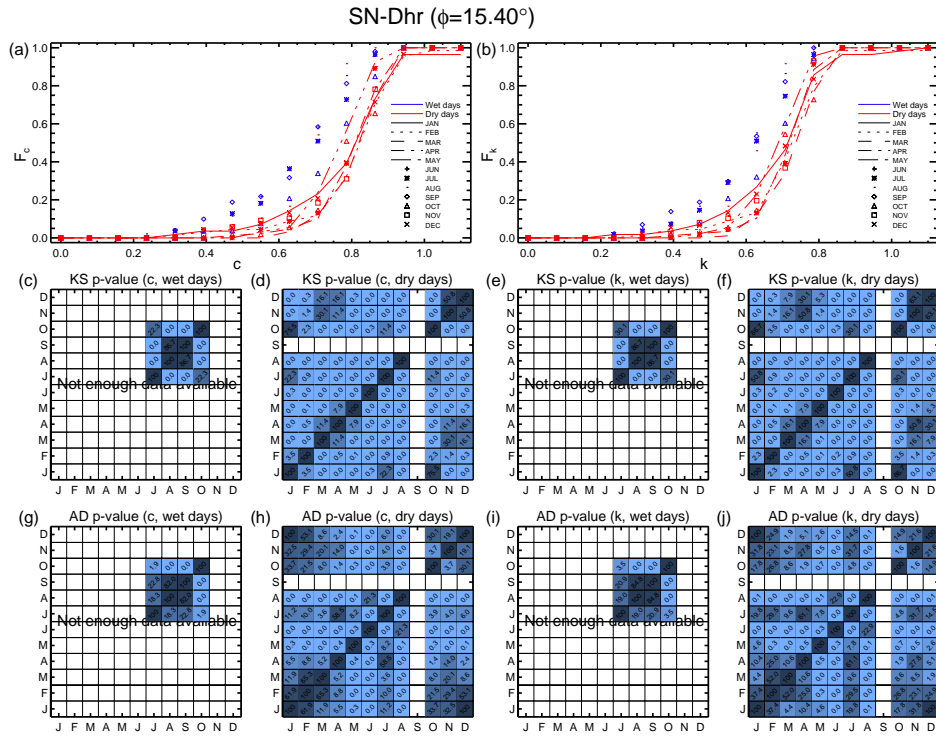

Figure S80. Monthly CDFs of (a) c, and (b) k. (c-j) p-value of the 2-sample KS and AD tests applied to all combinations of monthly CDF of c and k during wet (blue) and dry (red) days at US-Esm.
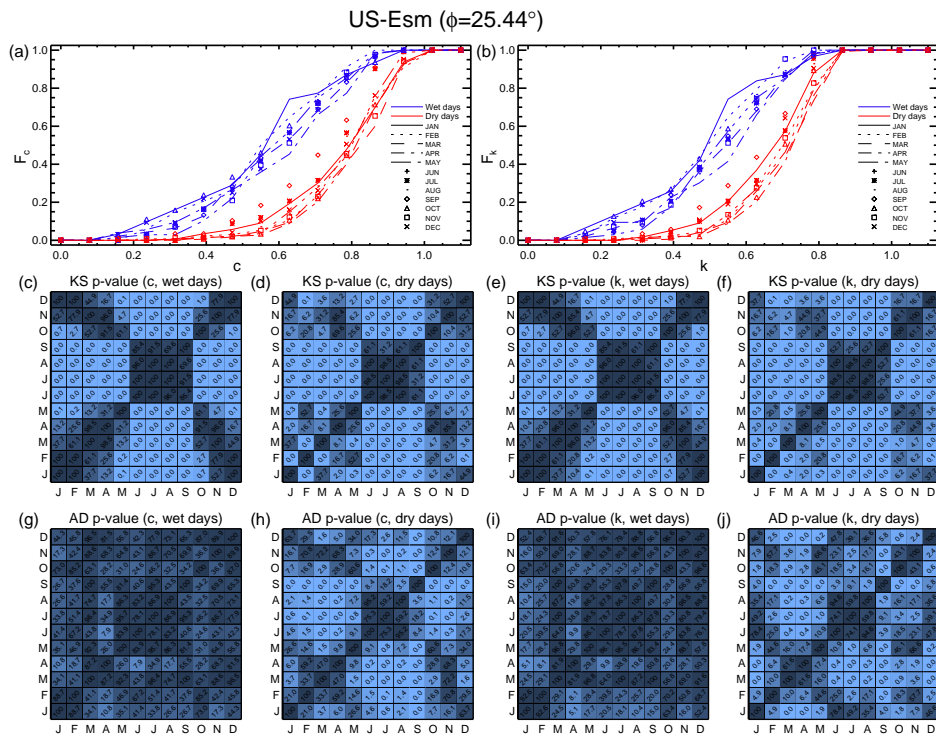
US-FPe (φ=48.31°)

Figure S81. Monthly CDFs of (a) c, and (b) k. (c-j) p-value of the 2-sample KS and AD tests applied to all combinations of monthly CDF of c and k during wet (blue) and dry (red) days at US-FPe.
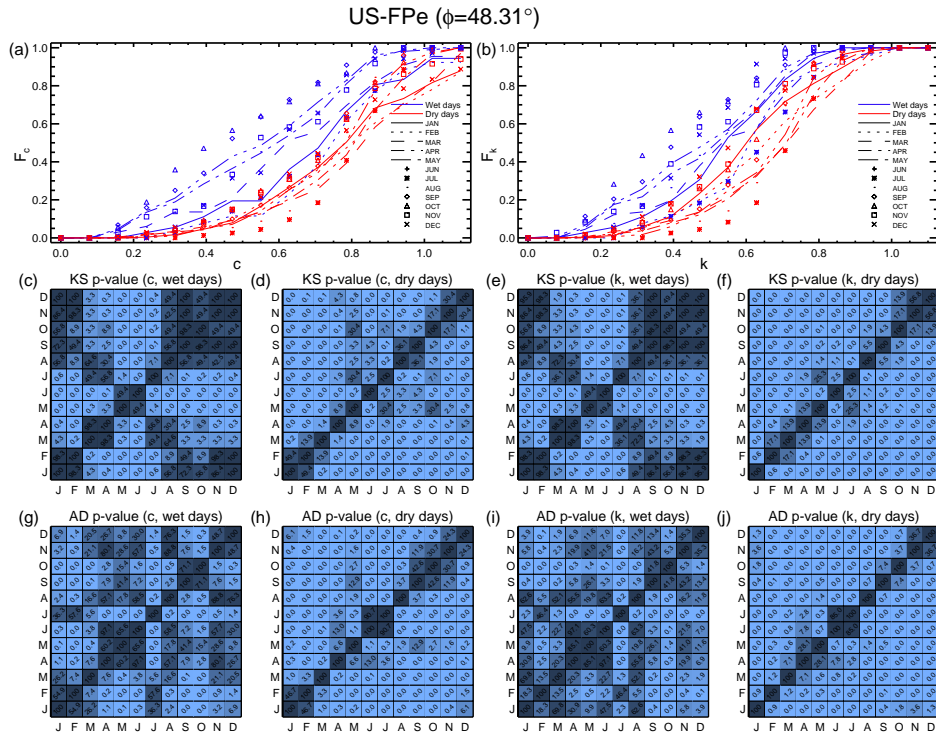
US-NC2 (φ=35.80°)

Figure S82. Monthly CDFs of (a) c, and (b) k. (c-j) p-value of the 2-sample KS and AD tests applied to all combinations of monthly CDF of c and k during wet (blue) and dry (red) days at US-NC2.
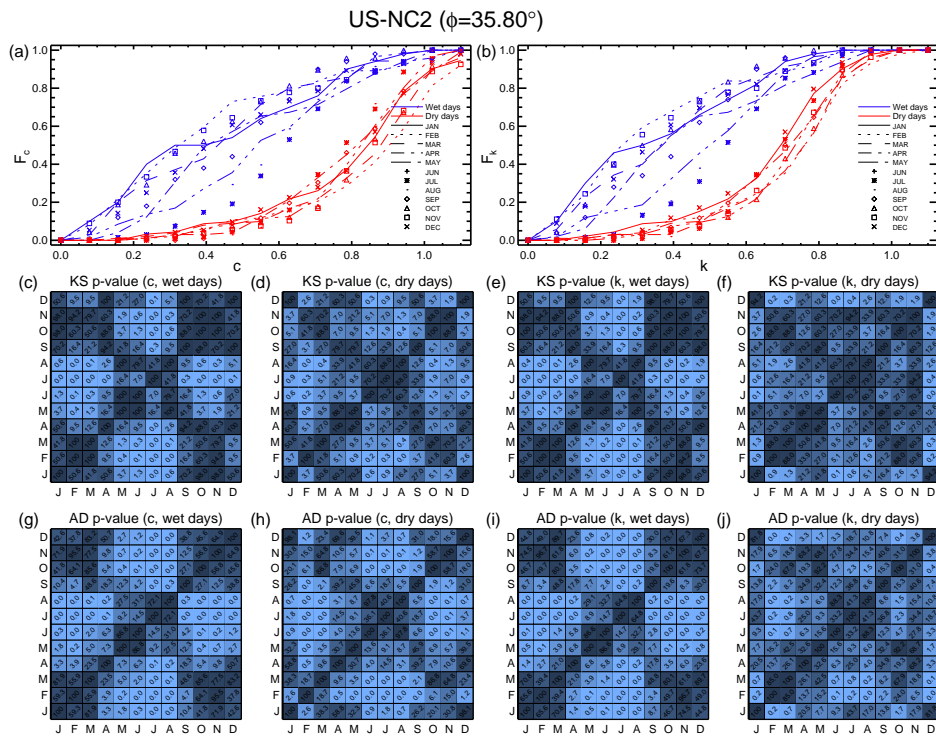
Figure S83. Monthly CDFs of (a) c, and (b) k. (c-j) p-value of the 2-sample KS and AD tests applied to all combinations of monthly CDF of c and k during wet (blue) and dry (red) days at US-SRM.
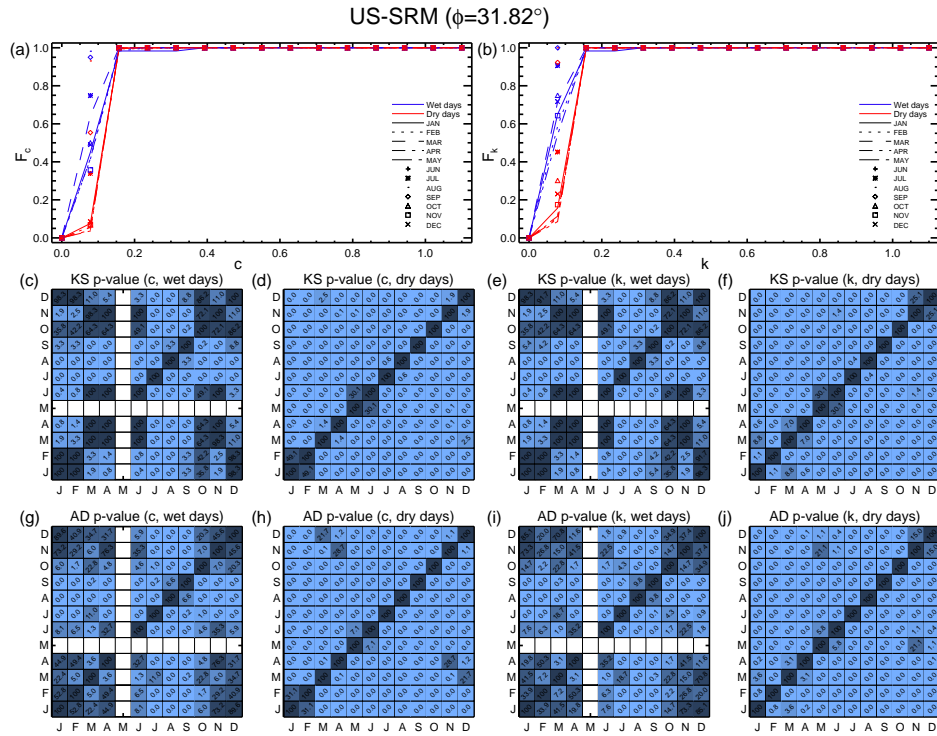

Figure S84. Monthly CDFs of (a) c, and (b) k. (c-j) p-value of the 2-sample KS and AD tests applied to all combinations of monthly CDF of c and k during wet (b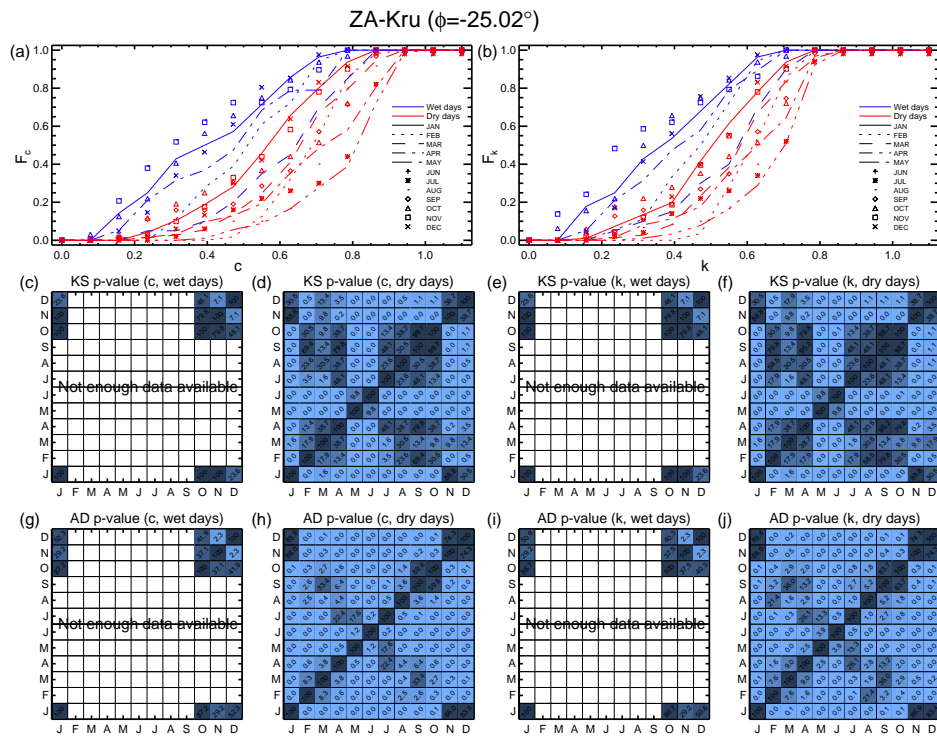lue) and dry (red) days at ZA-Kru.